HHS Public Access

Author manuscript

Chem Rev. Author manuscript; available in PMC 2020 January 23.

Published in final edited form as:

Chem Rev. 2019 January 23; 119(2): 797–828. doi:10.1021/acs.chemrev.8b00211.

Transition Metal Complexes and Photodynamic Therapy from a Tumor-Centered Approach: Challenges, Opportunities, and Highlights from the Development of TLD1433

Susan Monro[a], **Katsuya L. Colón**[b], **Huimin Yin**[a], **John Roque III**[b], **Prathyusha Konda**[c], **Shashi Gujar**[c,d,e,f], **Randolph P. Thummel**[g], **Lothar Lilge**[h], **Colin G. Cameron**[*,b], and **Sherri A. McFarland**[*,a,b,d]

[a]Department of Chemistry, Acadia University, Wolfville, Nova Scotia B4P 2R6, Canada;

[b]Department of Chemistry and Biochemistry, The University of North Carolina at Greensboro, Greensboro, North Carolina 27402, United States;

[c]Department of Microbiology and Immunology, Dalhousie University Halifax, Nova Scotia, Canada B3H 1X5;

[d]Department of Pathology, Dalhousie University, Halifax, Nova Scotia, Canada B3H 1X5;

[e]Department of Biology, Dalhousie University, Halifax, Nova Scotia, Canada B3H 1X5;

[f]Centre for Innovative and Collaborative Health Services Research, IWK Health Centre, Halifax, Nova Scotia, Canada B3K 6R8;

[g]Department of Chemistry, University of Houston, Houston, Texas 77204-5003, United States;

[h]Princess Margaret Cancer Centre, University Health Network, 101 College Street, Toronto, Ontario, Canada M6R1Z7

Abstract

Transition metal complexes are of increasing interest as photosensitizers in photodynamic therapy (PDT) and, more recently, for photochemotherapy (PCT). In recent years, Ru (II) polypyridyl complexes have emerged as the most widely studied systems for both PDT and PCT. Their rich photochemical and photophysical properties derive from a variety of excited-state electronic configurations accessible with visible and near-infrared light, and these properties can be exploited for both energy- and electron-transfer processes that can yield highly potent oxygen-dependent and/or oxygen-independent photobiological activity. Selected examples highlight the use of rational design in coordination chemistry to control the lowest-energy triplet excited state configurations for eliciting a particular type of photoreactivity for PDT and/or PCT effects. These principles are also discussed in the context of the development of TLD1433, the first Ru(II)-based photosensitizer for PDT to enter a human clinical trial. The design of TLD1433 arose from a tumor-centered approach, as part of a complete PDT package that included the light component and the protocol for treating nonmuscle invasive bladder cancer. Briefly, this review summarizes

[*]Corresponding Author: samcfarl@uncg.edu; cgcamero@uncg.edu.

SAM has received financial support from Theralase Technologies, Inc. (TLT). LL is a scientific consultant for Theralase Technologies, Inc. (TLT).

the challenges to bringing PDT into mainstream cancer therapy. It considers the chemical and photophysical solutions that transition metal complexes offer, and it puts into context the multidisciplinary effort needed to bring a new drug to clinical trial.

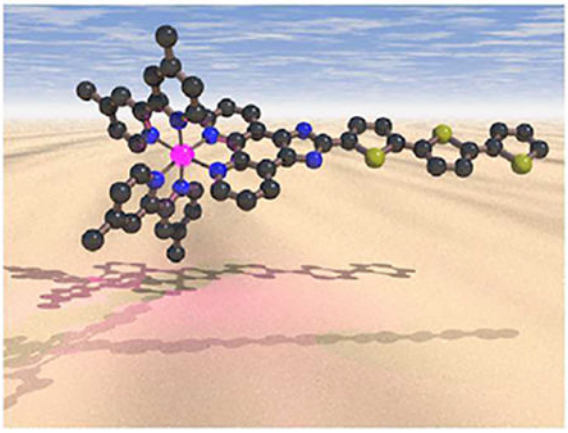

1. INTRODUCTION

This review provides an overview of the challenges and opportunities in developing transition metal complexes as photosensitizers for improved photodynamic therapy (PDT) and photochemotherapy (PCT). Its target audience includes researchers that are new to the field, researchers dedicated to translational outcomes, and those wanting to develop the most robust methods for assessing photosensitizer performance across different laboratories. It is assumed that the reader has a basic understanding of the photochemical and photophysical processes behind PDT/PCT and a good understanding of Ru(II) polypyridyl photophysics; any reader needing a primer should consult the sources cited at the beginning of the next section. This review was inspired by the challenges and opportunities that our own laboratory faced in developing TLD1433, the first Ru(II)-based photosensitizer to enter a human clinical trial (ClinicalTrials.gov Identifier: NCT03053635). It includes a discussion of the most influential published works that led us to develop TLD1433, emphasizing the multidisciplinary aspect of photosensitizer design for PDT/PCT.

1.1. What is PDT anyway?

Henderson and Dougherty edited a book in 1992, *Photodynamic Therapy: Basic Principles and Clinical Applications*, which provides a comprehensive overview of PDT.[1] Other useful resources include Bonnett's *Chemical Aspects of Photodynamic Therapy* (2000),[2] *Handbook of Photomedicine*[3] (2014), *Advances in Photodynamic Therapy: Basic Translational and Clinical*[4] (2008), as well as *Photodynamic Medicine: From Bench to Clinic*[5] (2016). There are also numerous informative reviews that discuss the basic concepts of PDT and its specific indications in photomedicine.[6–12] The large number of reviews and articles about PDT can overwhelm a newcomer trying to learn where to start and what information is the most relevant. Newer reviews rehash information from the older reviews with some concepts being lost in translation, and many articles cite information from seemingly randomly selected reviews that may or may not be applicable to the context of

interest. The 2017 review by Robinson *et al.* does an excellent job of collecting all of the advantages and challenges of PDT into a single article, complete with a discussion of all of the trials and studies related to the clinical application of PDT to cancer over the past ten years and a full tabulation of these review findings by tumor type, study goal, methodology, photosensitizer, outcome, and adverse events for each organ.[6]

The term PDT derives from the photodynamic effect, which was reported around the turn of the twentieth century when paramecia exposed to acridine were killed by light but survived in the dark (Figure 1). In its strictest definition, the photodynamic effect refers to the "damage or destruction of living tissue by visible light in the presence of a photosensitizer and oxygen",[2] and thus PDT is a therapy based on this effect. As such PDT can be exploited to destroy any unwanted entity, including eukaryotic cells, prokaryotic cells, and viruses. The more specialized term photodynamic inactivation (PDI) has emerged and is sometimes used to describe PDT against bacteria, fungi, and viruses, while PDT remains in familiar usage against cancer and neovasculature tissue.

The mechanisms of the photodynamic effect (and hence PDT) are inherently complex, but they generally fall into one of two categories: type I and type II photoprocesses (not to be confused with the Norrish type I and type II reactions of ketones and aldehydes[13] from organic photochemistry). However, the explosion of multidisciplinary research related to PDT has generated the haphazard, and often incorrect, use of such terms, but there have been attempts to set matters straight by defining the "ten tips for type I and type II photosensitized oxidation reactions".[14] Both Type I and Type II mechanisms have an absolute dependence on molecular oxygen (Scheme 1): Type II mostly involves energy transfer from the photosensitizer to ground-state $^3O_2$ to yield singlet oxygen ($^1O_2$), and type I involves photoinduced electron transfer that leads to the formation of superoxide ($O_2^{\bullet-}$) or hydroperoxyl radicals ($HO_2^{\bullet}$). Cadet and Greer emphasized that "photodynamic action is killing via Type I or Type II" photoprocesses and that the term "oxygen-independent photodynamic action should not be used".[14] Both Type I and Type II photosensitized reactions result in biomolecule degradation and ultimately tissue damage/destruction.

Even when considering the contribution of only these two photosensitization pathways, the distinction cannot be made easily, and they can be expected to occur together.[2] The distinguishing tests (e.g., lifetime in deuterated solvent, azide quenching, radical spin-trapping) do not reliably discriminate between $^1O_2$, and $O_2^{\bullet-}$ intermediates. Moreover, the detection of a minute quantity of a given species is not proof of the dominant mechanistic pathway. Lastly, such experiments are performed outside of a biological environment, which further complicates the interpretation of the actual operative mechanism(s) in vitro or in vivo, where it is difficult to obtain convincing mechanistic evidence.

In vitro and in vivo PDT effects likely arise from damage to numerous biological targets through multiple mechanistic pathways that change with tissue type, oxygenation status, and PDT regimen. While cell-free mechanistic experiments can reveal some useful information, the results cannot necessarily be extended to cellular environments or whole organisms, where absorption, distribution, metabolism, and excretion (ADME) (as it relates to the photosensitizer) and dosimetry (as it relates to the photosensitizer, light, and oxygen)

become influential factors. Nevertheless, the consensus appears to be that the predominant PDT mechanism is Type II and that $^1O_2$ targets unsaturated lipids and certain amino acid side chains as well as the nitrogenous bases of nucleic acids. Herein, we define PDT as the use of a photosensitizer, light (usually visible), and oxygen to generate cytotoxic reactive oxygen species (ROS). These three components of oncologic PDT are harmless individually, but they combine to destroy tumors, occlude tumor vasculature, and invoke an immune response in a two-stage procedure that consists of administration of the photosensitizer, followed by exposure of the affected tissue to light.[6]

1.2. What makes a good photosensitizer for PDT?

If one assumes that the Type II pathway is the most important mechanism for PDT and that $^1O_2$ is the most important mediator of the photodynamic effect, then molecules that have high quantum yields for $^1O_2$ formation (Φ_Δ) are desirable. The qualities of the so-called *ideal* photosensitizer are based on this premise and, for the most part, derive from both the attractive and unattractive properties of Photofrin®, the first photosensitizer clinically approved for PDT (Scheme 1).

Photofrin®, which is complex mixture of porphyrin-based oligomers, was approved in Canada in 1993 for the treatment of bladder cancer with PDT[16] but failed to become mainline therapy due, in part, to issues with prolonged skin phototoxicity and compromised bladder function.[9] Despite being the most widely used photosensitizer for oncologic PDT, it is known to have poor tissue selectivity and relatively low absorption of red light ($\varepsilon \approx 2{,}500$ M^{-1} cm^{-1} at 630 nm),[17] which is exacerbated by the poor tissue penetration of shorter wavelength visible light. These drawbacks spurred the development of higher-purity second-generation photosensitizers[18,19] aimed at increasing tumor selectivity to reduce the overall drug dose and thereby avoid the undesirable side effects associated with systemically-delivered photosensitizers. Some second-generation photosensitizers (which include derivatives of porphyrins, chlorins, bacteriochlorins, phthalocyanines, pheophorbides, bacteriopheophorbides, and texaphyrins) were also designed to absorb longer wavelengths of light in an effort to improve tissue penetration for treating deep-seated and/or solid tumors.[7,20,21]

The difficulty in simultaneously achieving high tumor affinity and optimal photophysical and photochemical properties for PDT in the second generation photosensitizers led to the design of third generation photosensitizers that actively or passively target tumors or tumor receptors to improve selectivity for malignant tissue. Active targeting most often involves covalent attachment of the photosensitizer to a ligand that will preferentially bind to surface receptors that are either unique to or overexpressed on tumors.[22] Examples include: monoclonal antibodies, antibody fragments, peptides, proteins such as transferrin, epidermal growth factor, insulin, LDL, certain carbohydrates, somatostatin, folic acid, and others. Photodynamic molecular beacons[23] and other photosensitizers that can be enzyme-activated (by tumor-associated proteases for example)[24] are particularly elegant examples of active targeting with additional selectivity for malignant tissue built into the design. Passive targeting, on the other hand, takes advantage of macroscopic differences between healthy tissue and tumors, often via the enhanced permeability and retention (EPR) effect.[25] In this

case, photosensitizers are carried by nanoparticles or liposomes that penetrate the leaky vasculature of tumors due to their compatible size. These nanoscale photosensitizer delivery systems also carry large payloads of photosensitizer molecules and act to solubilize these (often) hydrophobic structures. The rationale in both active and passive targeting in the third generation photosensitizers is that the targeting vehicle can be used to control localization so that the photosensitizer itself can be selected based on its photophysical properties rather than its tumor-targeting properties.[7]

A large number of new photosensitizers have been explored for their abilities to target certain subcellular organelles. For example, intracellular targeting of photosensitizers to mitochondria[26–31] has been exploited to promote PDT-induced apoptosis. While interesting on a fundamental level, this specificity is irrelevant if the photosensitizer does not accumulate in the tumor cells, the local environment is not well-oxygenated, or the light does not reach the photosensitizer. Moreover, observation of intracellular targeting in one type of cell at one point in time does not imply that this is a general property of the photosensitizer that can be universally applied. Often, these studies on intracellular targeting are performed in vitro on two-dimensional monolayers of a specific cell line at a specific time point without consideration of the tumor type and phenotype nor of the PDT regimen in the clinical setting. To date we are unaware of any intracellular targeted photosensitizers advancing to clinical studies.

Despite the introduction of multiple generations of photosensitizers for cancer therapy, and hundreds if not thousands of new compounds reported in the primary literature, only 3 have received regulatory approval by the FDA, and only 3 are approved worldwide (Tables 1–4, §1.5). Moreover, almost one-third of recent clinical trials still use the first-generation compound Photofrin®![6] The evolution of the generations of photosensitizers gives an idea of what the major priorities have been in terms of improvements: single agents rather than complex mixtures, enhanced aqueous solubility or formulation to achieve enhanced aqueous solubility, tumor selectivity for systemically-delivered photosensitizers, longer-wavelength absorption, and strong absorption at these longer wavelengths. In addition, many books and articles tout a standard list of properties for the *ideal* PDT agent: (1) effective $^1O_2$ generation, (2) large molar extinction coefficient in the PDT window (≈700–900 nm), with disagreement on this exact range, (3) preferential tumor accumulation and rapid systemic clearance, (4) amphiphilic structure, (5) no dark toxicity, (6) chemical stability, (7) solubility in injectable formulations, and (8) chemically pure and easy to obtain via high-yielding reactions.[4] Not surprisingly, no photosensitizer to date meets all of these criteria, and even if one did, it would not be widely applicable against a range of cancers and tumor phenotypes. In other words, attempting to create the ideal photosensitizer according to these criteria is unlikely to bring PDT into the mainstream for cancer therapy.

1.3. There is no ideal photosensitizer for PDT

One might argue that the basic premise of PDT makes it a priori not applicable to some of the most aggressive and drug-resistant tumors, which are often hypoxic.[32] Solid and deep-seated tumors also pose a similar challenge. At the very least, ideal property #1 should be restated to indicate that the $^1O_2$ quantum yields should remain high even at low oxygen

tension. In other words, the 20–50% quantum yields measured experimentally under normoxia (and often in organic solvent)[10,33] actually need to be larger to ensure ROS production in hypoxia. More importantly, new photosensitizers that can switch between oxygen-dependent and oxygen-independent mechanisms based on local oxygen concentration and/or that exploit oxygen-independent photochemistry will offer new avenues for treating hypoxic tissue with light-responsive photosensitizers.

The PDT window is the range of wavelengths over which tissue penetration is optimal. It has been reported as 700900 nm, 650–900 nm, 600–800 nm, 650–1200 nm, and other variations. It is limited at shorter wavelengths by light absorption by endogenous biomolecules and light scatter, and at the longer wavelengths by light absorption by water. In addition, it is constrained by the energy required to sensitize $^1O_2$ (94.5 kJ mol^{-1}, corresponding to quantum equivalents of about 1,270 nm). The triplet state of the photosensitizer must exceed this energy, and the lower-wavelength limit has been estimated at 850 nm due to thermal losses in the photophysical relaxation sequence.[10,33] Certainly, if the tumor is deep-seated and/or solid, tissue-penetrating near-infrared (NIR) light is advantageous. However, if the lesion to be treated is superficial and PDT will be applied topically, there is no reason to sacrifice PDT potency for deeper tissue penetration. In fact, deeper tissue penetration would be undesirable in such a case as it could damage underlying healthy tissue. Therefore, #2 should be restated to indicate that large molar absorption cross-sections are desirable in the wavelength range that makes sense clinically. In other words, the photosensitizer should absorb strongly at the activation wavelength where treatment depth matches tumor invasion depth.

Focus on tumor accumulation and rapid clearance historically arose from adverse events that occurred with systemic delivery of photosensitizers. The need to limit off-site toxicity, especially prolonged skin phototoxicity with Photofrin®, drove the development of the second- and third-generation photosensitizers for PDT according to these principles. However, intratumoral (IT) delivery and topical applications require high tumor retention and slow leakage from the tumor, especially in cases where it is desirable to give multiple PDT treatments without re-administration of the photosensitizer. The chemical structural elements that are best-suited for systemic or intraperitoneal delivery may not be those that are ideal for IT or topical delivery, and #3 and #4 should be rewritten to reflect this. It would make no sense to graft a synthetically-demanding and expensive targeting functionality onto a photosensitizer if it is not necessary for the clinical setting.

These are a few examples supporting the assertion put forward by Plaetzer and others: photosensitizer design in PDT research should be shifted from a photosensitizer-centered approach to a tumor-centered approach.[10] Accordingly, photosensitizers should be developed by starting with the requirements of the actual clinical situation and should optimize all aspects of the PDT regimen (photosensitizer type and dose, photosensitizer-to-light interval, light dose, etc.) for the clinical indication in question. In fact, they suggest that PDT research should move beyond focus on new photosensitizers and patents of those novel chemical entities, to promotion of complete PDT packages that would consist of the photosensitizer, the light source, and the specific protocol optimized for a given clinical indication. While researchers on the clinical side of PDT appreciate the importance of

proper dosimetry and protocol for the given cancer type and tumor phenotype of interest, reports about the development of new photosensitizers, usually authored by chemists, rarely acknowledge the light component and protocol nor do they focus on a specific tumor type. With this disconnect in mind, we set out to develop TLD1433 with medical biophysicists, industry partners, and clinicians, with the goal of treating nonmuscle invasive bladder cancer (NMIBC) with topical administration of the photosensitizer.

1.4. What are the most salient challenges to mainstream PDT?

Notwithstanding fifty years since its first oncological application, PDT has not become a mainstream modality for treating any type of cancer. At a molecular level, it may come down to oxygenation, tissue penetration, and metastasis. The absolute requirement for oxygen is a fundamental limitation of PDT so far. Oxygenation of tumors is highly variable and difficult to measure, and this presents a challenge in predicting which patients are most likely to benefit from PDT. Paradoxically, the PDT treatment itself can render the target tissue hypoxic and thus resistant to PDT. Poor tissue penetration by both light and photosensitizer can also limit the effectiveness of PDT. For larger, solid tumors, penetration of both throughout the tumor volume is crucial for achieving effective tumoricidal activity. Finally, PDT is viewed as a local treatment despite its ability to invoke antitumor immunity.[34–37] Approved protocols are optimized for local tumor ablation rather than for antitumor immunity. Gollnick and coworkers have demonstrated the importance of a two-step PDT protocol that would combine an immune-enhancing regimen to be followed by a tumor-ablating regimen; the parameters are not the same.[36–38] It is estimated that metastasis is responsible for about 90% of cancer deaths,[39] and it is impossible to deliver light to widely disseminated disease. For PDT to make an important contribution to improving survival rates in the most aggressive cases, the immune-enhancing facet of PDT must be exploited.

The poor adoption of PDT can be blamed on the clash of philosophy and pragmatism, which is responsible for the unfruitful photosensitizer-centered approach outlined earlier. In the pragmatic approach, an independent academic chemist synthesizes a new compound, and then studies its interactions with biological macromolecules and its photodamaging capacity in cell-free environments. In vitro testing is not available in most chemistry laboratories, and in vivo testing is rarer still. The very narrow and linear approach to characterizing the performance of these new photosensitizers is done most often in the absence of any specific clinical cancer indication target. New photosensitizers are rarely assessed alongside existing, clinically-approved photosensitizers, and the multidimensional complexity of PDT precludes a meaningful comparative analysis even when in vitro and in vivo screening is accessible to the chemist. This situation is further complicated by most academic laboratories not being able to purchase Photofrin® due to cost and the difficulties of procuring a “drug” by a non-physician. Without critical collaborations and partnerships — and an intellectual property (IP) strategy—, chemists are trapped in a bottom-up approach to photosensitizer design, and most photosensitizers languish, untested in the pre-clinical animal studies that precede translation and commercialization. At the same time, cancer biologists interested in PDT are stuck in a linear top-down approach, without access to new and better photosensitizers. The result is that very few new photosensitizers have both the physiological properties and the economic potential to reach extremely expensive human clinical studies. We posit that

significant progress in the field of PDT demands a lateral approach, where chemists develop new photosensitizers from a tumor-centered approach, alongside partners and investors, with a sound IP strategy (Figure 2). Multidisciplinary and multi-dimensional relationships are crucial; the traditional model of the lone research chemist in academia is outdated.

Pragmatically, the problems with photosensitizer distribution and dosimetry warrant a personalized approach to PDT delivery and robust clinical investigations. A number of reviews note that there is a lack of randomized controlled clinical trials of adequate power.[6] The equipment and expertise required for PDT is not standard clinical infrastructure. Where PDT studies are possible, different treatment protocols used in different small studies at different centers make comparison of clinical results difficult. There is generally a lack of commitment from the venture capitalists and government organizations that are able to fund large, multi-center trials. In addition, for ethical reasons, clinical trials have largely focused on PDT as an adjuvant, or on patients with advanced cancers that have failed other therapies (which leads to inherent bias towards poor outcomes).[10] The number of variables to be optimized for clinical PDT with new photosensitizers means that the time in clinical trials could be longer than other standard therapies, which adds significant cost and risk. All of these challenges underscore the importance of developing the photosensitizer, light parameters, and protocol together for a specific clinical indication from the very beginning of the drug discovery process. There is merit in considering panchromatic photosensitizers that could be optimally activated with any wavelength of light from visible to NIR given the difficulty in getting new photosensitizers approved. A panchromatic photosensitizer that is safe and well-tolerated in humans might enable the light parameters and protocol to be optimized so that treatment depth matches tumor invasion depth for personalized medicine. Ultimately, this may reduce cost, facilitate regulatory approval, and also position the photosensitizer to be developed simultaneously as part of an immunotherapeutic PDT package.

While PDT experts on the clinical side are aware of these issues, reports of new photosensitizers in the primary literature generally do not acknowledge the shortcomings of PDT research and the tenuous position of PDT as an anticancer modality. PDT runs a real risk of being completely dismissed if new photosensitizers and new approaches are not introduced in a timely manner. As with any innovative technology that depends on investment for commercialization, PDT is at a critical point on the Gartner hype cycle (Figure 3). If we do not bring PDT to the forefront for some clinical indication as mainline or adjuvant therapy soon, certainly it will become increasingly more difficult to find support for its development.

1.5. Tables of approved photosensitizers and those in clinical trials

Table 1.

Photosensitizers Approved Worldwide for Cancer Therapy.

GENERIC NAME	CHEMICAL NAME	STRUCTURE	λ_{ex} (nm) ε_{max} (M^{-1} cm^{-1})	CANCER TYPES
Porfimer sodium[a]	Photofrin®	Porphyrin	630 (3,000)	High grade dysplasia in

GENERIC NAME	CHEMICAL NAME	STRUCTURE	λ_{ex} (nm) ε_{max} (M^{-1} cm^{-1})	CANCER TYPES
				Barret's Esophagus, obstructive esophageal or lung cancer
5-Aminolevulinic acid (5-ALA)	Ameluz®; Levulan®	Porphyrin precursor	632 (5,000)[b]	Basal cell carcinoma, squamous cell carcinoma
Mithyl-5-aminolivulinati (MAL)	Mitvix®; Mitvixia®	Porphyrin precursor	635 (N.R.)[b,c]	Basal cill carcinoma

[a] Porfimer sodium (Photofrin®) withdrawn in EU for commercial reasons;

[b] λ_{ex} and ε_{max} refer to PpIX, the porphyrin produced as part of heme biosynthesis.

[c] N.R., not reported.

Table 2.

Photosensitizers in Clinical Trials in North America for Cancer Therapy.

GENERIC NAME	CHEMICAL NAME	STRUCTURE	λ_{ex} (nm) ε_{max} (M^{-1} cm^{-1})	CANCER TYPES
TLD1433	TLD1433	Ru(II) complex	525 (2,000)	Nonmuscle invasive bladder cancer (NMIBC)
Hexaminolevulinate (HAL)	Hexvix®, Cysview®	Porphyrin precursor	380–450 (N.R.)[a]	Bladder cancer, blue light cystoscopy (detection of tumours in bladder cancer patients)
2-[1-hexyloxyethyl]-2-devinyl pyropheophorbide-a (HPPH)	Photochlor®	Pheophorbide	665 (47,000)	Esophageal, lung, skin, and mouth and throat cancers; Cervical intraepithelial neoplasia, oral precancerous lesions
Chlorin e6-PVP	Photolon®	Chlorin	400, 665 (N.R.)[a]	Cervical intraepithelial neoplasia, oral precancerous lesions, cervical intraepithelial neoplasia, oral precancerous lesions
Indocyanine green (ICG)	ICG	Cyanine	800 (N.R.)[a]	ICG-guided PDT, medical diagnostic, near-IR identification
Rostaporfin (SnET2)	Purlytin	Phthalocyanine	664 (30,000)	Basal cell cancer (Recurrent), macular degeneration
Lemuteporfin		Benz oporphyrive deriviative	690 (N.R.)	Benign prostatic hypertrophy, mild acne (topical)
Motexafin lutetium (Lu-Tex)	Lutrin®; Optrin®; Antrin®	Metallotexaphyrins	732 (42,000)	Brain, breast, cervical and prostate; skin conditions and superficial cancers
(Sulfonated aluminum phthalocyanine) AlPcSn	Photosense®; Photosens®	Phthalocyanine	676 (200,000)	Stomach, skin, lip, oral, and breast cancer, age-related
Phthalocyanine 4 (Pc4)	Pc4	Phthalocyanine	675 (200,000)	Actinic Keratosis, Bowen's Disease, Skin Cancer, or Stage I or Stage II

GENERIC NAME	CHEMICAL NAME	STRUCTURE	λ_{ex} (nm) ε_{max} (M^{-1} cm^{-1})	CANCER TYPES
				Mycosis Fungoides
Synthetic hypericin	SGX301	Anthraquinone	410 (10,000); 590 (44,000)	Cutaneous T-cell lymphoma, psoriasis (topical)
Padoporfin (WST09)	Tookad®	Bacteriochlorophyll	763 (88,000)	Prostate cancer

[a]N.R., not reported.

Table 3.

Photosensitizers Approved Outside of North America for Cancer Therapy.

GENERIC NAME	CHEMICAL NAME	COUNTRY	STRUCTURE	λ_{ex} (nm) ε_{max} (M^{-1} cm^{-1})	CANCER TYPES
Temoporfin (mTHPC)	Foscan®	EU	Chlorin	652 (35,000)	Head and neck squamous cell carcinoma
Talaporfin (NPe6)	Laserphyrin®	Japan	Chlorin	664 (40,000)	Early centrally located lung cancer, malignant gliomas
LUZ111	Redaporfin®	Orphan Drug Designation (ODD) from EMA in Europe	Bacteriochlorin	749 (N.R.)[a]	Biliary tract cancer, advanced head and neck cancer
Padoporfin (WST09)	Tookad®	EU	Bacteriochlorophyll	763 (88,000)	Prostate cancer

[a]N.R., not reported.

Table 4.

Photosensitizers Approved for Other Therapies.

GENERIC NAME	CHEMICAL NAME	COUNTRY	STRUCTURE	λ_{ex} (nm) ε_{max} (M^{-1} cm^{-1})	CANCER TYPES
Indocyanine green (ICG)	ICG	USA	Cyanin	800 (N.R.)[a]	ICG-guided PDT, medical diagnostic
Verteporfin (BPD-MA)	Visudyne®	Worldwide	Chlorin	689 (34,000)	Age-related macular degeneration
Topical nanoemulsion of 5-ALA (BF200)	Ameluz®	USA	Porphyrin precursor	632 (5,000)[b]	Mild to moderate actinic keratosis on the face and scalp
Methyl-5-aminolevulinate (MAL)	Metvix®; Metvixia®	Worldwide	Porphyrin precursor	635 (N.R.)[a,b]	Non-hyperkeratotic actinic keratosis

[a]N.R., not reported.

[b]λ_{ex} and ε_{max} refer to PpIX, the porphyrin produced as part of heme biosynthesis.

2. MOVING BEYOND PDT: PHOTOACTIVE TRANSITION METAL COMPLEXES

2.1. Transition metal complexes in medicine

Transition metal compounds, which include coordination complexes and organometallic structures, have an interesting reputation in medicine. Despite the success of platinum-based anticancer drugs (used in nearly 50% of all cancer treatments), there remains a pervasive

fear that metals are too toxic to be considered in pharmaceutical formulations, and consequently, the development of medicinal *inorganic* chemistry has lagged conventional organic chemistry in pharmaceutical development. This ongoing (but misguided) concern arises from the toxicity of some forms of heavy metals, but fails to consider that the coordinated ligands and the oxidation state of the central metal ion determine the overall properties of transition metal complexes. As an analogy, many carbon-containing compounds are very toxic indeed, but we do not infer that all carbon-containing compounds are dangerous. Chemotherapeutics are toxic by design; the goal is to establish an acceptable therapeutic margin, where the therapeutic benefit outweighs any negative effects. The guiding principle is the same for both organic and inorganic drug development.

Metal coordination complexes and organometallics offer a wide range of oxidation states, coordination numbers, and geometries, yielding a virtually unlimited structural and chemical space. Metal complexes have been used to alter bioavailability, bind/release small molecules, inhibit enzymes, probe biological macromolecules such as DNA, label proteins, image cells, provide contrast as MRI agents, among other things.[40–42] Some act as catalysts to facilitate reactions that are simply not possible with organic compounds, and it is well-known that nature exploits metal complexes as cofactors in its most sophisticated biological reactions. Even the simple task of transporting oxygen requires a metal center. As noted by Sadler and Barry,[43] metal-based compounds offer biological and chemical diversity that is distinct from that of organic drugs, making them very attractive as pharmaceutical agents in the pursuit of new entities with novel mechanisms of action to treat drug-resistant diseases and conditions.

The properties of the “d” block transition metal complexes can be altered drastically or fine-tuned, owing to their modular three-dimensional architectures that can be easily modified by judicious selection of ligand-metal combinations, and these combinations can be designed with appropriate geometry for specific interactions with biological targets. Soliman *et al.* published a 2017 update on metal complexes in cancer therapy, highlighting some of these d-block properties.[44] Structural and electronic properties can be tailored by changing the identity of the metal and its metal oxidation state, which determines coordination number and geometry. This entails changes in physical properties and chemical reactivities, including charge, solubility, Lewis acidity, magnetism, the rates of ligand exchange, strengths of metal-ligand bonds, metal- and ligand-based redox potentials, ligand conformations, and outer-sphere interactions.[45] In addition, the ligands can be modified to contribute to biological activity as part of the intact complex or upon ligand dissociation.[46] Photophysical properties can also be manipulated in this way, and together these design aspects explain the attraction of metal complexes for photobiological applications.

2.2. Transition metal complexes as photoactive anticancer agents

It has been stated that hypoxia might well be the most validated target in cancer therapy,[47] underscoring a fundamental limitation of PDT with its exclusive reliance on molecular oxygen and ROS production for initiating phototoxic effects. When considering some of the molecular challenges to PDT — hypoxia and tissue-penetration — it is logical to look to the photophysics and photochemistry of transition metal complexes for next-generation photosensitizers. For example, researchers developing dye-sensitized solar cells (DSSCs) for

solar energy conversion have long exploited transition metal complexes as photosensitizers for efficient, long-lived charge separation.[48–50] These photophysical properties are also advantageous for photobiological applications. Even the photophysical properties of porphyrins and phthalocyanines have been improved for PDT by inserting transition metals into the macrocyclic structures,[51] but the focus in this review is on non-macrocyclic transition metal complexes for light-triggered anticancer therapy, with or without oxygen as a mediator.

In contrast to the $\pi\pi^*$ excited states that lead to PDT effects in organic photosensitizers, transition metal complexes offer many more excited-state electronic configurations (Scheme 2) that can be exploited in both oxygen-dependent and independent cytotoxic pathways. These configurations can be centered entirely on the metal (metal-centered, MC), within a single ligand (intraligand, IL), or involve both the metal and the ligand(s) in charge transfer states: metal-to-ligand charge transfer (MLCT) or ligand-to-metal charge transfer (LMCT). It is also possible to have a charge transfer excited state within a single ligand (intraligand transfer, ILCT), between two different ligands (ligand-to-ligand charge transfer, LLCT), or between two metal atoms in the case of a multimetallic complex (metal-to-metal charge transfer, MMCT). IL states are sometimes called ligand-centered (LC), and MC states are also called ligand field (LF) states. These excited states are further described by multiplicity, usually singlet or triplet. Triplet states are generally more easily accessed in metal complexes due to enhanced spin-orbit coupling induced by heavy atoms. This is an important consideration for at least two reasons. First, triplet states tend to be longer-lived, permitting the increased probability of a reaction between the sensitizer and a substrate. Second, oxygen-dependent and oxygen-independent phototoxic mechanisms originate from triplet states.

The large quantum yields for triplet state formation and the characteristic reactivities of the different excited-state configurations offer the opportunity to rationally design transition metal complexes with desirable photobiological mechanisms that are simply not possible with organic photosensitizers. The most studied transition metal complexes for this purpose are based on Pt(IV), Ru(II), and Rh(III),[52–59] followed more recently by Ir(III),[60,61] and finally Os(II).[62] The mode of light-controlled cytotoxicity generally falls into one of the following categories: (1) photosensitization reactions that involve ROS (PDT), (2) photosensitization reactions that do not involve ROS, (3) photothermal processes (photothermal therapy, PTT), and (4) photodissociation reactions involving the metal or photocleavage reactions on the ligand. Pathways 1–3 have the potential to be photocatalytic, requiring much lower photosensitizer dosing, while 4 is stoichiometric and requires higher doses for similar phototherapeutic effects and special storage conditions to prevent photochemical decomposition. These excited-state reaction pathways are not necessarily mutually exclusive for any given metal complex, and there is the possibility to favor one over another via the irradiation wavelength.[52]

Many terms have been used to describe the light-triggered anticancer activity of transition metal complexes via these various excited states and categories. These descriptions arose from the need to distinguish oxygen-independent cytotoxic mechanisms (that could remain effective in hypoxia) from the ROS pathways, namely $^1O_2$, that define PDT:

photochemotherapy (PCT), phototherapy, photoactivated cancer therapy (PACT), photoactivatable cancer therapy, photoactivated chemotherapy, and oxygen-independent PDT (which is semantically incorrect). For photosensitizers that invoke both PDT and oxygen-independent pathways, Turro and coworkers introduced the term dual action.[57,63,64] Still, the initial 1974 definition of photochemotherapy is broad and refers to any phototherapy mediated by a drug, which includes PDT.[2] The 2009 definition of photoactivated chemotherapy specifically refers to the use of a transition metal complex rather than an organic photosensitizer, and also includes PDT.[56] In this paper, we will use the term PDT to refer to the ROS pathways only, and PCT for oxygen-independent or dual-action pathways.

2.3. Selected examples of Ru(II)-based transition metal complexes for photobiological applications

Transition metal complexes derived from Ru(II) are among the most extensively studied systems for their photochemical, photophysical, and, more recently, photobiological properties. Much is known about the excited-state properties of the archetype polypyridyl complex $[Ru(bpy)_3]^{2+}$ and its related derivatives.[65–67] Ru(II) systems have been at the forefront of light-driven applications involving catalysis,[68] solar energy conversion,[48–50,69] luminescent sensing,[70] molecular switching,[71] and now anticancer therapies.[55,56] The longstanding interest in Ru(II) and its many complexes (both coordination and organometallic) stems from their kinetic stability combined with rich photophysical and electrochemical properties that are easily tunable from modular building blocks via straightforward synthetic routes.

The ligands in a Ru(II) complex can be designed to yield a wide variety of excited states that are accessible with visible light, each with distinct excited-state deactivation pathways, as described in §2.2. As for Ru(II) complexes and PDT, a simple literature search from the past ten years yields over 5,000 hits with Google Scholar and over 400 by SciFinder (Table 5). The field is too large to cover in a single review, but a few recent accounts have covered a lot of ground.[53–56,72–75] For this review, we have focused on a few examples to demonstrate the structural features that control the nature of the lowest-energy triplet excited states in Ru(II) complexes (see Chart 1 and the corresponding jablonski diagrams in Scheme 3). We also limit the discussion to the family of tris-bidentate diimine chelates of Ru(II), of which our own TLD1433 is a member, and the aspects of designing these complexes.

The representative examples below are based on the parent tris-homoleptic compound $[Ru(bpy)_3]^{2+}$, probably the most well-studied Ru(II) polypyridyl complex.[66] The photophysical and photochemical properties of derived systems are often contextualized relative to this parent compound. When photoexcited with visible light (~420 nm), the initially populated ^{1}MLCT state quickly relaxes to the lowest-energy ^{3}MLCT excited state (~2.1 eV) with almost unity efficiency. The lifetime of this ^{3}MLCT state is approximately 200 ns in aerated MeCN,[76] 1 μs in deoxygenated MeCN,[66] and 5 μs in 4:1 EtOH:MeOH glass at 77 K.[66] Quantum yields for emission (Φ_{em}) in deoxygenated MeCN and $^1O_2$ formation (Φ_Δ) in aerated MeCN at 298 K are 10%[77] and 56%,[78] respectively. The dissociative ^{3}MC state lies about 0.5 eV above the emitting ^{3}MLCT state,[79–81] making

$[Ru(bpy)_3]^{2+}$ photostable. The long triplet state lifetime, bright red luminescence, and efficient $^1O_2$ production from $[Ru(bpy)_3]^{2+}$ along with its well-characterized photophysics have created much interest in tuning these properties in other Ru(II) polypyridyl complexes for a variety of applications, including PDT and PCT.

$[Ru(bpy)_2(dppz)]^{2+}$ (where bpy=2,2′-bipyridine, dppz= dipyrido[3,2-*a*:2′,3′-*c*]phenazine) was first reported by Barton in 1990, followed by $[Ru(phen)_2(dppz)]^{2+}$ (where phen=1,10′-phenanthroline) in 1992.[71,82] Much like the parent $[Ru(bpy)_3]^{2+}$, the lowest-energy triplet excited state for the dppz complexes is ^{3}MLCT, but its luminescence is quenched in protic solvents. The environmental sensitivity of the ^{3}MLCT luminescence from $[Ru(bpy)_2(dppz)]^{2+}$ and $[Ru(phen)_2(dppz)]^{2+}$ are attributed to two distinct ^{3}MLCT configurations: a luminescent $^3MLCT^{prox}$ state and a dark $^3MLCT^{dis}$ state of lower energy.[83–87] Changes in the relative energies of these two states and their equilibrium with environment gives these Ru(II) dppz complexes the unique property of acting as molecular light switches for DNA, as the metal complex luminesces much more efficiently when bound to the nucleic acid. The ROS-generating capacity (albeit low) combined with this its ability to act as a luminescent sensor for DNA is an early example of the theranostic potential of Ru(II) polypyridyl complexes. Gasser and coworkers have further demonstrated this capacity for a number of Ru(II) phenazine-type complexes functionalized on the dppz ligand, highlighting their utility as PDT agents.[54,72,88–90]

A related compound $[Ru(phen)_2(dppn)]^{2+}$ (where dppn=benzo[*i*]dipyrido[3,2-a:2′,3′-c]phenazine), which is more π-extended than $[Ru(phen)_2(dppz)]^{2+}$ by one fused benzene ring, was first reported by Barton in 1992 and did not exhibit the DNA light-switch effect.[82] Complexes containing the dppn ligand were thus largely ignored until the DNA-damaging properties of $[Re(CO)_3(py)(dppn)]^+$ through indirect $^1O_2$ sensitization were reported in 1997 by Yam and coworkers.[91] Because the analogous Re(I) system based on dppz photocleaved DNA through direct guanine oxidation, it appeared that the photoexcited states of dppn metal complexes were different from those of dppz. This fundamental difference was further supported by the observation that $[Ru(phen)_2(dppz)]^{2+}$ displayed intense ^{3}MLCT emission in nonpolar solvents while $[Ru(phen)_2(dppn)]^{2+}$ did not.[82] Following that report, Thomas and coworkers published their investigation of the photophysical differences between dppz and dppn Ru(II) complexes in 2009.[92] They determined a triplet excited state lifetime of −12 μs in deoxygenated water and −62 μs in deoxygenated MeCN for $[Ru(bpy)_2(dppn)]^{2+}$ (versus the 180 ns lifetime of the emissive state of $[Ru(bpy)_2(dppz)]^{2+}$ in deoxygenated MeCN).[92,93] In addition, Φ_Δ for $[Ru(bpy)_2(dppn)]^{2+}$ in aerated MeCN was 83%, which is much larger than the 56% measured for $[Ru(bpy)_3]^{2+}$ in MeCN[78] or 53% for $[Ru(bpy)_2(dppz)]^{2+}$ in MeCN (16% in MeOH)[94]. The large value of Φ_Δ for $[Ru(bpy)_2(dppn)]^{2+}$ and its prolonged excited-state lifetime are consistent with the lowest-energy excited state being ^{3}IL and centered on dppn (Scheme 3), and this intra-dppn ππ* assignment was further supported by density functional theory (DFT) calculations.[92] The dppn ligand is more π-extended than dppz, placing the dppn-localized ππ* state lower in energy than the ^{3}MLCT state and thus accessible as a deactivation pathway. They speculated that the high photostabilities of Ru(II) dppn complexes combined with their efficient $^1O_2$ generation and large DNA-binding affinities might make such complexes useful as sensitizers for PDT.

Turro and coworkers reported the first experimental evidence for efficient DNA photocleavage by $[Ru(bpy)_2(dppn)]^{2+}$ in 2010.[94] This report followed previous work with the related bis-tridentate (3-(pyrid-2′-yl)-4,5,9,16-tetraaza-dibenzo[*a,c*]naphthacene) (pydppn) Ru(II) system, which also displayed a lowest-energy ^{3}IL state with extended lifetime of ~20 μs in deoxygenated MeCN and Φ_Δ of 92% in MeOH.[95,96] The [Ru(tpy)(pydppn)]$^{2+}$ (tpy [2,2′;6′,2′′]-terpyridine) complex photocleaved DNA and also facilitated the formation of DNA-protein and protein-protein cross-links in cells. The excited-state lifetime measured for $[Ru(bpy)_2(dppn)]^{2+}$ in MeCN by Turro's group was 33 μs with Φ_Δ=88% in MeOH. These lifetimes and $^1O_2$ yields were similar to those reported for [Ru(tpy)(pydppn)]$^{2+}$, in fact Φ_Δ was greater for the tridentate complex, yet $[Ru(bpy)_2(dppn)]^{2+}$ photocleaved DNA more efficiently and was able to act in the presence of ROS scavengers. They hypothesized that the ^{3}IL state was responsible for DNA damage indirectly via $^1O_2$ generation and that the ^{3}MLCT state might be capable of direct oxidation of guanine (G) nucleobases in DNA, leading to the more potent DNA damaging effects observed for the tris-bidentate complex. An excited-state reduction potential, E_{red}*, of approximately 1.64 V (vs. NHE) was calculated for $[Ru(bpy)_2(dppn)]^{2+}$ from E_{OO} estimated at 2.1 eV and $E_{1/2}([Ru]^{2+/+}]) = -0.46$ V (vs. NHE). Assuming an oxidation potential of G (vs. NHE) in water at pH 7 of +1.29 V (vs. NHE),[97] the driving force for G oxidation by excited $[Ru(bpy)_2(dppn)]^{2+}$ would be favorable (−0.35 V). DNA photocleavage through G oxidation has been reported for other complexes with favorable driving forces.[98–103] While no in vitro data was included to support photocytotoxicity in hypoxia, this example of dual reactivity with DNA (via a highly reactive, oxidizing ^{3}MLCT state and a long-lived $^1O_2$-generating ^{3}IL state) underscored the utility of **π**-extended Ru(II) complexes as dual-action PCT agents.

In 2014 we published the in vitro photocytotoxicity data for $[Ru(bpy)_2(dppn)]^{2+}$,[104] which was consistent with the potent DNA-damaging properties observed earlier in cell-free conditions by Turro and coworkers. We also showed that 625nm red light produced effective photoxicity in vitro, despite the molar extinction coefficient being below 100 M^{-1} cm^{-1}. Importantly, the red phototoxic effect and extremely high potency with shorter wavelengths of light were completely abrogated for $[Ru(bpy)_2(dppz)]^{2+}$, the related compound truncated by one fused benzene ring and lacking the lowest-lying ^{3}IL state and prolonged lifetime. While we did not carry out in vitro assays in hypoxia to confirm the dual-mode activity reported for the DNA experiments, our observation that spin-forbidden ^{3}IL states could be populated effectively with red light to yield photocytotoxic effects was a game changer for us. It meant that certain **π**-extended Ru(II) complexes, previously thought to be non-ideal PDT agents due to a lack of absorption in the PDT window, were now viable candidates. Multiwavelength PDT (or PCT) was now possible, via low-lying ^{3}IL states. Upon a close examination of the literature, we learned that Sadler and coworkers had reported similar anomalies, whereby DNA photoadduct formation could be induced with red light (647 nm) by Pt(IV) complexes with very low absorbance at this wavelength (<10 M^{-1} cm^{-1}).[105]

The prolonged lifetimes associated with lowest-energy ^{3}IL states, discussed above for contiguously-fused phenazine-type ligands, were actually first reported for metal-organic dyads in a 1992 study by Ford and Rogers,[106] whereby an organic chromophore was spatially isolated from the coordinating diimine ligand by a linker. In their 2005 review,

McClena-ghan and Campagna discuss a variety of these systems and the excited state dynamics that give rise to prolonged lifetimes from either pure ^{3}IL states or equilibrated ^{3}IL-^{3}MLCT states. In 1999, Ziessel and Harriman showed that the intrinsic lifetime for the ^{3}IL-^{3}MLCT equilibrated excited state of $[Ru(bpy)_2(5\text{-PEB})]^{2+}$ (5-PEB=5-(pyren-1-yl)ethynyl-2,2′-bipyridine) (Chart 1) was 42 μs at room temperature.[107,108] Later Castellano and Ziessel demonstrated that both $[Ru(5\text{-PEB})_2(bpy)]^{2+}$ and $[Ru(5\text{-PEB})_3]^{2+}$ yield pure ^{3}IL states that do not equilibrate, with lifetimes slightly longer than 50 μs in deoxygenated MeCN.[109–111]. Extending triplet lifetimes with ^{3}IL states, as illustrated by these examples, was desired for applications ranging from hydrogen production using solar energy to oxygen sensing, and it was also useful for chromophores in multicomponent chromophore-spacer-quencher supramolecular systems for more efficient electron- or energy-transfer over longer distances. In these reports, no emphasis was placed on these metal-organic dyads for photobiological applications. However, the properties that lend well to these applications, particularly oxygen sensing, are also desirable for PDT.

Thus, we became interested in Ru(II) dyads for PDT as we reasoned that the exceptionally long ^{3}IL lifetimes would make these systems extremely sensitive to excited-state quenchers (including O_2), and that pure ^{3}IL states would be accessible with red light as observed for $[Ru(bpy)_2(dppn)]^{2+}$. With coworker Thummel, we first demonstrated these principles for $[Ru(bpy)_2(5\text{-PEP})]^{2+}$ (5-PEP=5-pyren-1-ylethynyl-1,10-phenanthroline) (Figure 4) and the related 3-PEP and 4-PEP complexes in 2013.[112] Our Ru(II) dyads differ from the earlier dyad published by Ziessel and Harriman in that the (pyren-1-yl)ethynyl group was appended to phen instead of bpy, and the substitution position oriented the organic chromophore farther away from the metal but more aligned with the Ru-N coordination axis.[112,113] This change produced a pure ^{3}IL state in a Ru(II) dyad containing only one π-extended organic chromophore, whereas earlier examples required at least two organic triplets.[110,111] The pure ^{3}IL lifetimes of our 5-PEP systems reached 240 μs in deoxygenated MeCN and 3.4 ms in 4:1 EtOH:MeOH glass. These lifetimes were the longest reported for this state, and induced very potent in vitro phototoxic effects for this class of metal-organic dyads.[112] The responses could be magnified further in the presence of the protein transferrin (Tf) to achieve PIs greater than 10^4 (Figure 4b). Importantly, treatment with certain PDT regimens mediated by Ru(II) dyads such as $[Ru(bpy)_2(5\text{-PEP})]Cl_2$ was found to stimulate the hallmarks of immunogenic cell death (ICD) that are critical for antitumor immunity.[114]

The observed correlation between prolonged triplet excited state lifetimes and potent phototoxic effects from Ru(II) complexes with both contiguously-fused and tethered π-extended ligands indicates that lowest-lying ^{3}IL states may represent a general strategy for invoking potent photocytotoxic effects. These highly photosensitizing excited states may produce $^1O_2$ even at very low oxygen tension due to their long intrinsic lifetimes, making them excellent PDT agents according to the traditional definition. Depending on their excited state reduction potentials, they may also oxidize biological substrates to produce photodamage in the presence or absence of oxygen, making them dual-action PCT agents.

In 2002, oxygen-independent photoreactivity toward DNA was also demonstrated in trimetallic constructs of Ru(II) or Os(II) and Rh(III). The use of ^{3}MMCT excited states for oxygen-independent DNA photocleavage was pioneered by Brewer, who also showed in

vitro photobiological activity for these triads (albeit under normoxic conditions).[115–117] The lowest-energy ^{3}MMCT excited state was achieved by a symmetrical arrangement of two Ru(II) or Os(II) donor centers separated by a central Rh(III) acceptor bridged by 2,3-bis(2-pyridyl)pyrazine (dpp) ligands (Chart 1). The premise was that ^{3}MLCT states involving the terminal Ru(II) metals could undergo intramolecular electron transfer to the central Rh(III) to generate the lower-energy ^{3}MMCT state which was capable of photocleaving DNA with visible light in the absence of oxygen. This assertion was corroborated by testing the analogous system with 2,2′-bipyrimidine (bpm) as the bridging ligand (the bpm π^* acceptor orbital is lower in energy than the Rh do* acceptor orbital) or Ir(III) as the central metal (the Ir do* acceptor orbital is higher in energy than the dpp π^* acceptor orbital). In both cases the ^{3}MLCT state is the lowest-energy excited state and DNA photocleavage does not occur in the presence or absence of oxygen. While the mechanism for oxygen-independent DNA photocleavage was not definitively established for $[\{(bpy)_2Ru(dpp)\}_2RhCl_2]^{5+}$, it is known that photoexcitation of Ru(II) polypyridyl complexes can directly oxidize DNA in the presence of appropriate electron acceptors[118] and that Rh(III) complexes intercalated into DNA can serve as electron acceptors for excited Ru(II) chromophores via long-range electron transfer.[119] Therefore, it seems plausible that intramolecular electron transfer between Ru(II) and Rh(III) in the mixed-metal triad could result in a similar mechanism for oxidative DNA damage by the photooxidized Ru(III) center.

Similar intramolecular electron transfer can be accomplished in monometallic Ru(II) complexes with ligands that are capable of reductively quenching ^{3}MLCT excited states. In 2011, MacDonnell and Wolf showed that ^{3}ILCT states could be formed in Ru(II) complexes containing bithienyl groups appended to phen ligands by carboxamide linkages as demonstrated by the complexes $[Ru(phen)_2(PC\text{-}2T)]^{2+}$ (where PC-2T=N-(1,10-phenanthrolin-5-yl)-2,2′-bithiophene-5-carboxamide) (Chart 1) and $[Ru(PC\text{-}2T)_3]^{2+}$. The role of the bithienyl substituent is to reductively quench the Ru(III) initially formed upon photoexcitation to yield the ^{3}ILCT state, consisting of a charge-separated bithienyl radical cation and an anion localized on phen or delocalized onto the amide.[120] The intrinsic triplet lifetimes were ~3–6 μs, which are very long for a charge-separated state. It was hypothesized that recombination to reform the ^{3}MLCT state or back electron transfer to reform the ground state were energetically uphill, providing a unique opportunity to establish long-lived ^{3}ILCT states fueled by the ^{3}IL state as a triplet reservoir. These systems were of interest for energy-harvesting applications requiring vectorial charge-separation for follow-on reactions, but we had been simultaneously investigating these types of systems, namely, Ru(II) dyads with α-oligothienyl groups (including TLD1433), for photobiological activity. We viewed them as a novel platform for oxygen-independent photooxidation reactions that could translate to in vitro phototoxicity in hypoxia.

These examples involve potentially catalytic photosensitization and electron-transfer pathways. However, a very robust means of instilling oxygen-independent photoreactivity in Ru(II) polypyridyl complexes is through population of ^{3}MC excited states that lead to photoinduced ligand loss of weakly coordinated ligands.[58,74,75] Introducing steric strain in the coordination sphere with bulky ligands lowers the energy of dissociative ^{3}MC states, making them accessible from the initially-populated ^{3}MLCT state. In 2012, Glazer and coworkers showed that strained $[Ru(bpy)_2(LL)]^{2+}$ (LL=6,6′-dimethyl-2,2′-bipyridine (6,6′-

dmb) or 2,2′-biquinoline (biq)) complexes photoeject 6,6′-dmb or biq, respectively, upon exposure to visible light, and subsequently form covalent adducts with DNA.[121,122] These photocisplatin agents were phototoxic in vitro, and this activity (although attenuated) extended to hypoxic tumor spheroids. While this approach is advantageous for conditions of severe hypoxia/anoxia, the process is stoichiometric and the compounds are not stable to ambient light. Most examples have very low $^1O_2$ quantum yields and thus cannot take advantage of oxygen when it is present. However, dual-action photocisplatin agents, such as $[Ru(bpy)(dppn)(CH_3CN)_2]^{2+}$, developed by Turro and Dunbar generate $^1O_2$ in high yield and also undergo photoinduced ligand exchange.[123] PCT agents that simultaneously exploit these two distinct mechanisms represent a strategy for ensuring photobiological activity regardless of oxygen tension.

These examples were selected to highlight the different reactive excited states of Ru(II) polypyridyl complexes, but not to serve as a comprehensive review of photoactive Ru(II) polypyridyl complexes. It is worth noting that there are a number other elegant examples of oxygen-independent light-responsive Ru(II) complexes, where the metal center itself participates in the photochemical reaction through ^{3}MC states (as discussed above) as well as those where the photochemical reaction can take place on a ligand through organic photochemical reactions. Some of these approaches are highlighted in a recent 2O17 review by Szymanski,[53] and elsewhere.[58,75]

2.4. Determining the best Ru(II)-based transition metal complexes for PDT/PCT

If one focuses exclusively on the photosensitizer, and ignores the multi-dimensional nature of PDT/PCT (e.g., the regimen, and the intended clinical application), how can one quantitatively compare all of the different light-responsive agents in the literature to establish structure-activity relationships (SARs) for photoactive Ru(II) compounds? That is, what combination of chemical, photophysical, and biological properties are best for PDT/PCT? In many early studies, “activity” was measured as the capacity to photocleave DNA, using supercoiled plasmid DNA as the probe in an agarose gel mobility-shift assay. ROS (or other reactive intermediates) induced single-strand and double-strand breaks, covalent modification, and intercalative binding can all be discerned by distinct DNA topological changes that affect electrophoretic mobility in a characteristic manner. Some of these studies were carried out with DNA as the desired intracellular target, while others simply used DNA as a convenient probe for photodamage on the premise that this photodamage would translate to other biological targets.

There are several problems in using the plasmid DNA assay for assessing PDT/PCT potential. First, some compounds that are excellent in vitro PDT/PCT agents interfere with the intercalating stain used to image the DNA bands on the gel; the result is nothing visible on the gel. Second, some Ru(II) compounds that are excellent DNA photocleavers in the gel assay give no phototoxicity in the cellular assay. Third, some Ru(II) compounds that give no photocleavage in the DNA experiment produce good phototoxicity in the cellular assay. And finally, the DNA photocleavage profiles still cannot be compared with other published DNA photocleavage data because no two labs appear to run the assay the same way or deliver the same light dose from the same light source. Moreover, most published experimental details

do not even describe the light wavelength/spectral output, the fluence, or the irradiance used for the experiment. These are key factors for triggering the PDT/PCT response, but their significance is often overlooked; reproducing another lab's results is often impossible.

The problems with relying on DNA photocleavage in normoxia, as above, are compounded when investigating hypoxic response. Much of the oxygen-independent excited state reactivity discussed in §2.3 was inferred from DNA photocleavage assays that either incorporated various ROS scavengers or were degassed. Degassing microliter volumes (according to experimental details, inert atmosphere boxes were not used) is not simple, and the process invariably changes the concentrations of DNA and photosensitizer. The addition of ROS scavengers produces inconsistent results. For example, one could use three different $^1O_2$ scavengers (or three different concentrations of the same scavenger) and likely get three different results.

The trend lately is to test new photosensitizers for PDT/PCT with in vitro phenotypic screening. However, the number of variables in cellular assays is even greater than in the cell-free DNA photocleavage assay. For this reason, it is mostly meaningless to make quantitative comparisons of literature compounds that were not tested under identical conditions. Yet, photocytotoxicity is frequently cited in terms of absolute numbers that refer to effective photosensitizer concentration (EC_{50}, LD_{50}, IC_{50}, etc.), with no information regarding the light dose. In addition, most laboratories do not perform cellular assays in hypoxia, probably due to lack of access to the appropriate equipment. Some do employ 3D tumor spheroids that have regions of hypoxia, but these multicellular spheroid assays suffer from the same experimental variability across laboratories. A notable improvement to photosensitizer discovery for PDT/PCT would be a standardized cytotoxicity/photocytotoxicity assay in normoxia and a move toward doing the same for various levels of hypoxia.

In our laboratory, we set out to use a standardized in vitro assay to screen as many transition metal complexes as possible: our own, those of collaborators, and others published in the literature. There were two reasons: (1) to generate a SAR database for PDT/PCT effects in transition metal complexes, and (2) to understand which photosensitizers really are the most potent. Our longer-term goal was to develop a clinical PDT/PCT agent by making strategic partnerships when the best photosensitizers were identified. We cannot overemphasize the importance of establishing a standardized phenotypic screen as this is critical to selecting the top-performing photosensitizers in normoxia and hypoxia. The next section provides more details about the screen we use to compare our own photosensitizers and those of other researchers in longitudinal studies.

3. PHENOTYPIC SCREEENING: THE IMPORTANCE OF THE STANDARDIZED IN VITRO ASSAY

Prior to 2010, we spent a lot of time developing an in-house standardized in vitro PDT/PCT assay to be used for screening our compounds and those from other laboratories, as well as published compounds for which there was no cellular data, to try to establish SARs for metal complexes as traditional chemotherapeutic agents and as photosensitizers for PDT/

PCT. SAR studies are standard in the field of medicinal chemistry, which usually investigates organic compounds as therapeutics. There was a clear need for the same type of knowledge database for inorganic compounds, underscored by the fact that it is much more difficult to get metal complexes accepted for the NCI-60 Human Tumor Cell Lines Screen as part of the NIH/NCI Development Therapeutics Program (DTP). In addition, an NIH/NCI-supported standard screen for photocytotoxicity simply does not exist at this time. With a standardized cytotoxicity-photocytotoxicity assay, we would be able to sort through the thousands of published metal complexes, as well as new ones, and set filter rules for the most promising PDT/PCT leads.

It is somewhat difficult for a chemist to appreciate the complexity, inconsistency, and unpredictability of biological samples. There is a tendency to record a single EC_{50} (also referred to as IC_{50}, although more accurately IC refers to inhibition not lethality) value from an in vitro dose-response assay, and publish it as an absolute parameter that describes the anticancer activity of the given compound. But really this parameter is meaningless without the context of the experiment (the assay conditions) and a reference compound screened the exact same way. The challenge in accurately assessing the anticancer potential of new and existing compounds grows exponentially with PDT/PCT, since there are many more variables to consider: compound, light wavelength and intensity, oxygen, photosensitizer-to-light interval, and regimen, to name a few.

The premise behind the PDT/PCT assay is that two dose-response assays are run in parallel in two separate microtiter plates, with one plate kept in the dark (to obtain the dark EC_{50}, which is a measure of cytotoxicity of the compound as a traditional chemotherapeutic) and the other plate exposed to a light treatment (to obtain the light EC_{50}, which is a measure of the photocytotoxicity of the compound as a PDT/PCT agent). Each plate contains at least triplicate data points for each concentration and the appropriate control wells of cells that were not treated with compound. The phototherapeutic index (PI) is obtained as the ratio of the dark EC_{50} to the light EC_{50}, and is a measure of the PDT/PCT effect. As of 2012, PIs of 200 were among the largest reported, and since that time, we have achieved PIs > 10^5 (§4.2) and have published many examples beyond 1000. Our most potent light EC_{50} values are sub-picomolar (§4.2) and our best published values are low nanomolar. But as stated earlier, these descriptors mean little without knowing the light dose applied and other assay conditions. The light dose and oxygen concentration should be considered as drug components, and are therefore at least as important as the identity of the photosensitizer.

There are many less obvious variables must be carefully controlled in designing a standard in vitro PDT/PCT assay. Parameters that we have found to cause inconsistencies in cell assay results include, but are not limited to: (1) identity of cell line (tissue type, morphology, and other properties), (2) cell growth properties (suspension versus adherent), (3) cell passage number, (4) cell viability, (5) cell seeding density, (6) cell culture growth medium, (7) cell culture growth medium suppliers, (8) photosensitizer vehicle, (9) microplates (TC-treated versus non-treated), (10) cell counting method, (11) cell viability dye and method used, and (12) microplate reader and reading mode (absorption, fluorescence, luminescence and top-read versus bottom-read). Incubation times also present variables that can fundamentally alter experimental outcomes: (1) time interval between cell seeding and

compound delivery, (2) time interval between compound delivery and addition of a cell viability dye, and (3) time interval between the addition of the cell viability dye and reading the plate. Finally, the storage condition of the compound (identity of the vehicle and temperature) can affect assay results, particularly if the compound is somewhat hydrophobic and tends to aggregate (or adhere to glass or polypropylene tubes) when stored as a stock solution.

For the PDT/PCT plate, the time interval between compound delivery and irradiation as well as the interval between irradiation and the addition of the cell viability dye are important. No high-throughput cell viability dye is without limitations, regardless of the read mode (i.e., absorption vs. emission). In fact, performing the exact same experiment with the same dye in two different modes can give different results. This problem is exacerbated in the case of PDT/PCT because the photosensitizers are designed to be highly absorbing (and often luminescent) in the same wavelength region as the cell viability indicator. At high concentration, the photosensitizer itself interferes with the cell viability reading at low cell counts for both suspension (Figure 5) and adherent (Figure 6) cells. Of the hundreds of papers in the literature, there are no figures showing this raw data and no comments about this pervasive problem (we have been guilty of this too). Our solution is to manually count cells at the concentrations where interference occurs to confirm that the cell count is zero; clearly, this only works for a very potent photosensitizer where cell kill is 100% at those interfering concentrations.

Notwithstanding the difficulties, in vitro assays are crucial for assessing compound potential and building SAR libraries. They necessitate standard conditions that are robust and invariant. Even the personnel who maintain the cell lines and perform the assays should be recognized as variables. Wherever practical, all the variables (including the people) should not be altered. The standard assay (Schemes 4 and 5) that we iteratively developed over the years is performed in two cancer cell lines (SKMEL28 melanoma as an adherent cell line and HL60 as a suspension cell line) and one noncancerous cell line (CCD-1064SIC normal skin fibroblasts). Assays are performed under normoxia (20% CK, 5% CO_2), typically on cells between passage 5 and 10. Briefly, the assays are performed on 100 μL volumes with cells added in 50 μL aliquots to 25 ʾL of warm culture medium (37 °C) already present in the wells. The cells are left to incubate in the wells for 3 h at 37 °C, and then 25 μL of phosphate-buffered saline (PBS) (control) or serially diluted photosensitizers made in PBS (37 °C) are added to bring the cells to the same density used in the NCI-60 Human Tumor Cell Lines Screen (different densities are used for different cell lines). The photosensitizers are prepared as 5-mM stock solutions in water containing 10% DMSO (v/v), with DMSO added first. The 5-mM stock solution of each photosensitizer is serially diluted using phosphate-buffered saline (PBS) to obtain nine concentrations (1.2 mM to 4 nM) such that 25 μL aliquots of these dilutions yield final concentrations of 1 nM to 300 μM in the 100-μL assay volumes. The 5-mM stock is stored at −20 °C and used for multiple assays.

After the 16 h incubation period at 37 °C/5% CO_2, the microplates are removed and either kept in the dark under ambient conditions or exposed to a light treatment for approximately 1 h. Note that we do not replace the cell culture medium before illumination, and we do not use phenol red-free medium; some laboratories do. The microplates are further incubated at

37 °C/5% CCh for 48 h and then treated with 10 μL of 0.6 mM resazurin (sold commercially as alamarBlue™ Cell Viability Reagent) prepared according to a patented procedure to allow for short development times.[124] Two to three hours later (when control wells read ≥10,000 counts) the plates are read in emission mode using λ_{ex}=530 nm and λ_{m}=620 nm. Cell viability is reported as a percentage relative to control wells on the dark plate containing cells only. Any loss in cell viability due to the light treatment alone is evident when comparing the control cells on the dark plate with those on the light plate. EC_{50} values are calculated from sigmoidal fits of the dose-response curves for dark (cytotoxicity) and light (photocytotoxicity) treatments using Graph Pad Prism 6.0 according to Equation 1, where y_i and y_f are the initial and final fluorescence signal intensities. EC_{50} values determined in this way are generally reproducible to within ±25% in the submicromolar regime; ± 10% below 10 μM; and ±5% above 10 μM. PIs are calculated from the ratio of dark to light EC_{50} values obtained from the dose-response curves for a particular cancer cell line. Selectivity factors (SFs), a measure of the selective cytotoxicity of the compounds toward cancer cells over normal cells, are calculated from the ratio of the dark EC_{50} values for SKMEL28 melanoma cells and CCD-1064SIC human skin fibroblasts. Enhanced SF values are most important when considering the photosensitizer as a chemotherapeutic but can also be advantageous for PDT/PCT if the selectivity indicates preferential uptake by cancer cells.

$$y = y_i + \frac{y_i - y_f}{1 + 10^{\left(\log \mathrm{EC}_{50} - \mathrm{x}\right) \times (\mathrm{Hillslope})}} \quad (1)$$

We carry out our standard assay using two different light treatments: visible light (400–700 nm, 34.7 mW cm^{-2}) using a 190 W BenQ MS 510 overhead projector or red light (625 nm, 27.8 mW cm^{-2}) from an LED array (PhotoDynamic Inc., Halifax, NS). Irradiation times using these two light sources are approximately 48 and 60 min, respectively, to yield total light doses of 100 J cm^{-2}. We periodically confirm that the spectral output from the two light sources is consistent using an Ocean Optics USB4000 spectrometer interfaced with a portable fiber optic spectrophotoradiometric detector. The compound $[Ru(bpy)_2(dppn)]CL$ is used as a reference to validate the assay over time (Figure 7). The variability of the light component of PDT/PCT is one reason why it is impossible to carry out quantitative comparisons of photosensitizers from different laboratories in the literature. Moreover, the light fluences and irradiances are often not included in reports of new photosensitizer activity, and some articles even omit the light source used.

To make a robust comparison between a new compound and one from the literature, it is always best to screen them side-by-side using identical assay conditions. In 2010, Plaetzer and coworkers published the first comparative in vitro study of different photosensitizers employed in PDT under identical conditions,[125] and later published a tutorial on the in vitro characterization of new photosensitizers for PDT/PCT and PDI that highlights many of the factors that can affect assay results and should be a standard resource for researchers in the field.[126]

The inclusion of a detailed standard assay procedure may be somewhat out of character for a review article. We feel that this is an important issue that deserves attention, particularly in the context of a review, because of the pitfalls of comparing PDT/PCT activity as explained earlier. We also hope that this description will help to anchor a common starting point for new researchers in the field and to raise awareness of a common problem.

The in vitro assay should not be construed as a predictor of in vivo performance as a PDT/PCT agent. Rather, it serves only as a go/no-go decision in identifying photosensitizers to move forward through biological assays and models of increasing complexity, many of which will fail when scrutinized in more biologically relevant models. The assay also serves as the foundation of our metal complex SAR database, and we continue to screen as many compounds as we can from our own libraries and those of others. Once a hit (nanomolar light EC_{50} with PI>1,000) is identified in the standard assay, the photosensitizer and light protocol can be further optimized for a particular translational outcome. With a target clinical indication in mind, we (in collaboration with our industrial partner Theralase Technologies, Inc. (TLT)) have used the filter shown in Figure 8 to develop TLD1433 for treating NMIBC with PDT.

4. THE SHORT STORY OF TLD1433

4.1. Design aspects from basic principles

TLD1433 is the chloride salt of a racemic (ΔΛ) monometallic Ru(II) dyad derived from an ionizable imidazo[4,5-*f*][1,10] phenanthroline (IP) ligand appended to an α-terthienyl (3T) as the organic chromophore and two 4,4′-dimethyl-2,2′-bipyridine (4,4′-dmb) coligands (Chart 2). To our knowledge, TLD1433 is the first Ru(II)-based photosensitizer to advance to human clinical trials (ClinicalTrials.gov Identifier: NCT03053635). For this reason, we will present the short history of its development and current standing in the hope that it may be of interest to other researchers investigating transition metal complexes for photobiological applications. The structural features that define TLD1433 were ultimately selected based on the desired in vitro and in vivo performance of the compound as well as considerations related to patentability, cost, and clinical indication. However, certain design aspects were driven from first principles rooted in Ru(II) polypyridyl photophysics based on some of the important examples discussed in §2.3. The choices for the molecular components of TLD1433 are discussed individually below, and the selection of TLD1433 over other photosensitizers is discussed separately in §4.2.1.

4.1.1. Ru(II) as the central metal ion.—Ru(II) was chosen as the metal center because of (1) the extensive literature available on how to manipulate excited state energies via structural modification, (2) the rich photophysical and photochemical properties known for some of its polypyridyl complexes, and (3) the availability of well-established synthetic procedures for preparing coordination and organometallic complexes from this metal ion. We reasoned that a potent and versatile Ru(II)-based photosensitizer would be one that could sensitize $^1O_2$with very high efficiency, but also one that could participate in inter- or intramolecular electron-transfer reactions (with or without oxygen).

4.1.2. Lowest-energy ^{3}IL state.—Our approach to designing photosensitizers with very high sensitivities to trace oxygen was to exploit excited states with extremely long intrinsic lifetimes (>>1 μs), namely ^{3}IL states. The increased ππ* character of ^{3}IL states prolongs their intrinsic triplet excited-state lifetimes due to the decreased radiative (k_r) and nonradiative *(k_{nr})* decay rates between states of different multiplicity in organic chromophores with reduced spin-orbit coupling (SOC) constants. Even when equilibrated with ^{3}MLCT states, such states have been shown to be almost íyg× more susceptible to oxygen quenching compared to pure ^{3}MLCT states, with >75% of these^{3}MLCT-^{3}IL states being quenched even in hypoxia (3.5% O_2).[127] This sensitivity would be expected to be even higher for pure, nonemissive ^{3}IL states, and this forms the basis of optical oxygen sensing, where the goal is to make the sensor's luminescence extremely responsive to oxygen. In this case, changes to luminescence intensity (or excited-state lifetime) in the presence of an excited-state quencher is described by the Stern-Volmer relationship: $I_O/I = \tau_0/\tau = 1+k_q\tau_0$ [Q], where $k_q\tau_0$ is the Stern-Volmer constant *(K_SV)* and *$Q=pO_2$*. *K_SV* depends directly on the rate of O_2 diffusion, oxygen solubility, and the intrinsic lifetime of the lumophore.

Given that the excited-state quenching pathway for these lumophores involves $^1O_2$ sensitization as an important deactivation channel, it stands to reason that a straightforward way of maintaining $^1O_2$ production at low oxygen tension for a photosensitizer is to increase its intrinsic excited-state lifetime. We posited that Ru(II) polypyridyl complexes possessing ^{3}IL states with energies <2.1 eV, intrinsic lifetimes >20 μs, and K_SV>O.25 $Torr^{-1}$ would be potent PDT agents with the potential to act in hypoxia. We also recognized that losing some excitons to the less sensitive, but emissive, ^{3}MLCT channel might be advantageous for theranostic applications: potent PDT from ^{3}IL states and diagnostic imaging via luminescence from ^{3}MLCT states. The ^{3}MLCT state is also sensitive to oxygen and can be used to report not only on spatiotemporal localization of the photosensitizer but also on oxygen concentration via luminescence- or lifetime-based measurements, which has been recently demonstrated for TLD1433.[128]

4.1.3. Bis-heteroleptic Ru(II)-orqanic dyad with diimine ligands.—The tris-diimine coordination environment of Ru(II) polypyridyl complexes is optimally suited for installing lowest-energy ^{3}IL states. The triplet state energies in the parent $[Ru(bpy)_3]^{2+}$ follow the order ^{3}IL > ^{3}MC > ^{3}MLCT, and its excited state dynamics (with visible light excitation at room temperature) are thus controlled by the lowest-energy ^{3}MLCT states that lie approximately 2.1 eV above the ground state and 0.5 eV below the dissociative ^{3}MC state.[79–81] We chose to increase π-conjugation on one of the ligands to give ^{3}MC > ^{3}MLCT > ^{3}IL, with ^{3}IL energies <2.1 eV to for lowest-lying *pure* ^{3}IL states with prolonged lifetimes. This can be achieved best by extending π-conjugation along the M-N coordinate (Scheme 6, blue arrow), as exemplified by $[Ru(bpy)_2(dppn)]^{2+}$ (Scheme 6, red ligand). Extension orthogonal to the M-N bond (Scheme 6, green arrows), an alternate way of extending π-conjugation, was not considered as it does not preferentially lower the energy of the ^{3}IL state. Rather, it also lowers the energies of both the ^{3}MLCT and dissociative ^{3}MC states, and the resulting complexes, $[Ru(bpy)_2(biq)]^{2+}$ (biq=2,2′-biquinoline) as an example, undergo photoinduced ligand loss and have much shorter triplet lifetimes (,τ_0<,=0.27 μs).[66]

There are several ways that π-expansion can be introduced into Ru(II) polypyridyl complexes, including the incorporation of: (1) contiguously-fused diimine ligands, (2) diimine ligands with tethered organic chromophores, and (3) diimine ligands with organic chromophores tethered via a linker (Chart 3). We chose arrangement (2) to spatially isolate the tethered organic chromophore from the Ru(II) center to limit its communication with the chelating diimine ligand, thus potentially giving the organic moiety more ππ* character and enabling better charge separation (vide infra). We call this π-extended ligand the functional ligand (or PDT ligand) due to its role in contributing the accessible ^{3}IL state. Triplet excited state lifetimes tend to lengthen with the number of these functional ligands in the complex. For example, the triplet excited state lifetimes for $[Ru(bpy)_2(LL)]^{2+}$, $[Ru(bpy)(LL)_2]^{2+}$, and $[Ru(LL)_3]^{2+}$ (where LL=5-PEB) are 42, 57, and 65 μs, respectively, with ^{3}IL purity increasing in the same order.[107,111] Despite the fact that the tris-homoleptic complex possesses^{3}IL states that are most sensitive to trace oxygen, we chose the bis-heteroleptic $[Ru(bpy)_2(LL)]^{2+}$ scaffold, with only one functional ligand, to maximize aqueous solubility and reduce aggregation.

We chose 4,4′-dmb as the two coligands to be combined with the functional ligand. Small coligands that adopt optimal dihedral and bite angles[129,130] were desirable to enhance the stability of the complex, and methyl-substituted bpy was preferred over unsubstituted bpy to further minimize aggregation effects and enhance aqueous solubility. Finally, IP was selected as the chelating ligand for incorporating the organic chromophore because it is very easy to prepare IP ligands with organic units appended at C2 from the simple Radziszewski condensation of 1,10-phenanthroline-5,6-dione with the appropriate organic aldehyde.[131] In addition, the IP ligand can adopt three different ionization states,[132,133] making it possible to alter the charge on the overall complex with pH changes. We hypothesized that the lower extracellular pH of cancer cells[134] might shift the IP equilibrium toward the cationic form, facilitating a preferential interaction with negatively membrane phospholipids of cancer cells. We also wished to investigate pH effects on the excited state dynamics of Ru(II) complexes with amphoteric groups that could adopt multiple ionization states over the physiological pH range.[135]

4.1.4. Chloride as the counter ion.—The tris-chelates of Ru(II) derived from neutral diimine ligands carry two counter ions to balance the +2 oxidation state of the metal center. These counter ions influence solubility, and they can also affect (photo)biological activity. We chose chloride as the counter ion because (1) it renders the Ru(II) metal complex soluble in aqueous media, and (2) it is biologically compatible.

4·1.5. Racemic mixture.—TLD1433 is produced as a racemic mixture of Δ and Λ isomers to avoid the cost associated with enantiomeric resolution on the quantities required for human clinical studies. The toxicity profile of the racemic mixture is acceptable for local administration to the bladder.

4.1.6. α-Terthienyl as the organic chromophore.—The defining feature of TLD1433 is the α-terthienyl (3T) group that was selected as the organic chromophore and incorporated as the IP-3T functional ligand. There are many possible choices of π-expansive organic chromophores for instilling low-energy, long-lived ^{3}IL states in Ru(II) dyads.[109]

There are two primary reasons why α-oligothiophenes became our organic chromophore of choice. First, we required a means of generating charge-separated ^{3}IL states in a monometallic construct for electron-transfer reactions that could potentially take place in hypoxia. We were inspired by Brewer's use of intramolecular electron transfer to achieve oxygen-independent photooxidizing ^{3}MMCT states in trimetallic Ru-Rh-Rh systems, but sought to reduce the number of metal atoms in the photosensitizer (due to cost and availability) and to lower the molecular weight of the compound. Second, our simple, monometallic Ru(II) complex should be patentable based on composition (i.e., its unique, unreported structure) as well as utility, and Ru(II) dyads constructed from IP appended to α-oligothiophenes had not been reported.

α-Oligothiophenes have been of interest for more than 20 years, especially because of their unique molecular and material characteristics at higher *n*. These highly conjugated oligomers and polymers have utility as nonlinear optical components, for charge storage, and in molecular electronics.[136] Thiophene rings linked through the 2–2′ position exhibit such properties, with a ππ* gap that decreases asymptotically with the number of rings,[137] and close-lying molecular orbitals that coalesce into band-like electronic structures (reminiscent of semiconductors) as the number of rings becomes sufficiently large.[138]

Polythiophene and its derivatives are generally able to donate and accept electrons fairly easily without decomposition.[139] Optical absorption leads to symmetry-allowed excited states and excitons that can be further manipulated into relatively long-lived charge separation in the presence of suitable electron donors or acceptors,[138] illustrating the applicability of such arrangements to solar energy conversion. Triplet states are accessible from intersystem crossing (ISC) of a singlet exciton, with a relatively high exchange energy of around 0.7 eV in conducting polymers in general[140] and 1.75 eV for 3T specifically.[141] It has been shown[142] that the triplet exciton has a "natural" size of *n*=3–4 thiophene rings, but the quantum yield of triplet state formation decreases as the number of rings increases, leveling off at around five rings.[136] Consequently, we were interested in oligothiophenes of smaller *n* for photobiological applications since they are good $^1O_2$ generators[141,143] and can also reductively quench the ^{3}MLCT excited states of Ru(II) polypyridyl complexes.[120]

The triplet states of bithiophene (2T) and longer oligomers up to *n*=11 have been explored. Their intrinsic lifetimes range from a few tens of microseconds (in fluid solution at ambient temperature) to hundreds of microseconds at 77 K. The triplet state energy of 3T was estimated at 1.72 eV,[141] with the energies of the longer oligomers (4T-11T) decreasing as 1/n to 1.57 eV for 11T. These triplet excited states participate in both energy- and electron-transfer processes with appropriate acceptors to form $^1O_2$ and *n*T radical cations ($nT^{+\bullet}$), respectively.[142] To some extent, the relative contribution of each pathway to excited-state decay is controlled by *n* and the environment. We hypothesized that this partitioning could be exploited for type I/II PDT effects as well as electron-transfer reactions that may not require oxygen. We previously described these systems as Type I/II photosensitizers,[144] but here we use the term dual-action PCT (or PDT/PCT) agents to acknowledge that oxygen-independent pathways for photodamage may be operative in hypoxia.

The photocytotoxicity of 3T and several of its natural and synthetic analogs had already been demonstrated, and this activity was attributed to the efficient production of ROS.[141,143,145] In fact, plants of the Asteraceae family are known to produce this class of UV-active phototoxins as secondary metabolites to protect against pathogens.[146] Incorporation of 3T into a Ru(II) dyad construct would allow indirect access to these photosensitizing $^3\pi\pi^*$ states with longer-wavelength visible light, owing to the Ru(II) ^{1}MLCT state acting as an antenna to funnel excitation energy to the ^{3}IL state centered on 3T (Scheme 7). It might also provide direct access to ^{3}IL states via a one-photon, spin-forbidden $S_0 \rightarrow T_n$ transition, owing to increased SOC afforded by the heavy Ru(II) center. The triplet state energy of the free 3T at 1.72 eV (approximately 725 nm) conveniently falls in the so-called optimal PDT window, where light penetrates tissue most effectively. In addition, 3T should have the ability to reductively quench the photoexcited Ru(III) center, forming the intramolecular charge-separated ^{3}ILCT state on 3T, reminiscent of what was observed for $[Ru(PC\text{-}2T)_3]^{2+}$ (Chart 1).

We reasoned that this ^{3}ILCT state could (in theory) participate in intermolecular charge transfer reactions with (1) biological substrates, (2) oxygen, or (3) another Ru(II) dyad in its ground state or triplet state (Equations 2–5). The latter would enable the Ru(II) dyad to act as a *supercatalyst*, creating more than one reactive species per photon absorbed via autoionization and other chain reactions. The importance of these relative pathways would depend on *n* and the presence of electron donors (such as DNA guanines or other reduced dyads). Alberto and coworkers carried out a theoretical exploration of this Type I/II photoreactivity in 2016 for two of our $[Ru(LL)_2(IP\text{-}nT)]^{2+}$ families, where LL=bpy or 4,4′-dmb and *n*=1–4.[147] Their calculations showed that with increasing n, the triplet states become weaker electron donors and thus not able to form superoxide directly in water (Equation 2). However, they confirmed (from calculated vertical electron affinities and ionization potentials) that the triplet states of all the compounds could be reduced through autoionization reactions (Equations 3–4). The reduced Ru(II) dyads could then form superoxide (Equation 5) due to the higher electron affinity of molecular oxygen compared to the reduced photosensitizer. The calculations also showed that superoxide itself could act as a reducing agent for Ru(II) dyads in their triplet states, which might be one mechanism for the potent photocytotoxicities of these compounds. No calculations were performed using biological substrates in the computational report, but we observe experimentally that reducing agents such as glutathione (GSH)[148] greatly enhance the photodamaging properties of TLD1433 and its relatives.[144]

$$PS(T_1) + {}^3O_2 \rightarrow PS^{\bullet +} + O_2^{\bullet -} \quad (2)$$

$$PS(T_1) + PS(S_0) \rightarrow PS^{\bullet +} + PS^{\bullet -} \quad (3)$$

$$PS(T_1) + PS(T_1) \rightarrow PS^{\bullet +} + PS^{\bullet -} \quad (4)$$

$$PS^{\bullet -} + {}^3O_2 \rightarrow PS + O_2^{\bullet -} \quad (5)$$

4.2. Photobiological properties

4.2.1. How was TLD1433 selected?—TLD1433 was selected from a group of Ru(II) dyads that incorporate α-oligothiophenes as part of a small SAR study (Chart 2) that was created based on the guiding design aspects outlined in the previous section. The members of the library were included to test certain hypotheses regarding SARs and to identify the most versatile and potent photosensitizer for further development. For example, a comparison of TLD1433 and TLD1411 demonstrated that the aqueous solubility of the photosensitizer increased substantially with the addition of the methyl substituents to the bpy coligand core. The position of the methyl groups on the bpy rings was crucial as 6,6′-substitution, illustrated in $[Ru(6,6'\text{-dmb})_2(IP\text{-}3T)|Cl_2$, produced a crowded coordination sphere that resulted in stoichiometric ligand loss, albeit oxygen-independent, with visible irradiation.[149] Replacement of the central Ru(II) metal with Os(II) lowered the energy of the MLCT and ^{3}MLCT states and red-shifted the absorption as expected, but also decreased the triplet state lifetime and attenuated the photocytotoxic effect even with red light activation (Figure 9). Finally, a systematic change in the number of thienyl groups in the chain highlighted the importance of n for increasing $^1O_2$ quantum yields, inducing potent in vitro phototoxic effects with visible light, and invoking the “red” PDT effect (i.e., PDT occurs at λ_{ex} where molar extinction coefficients are <100 M^{-1} cm^{-1}) (Figure 10). Some of these comparisons, and others, are discussed in more detail in our 2015 review on the family that includes TLD1433.[144]

All the compounds in Chart 2 are nontoxic in the dark (EC_{50}>100 μM) in our standard in vitro assay. However, their light EC_{50} values and PIs vary considerably. This observation is nicely illustrated by comparing n=1–4 (Figure 10). The data also show that the light component can be manipulated to greatly amplify the phototoxic effects of α-oligothienyl-based Ru(II) dyads. All have molar extinction coefficients that are <100 M^{-1} cm^{-1} at 625 nm, yet as n increases from 1 to 4, the red EC_{50} potencies increase from >100 μM for n=1 to −1.5 μM for n=4, with TLD1433 at 2.3 μM. Computational studies[147] support the notion that the red PDT effects in this series stem from direct population of ^{3}IL states that are of increasingly more ππ* character at n≥2. The photocytotoxicity from direct population of^{3}IL states spans a range of just over 70-fold on going from n=1 to 4, while initial population of ^{1}MLCT states leads to triplet states that are much more sensitive to the number of thienyl rings in the organic chromophore. There is an abrupt change in visible light potency on going from n=2 to 3, and then again from n=3 to 4. The visible EC_{50} values documented for TLD1433 and TLD1633 (Chart 2) are much smaller than any that have been measured previously against any cancer cell line in our standard assay. While the PIs for these two compounds are always orders of magnitude larger than those of other systems, they are also

much more prone to batch-to-batch variability. Moreover, these extremely high potencies that are observed for α-oligothienyl-containing systems suggest that these photosensitizers act through a different mechanism than many other π-expansive Ru(II) dyads. Our current hypothesis is that TLD1433 and TLD1633 act as supercatalysts, producing more than one ROS or other reactive species per photon absorbed per molecule when electron-transfer reactions are involved (Scheme 7, Equations 2–5).

For comparison, we show the (photo)cytotoxicity data for two other families of Ru(II) dyads (Figure 11), but collected on a different cell line. Ru(II) dyads derived from the π-expansive azaaromatic dppn ligand or the pyrenyl 5-PEP ligand, while good photosensitizers with PIs of 670 and 4,300, respectively, always have light EC_{50} values in the 50–500 nM range (never subnanomolar). Other related family members are included to demonstrate that there is a critical degree of reconjugation for potent in vitro PDT effects. The data also highlights that $[Ru(bpy)_2(dppz]CL$, the DNA light switch complex and a less effective $^1O_2$ generator, has no phototoxic effects.

Considering the potency of TLD1633, it may seem odd that TLD1433 was selected instead. TLD1433 was prioritized over the other compound for a number of reasons, including: (1) there were more synthetic steps required for producing TLD1633, and those steps were low yielding (unoptimized at that time) and required expensive catalysts, (2) there was more batch-to-batch variability with TLD1633, (3) the theranostic capacity of TLD1433 was greater (i.e., its luminescence quantum yield was higher), and (4) we were relatively far along in our pre-clinical studies with TLD1433 by the time the synthesis of TLD1633 was optimized to produce the larger batches required for in vivo studies.

4.2.2. What excited-state model accounts for the potency ofTLDi4jj?—Scheme 7 illustrates the excited-state relaxation pathways available to TLD1433 with photoexcitation into the ‘MLCT band. Rapid ISC to form triplet excited states occurs with near-unity efficiency. Population of the emissive ^{3}MLCT state is responsible for the intense luminescence of these compounds when bound to DNA or accumulated in cancer cells or tissue (Figure 12), while population of the much longer-lived α-terthienyl-based ^{3}IL states results in potent photocytotoxicity. From transient absorption studies and the photophysical model reported for $[Ru(bpy)_2(PC\text{-}2T)|^{2+}$,[120] we propose that two IL configurations are possible: a relatively nonpolar ^{3}IL state with increased ππ* character that sensitizes $^1O_2$, and an ^{3}ILCT state that is polarized and poised to participate in electron-transfer reactions with oxygen (or biological substrates) and autoionization reactions that also produce ROS. In this model, it is the ^{3}ILCT state that is responsible for the unusual potency of TLD1433 (and likely TLD1633 as well). The ^{3}MLCT is also capable of producing $^1O_2$, but with far less efficiency relative to the ^{3}IL states.

Concerning the red PDT effect, it is possible that direct absorption to the ^{3}IL state provides a pathway for generating $^1O_2$, but not the electron-transfer reactions that give rise to supercatalytic potency. These chain reactions may originate from the ^{3}ILCT state that can only be accessed via higher-lying MLCT states with sufficient mixing, which would explain why visible light (enriched with the bluer wavelengths) produces exceptional potencies, while red light has an upper limit near 1 μM.

4.2.2. Does TLD1433 act as an oxygen-independent PCT agent in vitro?—

Much remains to be elucidated about TLD1433 and some of its related derivatives of n=3 and higher. While TLD1433 is a very potent photosensitizer in normoxia with almost unity efficiency for $^1O_2$ production at ambient pO_2, its ability to maintain photocytotoxic effects in hypoxia is highly dependent on the type of cell and cell line. In fact, TLD1433 loses all of its PDT effects against the glioma (U87) cancer cell line under hypoxic conditions, but becomes even more active against the microorganisms *S. aureus* (SA) and methicillin-resistant *S. aureus* (MRSA) in hypoxia.[150] Under cell-free conditions, TLD1433 photodamages DNA in the absence of oxygen and in the presence of ROS scavengers,[144] but this oxygen-independent activity does not always translate to photocytotoxicity. We are currently investigating photocytotoxicity in a wide panel of cell lines in normoxia and various levels of hypoxia using the standard assay with 2D monolayers as well as 3D spheroids and patient-derived organoids to better understand the variable oxygen-dependence of this compound under the most relevant conditions.

4.2.3. Where does TLD1433 localize in cancer cells and what is the mechanism of cell death?—

The localization of compounds and photosensitizers in cells depends on many factors: (1) the cancer cell type, (2) whether the cells are growing as 2D monolayers or 3D tumor spheroids, (3) the concentration of the photosensitizer employed, (4) the experimental procedure used to assess localization (e.g., ICP-MS versus LSCM), (5) the time point for assessment, (6) the cell seeding density, (7) the presence of antibiotics in the cell culture medium, and (8) whether the cells have been exposed to light, even ambient light (visible light activates the photosensitizer, which results in photoactivated cellular uptake[151]), among others. Delineating the mechanism for cell death is further complicated by the number of variables associated with the light parameters and dosimetry, and how these aspects change on going to increasingly more sophisticated models. We can appreciate that there is interest in how photosensitizers, including TLD1433, can potentially interact with and inside cells and what cellular pathways are responsible for cell death at the molecular level, as well as subcellular targeting of organelles. However, whatever is observed in simple 2D monolayers, which is not at all representative of real tumors and their complex pathophysiology, most likely does not translate directly to in vivo models. For this reason, we (in collaboration with TLT) have focused much of our effort on understanding the macroscopic interactions between TLD1433 and tumors (both subcutaneous and orthotopic models), which are those that are most relevant for clinical development. Moreover, our attention is also aimed at understanding the PDT regimens that are best for stimulating antitumor immunity in vivo, rather than a single focus on maximizing tumor ablation and its mechanism in vitro.

4.3. Translation and commercialization highlights

4.3.1. Timeline: from bench to clinical trial.—

TLD1433 was synthesized in May 2011, and six years later, it was administered to the first patient in a clinical trial for NMIBC (Figure 13). Compared to hundreds of other photosensitizers previous evaluated in our standard assay, TLD1433 and some of its close relatives were superior. Rather than publish these initial findings, we partnered with TLT to develop this class of compounds for clinical use. From here on, “we” refers to this key partnership between our academic group and TLT.

We submitted a provisional patent application in April 2012, and in 2016 the first US patent (9,345,769) was issued, followed by a second US patent (9,676,806 B2) in 2017. In October 2014, we provided our standard operating procedure (SOP) for preparing TLD1433 to Sigma-Aldrich Fine Chemicals (SAFC, Wisconsin) for scale-up and GMP production. Approximately one year later, the GMP production was complete, but it would take another year to obtain all the approvals to go to a trial. Six months later, the first patient was treated with TLD1433, making it the first Ru(II)-based photosensitizer to enter a human clinical trial for treating cancer with PDT.

4.3.2. Pre-clinical studies and device development.—While this review focuses primarily on the design and development of TLD1433 from chemical and photophysical principles, it is important to point out the enormous effort that went into its pre-clinical development in partnership with TLT, plus the engineering of the proprietary medical laser system (TLC-3200) and the dosimetry fiber optic cage (TLC-34000) that are being used in the clinical trial. Many animal models and testing of increasing levels of sophistication were required to establish confidence in the technology and satisfy various approval requirements. The development of the complete PDT package based on TLD1433 as the photosensitizer was a multidisciplinary effort that required the expertise and contributions from chemists, biologists, medical biophysicists, engineers, clinicians, investors, industrial partners, and lawyers.

4.3.3. Clinical trial.—In March 2017, TLD1433 was administered to the first patient in a human clinical trial (ClinicalTrials.gov Identifier: NCT03053635), “Intravesical Photodynamic Therapy (PDT) in BCG Refractory High-Risk Non-muscle Invasive Bladder Cancer (NMIBC) Patients”, sponsored by TLT. The trial was carried out at the University Health Network (Toronto, Ontario, Canada) under principal investigator Dr. Girish Kulkarni with Dr. Michael Jewett as Chairman of TLT’s Medical and Scientific Advisory Board. It was a phase lb, open-label, single-arm, single-center study on patients with NMIBC (Ta, Ti, and/or Tis) who had either refused or were not candidates for a radical cystectomy.

The study plan consisted of nine participants, each assigned to one of two phases. (1) Three subjects receive PDT at half of the projected therapeutic dose of TLD1433 (0.35 mg cm^{-2}) and are monitored for safety and tolerability. (2) If the treatment of the first three patients in the first phase does not raise safety concerns after one month of patient follow-up (based on the judgement of a safety monitoring committee), then six subjects receive PDT with the full therapeutic dose of TLD1433 (0.70 mg cm^{-2}) and are monitored for 180 days.

The primary endpoint of the trial was an evaluation of safety and tolerability, assessed by the incidence and severity of adverse effects (up to completion of the follow-up phase at 180 days). The secondary endpoint was the determination of pharmacokinetics as the maximum observed concentration (C_{max}) of TLD1433 in the blood and urine, as well as the area under the curve from time zero to the last quantifiable concentration ($AUC_{O\text{-}t}$). The exploratory endpoint was efficacy, which was assessed in terms of recurrence and survival. The recurrence endpoint was either recurrence-free survival rate at three and six months or recurrence rate at three and six months. The survival endpoint was either overall survival during the study, or overall survival rate at three and six months.

The protocol used in this study is available at ClinicalTrials.gov. Under general anesthesia, patients were infused with TLD1433 (directly into the bladder) for one hour. The light dose was then delivered after TLD1433 had been completely rinsed from the bladder. Removal of unbound TLD1433 followed by uniform illumination of the entire bladder was possible because TLD1433 is almost 2OO× more selective for bladder tumors than normal, healthy urothelial tissue. TLD1433 was supplied as a lyophilizate, packaged in amber borosilicate glass vials stored at room temperature, and was reconstituted in sterile water just before administration to obtain the final clinical dilution determined by bladder volume. Patients were required to restrict fluid intake for twelve hours before TLD1433 administration. Before instillation, a transurethral catheter was inserted and the bladder was drained. TLD1433 was then infused intravesically for one hour, followed by three washes with sterile water. The bladder was then distended with a fourth instillation of sterile water to prevent any folds that would compromise uniform light delivery. Next, an optical fiber with a spherical diffuser was positioned in the center of the bladder, and irradiance sensors were placed via a cage on the bladder wall surface. The assembly was locked in place with an endoscope holder. The irradiance (mW cm^{-2}) was integrated at all sensors, until the target radiant exposure of 90±9 J cm^{-2} was achieved, and then the laser was turned off. The total irradiation time depended on the bladder size and the tissue optical properties of the individual bladders.

The first of the three patients in the first phase of the study was treated March 30, 2017. The primary, secondary, and exploratory (at 90 days post-treatment) endpoints were successfully achieved for all three patients treated with the maximum recommended starting dose. At 180 days post-treatment, the three patients treated with the sub-therapeutic dose of TLD1433 recurred, although there was no sign of progression.

The fourth patient, and the first of the six patients to receive the therapeutic dose of TLD1433 in the second phase of the study, was treated on August 1, 2017. The primary, secondary, and exploratory (at 90 days post-treatment) endpoints were achieved, but this patient presented with metastatic urothelial carcinoma 138 days post-treatment (presumably due to disseminated bone micrometastases present at the time of treatment).

The clinical procedure was optimized (details not disclosed) commencing with the fifth patient. Patients five and six were treated in January and February of 2018, respectively, and met the established primary, secondary, and exploratory 90-day endpoints with no evidence of tumor recurrence. While an additional three patients were part of the original trial design, TLT's Medical and Scientific Advisory Board unanimously voted for early termination of the study in May 2018 based on successfully achieving the primary and secondary endpoints (and exploratory endpoint at 90 days) in six patients. Since that time, patients five and six also met the exploratory efficacy endpoint, with no evidence of disease at 180 days. The next step is an international, multi-center phase II study for NMIBC with efficacy as the primary endpoint in a much larger patient population.

4.4. Future direction

The future is bright for transition metal complexes and PDT/PCT, and many research groups are demonstrating the potential of Ru(II) compounds in this application. Areas to watch

include (1) the creation of photosensitizers and photo-sensitizer-vehicle conjugates that are highly selective for tumors over normal tissue (yet general enough to be used on multiple cancer types), offering improved safety margins for systemic delivery, (2) the design of x-ray activatable photosensitizers that exploit the best attributes of both radiotherapy and PDT for hard-to-treat tumors, and (3) the development of PDT/PCT regimens that stimulate antitumor immunity, which would move PDT/PCT from being viewed as a local treatment to one that can prevent or even target metastatic tumors. A few illustrations involving TLD1433 are highlighted below.

4.4.1. Rutherrin®.—Despite light-mediated cancer therapy being inherently selective by confining the light treatment to malignant tissue, intravenous (IV) delivery of previous photosensitizers has caused unwanted side effects due to off-target accumulation. Thus, there is a continued need to develop better selectivity strategies for photosensitizers that will be administered systemically. There has been ongoing interest by a number of research groups in the use of the protein transferrin (Tf) to carry metal-based drugs as cargo to Tf-receptors that tend to be overexpressed on cancer cell surfaces.[152–158] Ru(II) transition metal complexes, including photosensitizers, have been shown to exhibit nonselective binding to both holo- and apo-Tf. This is also the case for TLD1433 and its derivatives, where Tf-binding both enhances and red-shifts the molar extinction coefficients of some of these photosensitizers under certain conditions. TLT has demonstrated that the photophysical properties of TLD1433 are improved by premixing TLD1433 and Tf, which includes reduced photobleaching, and that overall PDT efficacies are improved with a significant decrease in toxicity.[154] The TLD1433-Tf conjugate was named Rutherrin®, with a Canadian patent pending, and is currently under clinical development for glioblastoma multiforme (GBM) and non-small cell lung cancer (NSCLC). Rutherrin® is able to cross the blood brain barrier (BBB) when sys-temically delivered to rats, with higher uptake by GBM cells relative to normal brain tissue. Activation of Rutherrin® with 808 nm light improved survival in this very aggressive animal model of GBM. They have also demonstrated that Rutherrin® can be activated by x-rays (20 Gy, 225 keV), and the next step is to investigate whether GBM tumors can be safely and effectively destroyed when Rutherrin® is activated transcranially with x-rays. Such developments have the potential to change the way brain tumors are treated, and to improve overall survival for what are now terminal diagnoses.

4.4.2. Immunomodulating PDT/PCT.—Antitumor immune responses, if successfully established, can protect against existing as well as relapsing cancer cells. Recently, certain photosensitizers and PDT regimens have been recognized for their capacity to train a host's immune system against cancer and promote the development of antitumor immunity.[34–38,159,160] Such PDT-induced antitumor immune responses have the capacity to target cancer cells at local sites *and* metastatic niches, and thus hold the key to establishing long-term cancer-free health. As such, the development of novel photosensitizers and regimens of immunomodulatory potential represent the frontier in the field of PDT (and PCT) research, and promise to yield the next generation of cancer immunotherapeutics. TLD1433 and its PDT regimen have been shown to induce antitumor immunity in a mouse model of colon cancer, and there is hope that this could translate to humans. We are actively developing other immunomodulating transition metal complexes and PDT/PCT regimens for melanoma

specifically. As chemotherapy and radiotherapy are ineffective toward melanoma, outcomes could be improved with better adjuvant therapies that can be administered alongside surgery.

5. CONCLUSIONS

PDT activity has been known generally for over a century and as a cancer treatment for nearly half as long, and recent developments have demonstrated remarkable potency. However, no light-activatable prodrugs have emerged as a mainstream cancer treatment. This review and others have discussed the major obstacles to introducing PDT as a viable alternative to conventional cancer therapy approaches (e.g., surgery, radiotherapy, and chemotherapy). These major obstacles are: (1) its absolute dependence on molecular oxygen, (2) the paucity of photosensitizers that can be activated by tissue-penetrating near-infrared light, (3) poor or zero tumor selectivity for systemically-delivered photosensitizers (especially first-generation photosensitizers), (4) the inability to treat metastases using the current protocols, which are optimized for primary tumor ablation, (5) the lack of randomized, controlled clinical trials of adequate power, (6) the equipment required, although relatively inexpensive, is not standard clinical infrastructure, (7) the use of different treatment protocols that prohibit the comparison of treatment outcomes in small studies across different centers, (8) the lack of commitment and funds for PDT research, (9) the fact that the first-generation photosensitizer Photofrin® is still used in almost one-third of recent trials, and (10) the pervasive photosensitizer-centered approach to the design of next-generation photosensitizers for PDT rather than the development of complete and optimized PDT *packages*.

While there is no “ideal” photosensitizer, those derived from transition metal complexes offer many advantages. First, metal-based compounds can adopt a larger number of oxidation states compared to their organic counterparts, which allows a variety of bonding modes and geometries. The structural and chemical space that can be sampled with minor modification is vast. Second, inorganic complexes possess a much wider range of accessible excited-state electronic configurations, with characteristic photophysical and photochemical properties. They readily participate in energy- and electron-transfer processes upon photoexcitation, yet can remain very kinetically stable. Finally, coordination complexes have a modular architecture, whereby photophysical and chemical properties can be tuned through judicious choice of metals and ligands to achieve potent photobiological effects. As such, they have been of particular interest as systems that can yield PDT effects at low oxygen tension, operate via oxygen-independent photochemical processes for PCT, and/or be activated with tissue-penetrating near-infrared light. When designed from a tumor-centered approach, they can also stimulate important immunological responses.

The potential of transition metal complexes for PDT/PCT has been demonstrated in a number of Ru(II) polypyridyl systems investigated as in vitro photobiological agents. One example is TLD1433, which is the first Ru(II)-based photosensitizer for PDT to enter a human clinical trial. This system exploits long-lived triplet ^{3}IL and ^{3}ILCT states for $^1O_2$ sensitization and for electron-transfer pathways, respectively, producing extremely potent photocytotoxic effects. It also exploits ^{3}MLCT states that luminesce brightly in cancer cells and tumors, giving this photosensitizer an added theranostic capacity. Its design emerged

from a knowledge of fundamental photophysical and chemical principles that were derived from the SARs of a large number of transition metal complexes studied in a standardized phenotypic in vitro (photo)cytotoxicity assay.

The standardization of this assay was key to comparing different photosensitizers. It is well known that there is a problem with reproducibility of biological results between different laboratories. With PDT/PCT, this problem is exacerbated by the added variables associated with light delivery and dosimetry. The solution is to screen compounds of interest and reference photosensitizers through a standardized assay in-house, rather than relying on published data for comparison. This approach has enabled us to make quantitative comparisons of the performance of our photosensitizers against others, which ultimately made the case for investing the time and money to move TLD1433 forward.

TLD1433 progressed from the bench to a clinical trial in six years thanks to efforts of a highly productive and motivated multidisciplinary team of chemists, biologists, medical biophysicists, engineers, clinicians, investors, industrial partners, and lawyers. The early identification of the target indication — NMIBC — facilitated the parallel development of the compound, the medical device, and the PDT package via a tumor-centered approach. The creation of a photosensitizer is only one moving part in a much bigger machine, and researchers making these compounds ought not lose sight of the big picture.

The phase Ib study of TLD1433, focused on safety and tolerability, was deemed a success, and a much larger, multicenter phase II study with efficacy as the primary endpoint is being planned. We hope that this development process, i.e., as part of a complete PDT package, might serve as a model for bringing improved transition metal complex photosensitizers to clinical studies. The key is to capitalize on the strengths of a multidisciplinary team, and to identify the right photosensitizer and the right light protocol for a target clinical indication.

ACKNOWLEDGMENTS

SAM, CGC, RPT, and SG thank the National Cancer Institute (NCI) of the National Institutes of Health (NIH) (Award #Ro1CA222227) for support. The content in this review is solely the responsibility of the authors and does not necessarily represent the official views of the National Institutes of Health. SM and SG thank the Canadian Institutes of Health Research (CIHR), the Beatrice Hunter Cancer Research Institute (BHCRI), and the Dalhousie Medical Research Foundation (DMRF) for support. SM also acknowledges TLT and the Natural Sciences and Engineering Council of Canada (NSERC), the Canadian Foundation for Innovation (CFI), the Nova Scotia Research and Innovation Trust (NSRIT), Acadia University, and the University of North Carolina at Greensboro for support. RPT thanks the U.S. Department of Energy, Office of Science, and Office of Basic Energy Sciences under award no. DE-FG02–07ER15888 as well as the Robert A. Welch Foundation (grant E-621) for support.

Biographies

Susan Monro received her BSc degree in Chemistry and Biology in 2008, and her MSc in Chemistry in 2011, from Acadia University under the supervision of Prof. Sherri McFarland. She has worked with Prof. McFarland since 2007 as a senior researcher and lab manager, concentrating on several areas such as chemical synthesis and biological assessment and evaluation of photosensitizers. Her current research work focuses on the photobiological effects of metal-based photosensitizers, including ROS accumulation in cell systems.

Katsuya Colón received his Bachelor of Science degree in biochemistry from the University of North Carolina Greensboro (UNCG) in May 2018 under the supervision of Prof. Sherri McFarland. He is currently a graduate student in the chemistry program at the California Institute of Technology. His current research interests are in the synthesis of inorganic photosensitizers for photodynamic therapy, development of chemical probes to study biological processes, and studying the role of glycans in neurobiology.

Huimin Yin received her Bachelor of Science degree in biology at Acadia University in 2012. From 2012 to 2014, she worked as a research associate evaluating photoactive transitions metal complexes for cancer therapy under the supervision of Prof. Sherri McFarland at Acadia University. She then joined the Master of Science degree program at Acadia University and earned her MSc in Biology in 2016 under Prof. McFarland's supervision.

John Roque III received his Bachelor's degree in chemistry from the University of Rhode Island in 2016. Currently, he is a Ph.D. student in the medicinal biochemistry program at the University of North Carolina at Greensboro (UNCG) under the mentorship of Prof. Sherri McFarland. His current research interests are focused on panchromatic and hypoxia-active photosensitizers for photodynamic applications.

Prathyusha Konda received her B. Tech. from the Indian Institute of Technology (IIT; Chennai, India). She is pursuing her Ph.D. with Prof. Shashi Gujar at Dalhousie University, Halifax, NS. Her research interests include immunomics and immunotherapies of cancers.

Shashi Gujar, a Veterinarian-turned-immunologist, finished his Ph.D. in Immunology and Infectious Diseases, at Memorial University of Newfoundland, Canada in 2008–2009. He then pursued his post-doctoral training under the mentorship of Dr. Patrick Lee, known for his pioneering discovery on using benign human virus, reovirus, to kill cancers, at Dalhousie University, in Halifax, Nova Scotia, Canada. He was then appointed as an Assistant Professor in the Department of Pathology, Dalhousie University (in 2016), wherein he established an Immunotherapy research program. His current research interests include molecular biology, immunology, oncolytic viruses and metabolism, which are geared towards developing novel immune-based interventions to enhance human health outcomes, especially in the context of cancer.

Randolph P. Thummel received his B.Sc. degree from Brown University (Providence, RI) in 1967, and obtained his Ph.D. degree from the University of California Santa Barbara (UCSB) in 1971 in synthetic and physical organic chemisty. From 1971–1973, he completed an NIH post-doctoral fellowship at The Ohio State University. He was appointed full professor in 1987 at the University of Houston. Prof. Thummel has been a Fullbright Research Scholar, and is currently the distinguished John & Rebecca Moores Professor of Chemistry. His research group has published over 200 peer-reviewed articles in the area of azaaromatic systems and polypyridine-type ligands. Currently, his research interests include the design and synthesis of ruthenium polypyridyl complexes for artificial photosynthesis and photobiological applications.

Lothar Lilge received his Ph.D. degree in experimental physics 1992 from the Westfaehlische Wilhelms University in Muenster, Germany under Prof. Franz Hillenkamp. He completed post-doctoral training under Prof. Brian Wilson at McMaster University (Hamilton, Ontario Canada). He was appointed full professor at the University of Toronto (Ontario, Canada) in 2009. Since 2009 he has been a Senior Scientist at the Princess Margaret Cancer Centre, University Health Network (Toronto, Ontario Canada). His current research interest encompasses photodynamic therapy and optical techniques for breast cancer pre-screening and breast cancer risk assessment. Related to photodynamic therapy in particular, his interests also include evaluating novel photosensitizers, modulation of the tissue response to photodynamic therapy, and establishing personalized treatment planning.

Colin G. Cameron earned his Ph.D. degree in electrochemistry in 2000 from the Memorial University of Newfoundland (MUN) under Prof. Peter Pickup, and completed a post-doctoral fellowship at the California Institute of Technology with Prof. Michael S. Freund. He then worked for Defence Research Development Canada (DRDC) as a senior defense scientist for 14 years, where he led a number of high profile research programs for the Canadian government. In 2012, Dr. Cameron and Prof. Sherri A. McFarland founded the biotech start-up PhotoDynamic, Inc. to commercialize photoactive plant extracts as oral antimicrobials. In 2016, he left Canada and joined the University of North Carolina at Greensboro to manage a new research program on immunomodulating ruthenium photosensitizers with Prof. McFarland.

Sherri A. McFarland received her Ph.D. in organic chemistry in 2003 from the University of California San Diego (UCSD) under Prof. Nathaniel Finney. From 2003–2005, she completed a post-doctoral fellowship under Profs. Norman Schepp and Francis Cozens at Dalhousie University (Halifax, Nova Scotia Canada). She was appointed full professor in 2014 at Acadia University (Wolfville, Nova Scotia Canada), and then relocated to the University of North Carolina at Greensboro (UNCG) as full professor in 2016. She also founded a bio-tech start-up PhotoDynamic, Inc. in 2012 and served as President and CEO from 2012–2015, and now serves as CSO. Her current research interests include medicinal inorganic chemistry and investigating the photophysics/photochemistry/photobiology of both synthetic inorganic compounds/materials and photoactive natural products toward anticancer and antimicrobial applications.

ABBREVIATIONS

Φ_Δ	quantum yield for $^1O_2$ production
BBB	blood brain barrier
DFT	density functional theory
bpy	bipyridine
4,4′-dmb	4,4′-dimethyl-2,2′-bipyridine
6,6′-dmb	6,6′-dimethyl-2,2′-bipyridine

DSSC	dye-sensitized solar cell
dpp	bis(2-pyridyl)pyrazine
dppn	benzo[*i*]dipyrido [3,2-*a*:2′,3′-c]phenazine
dppz	dipyrido [3,2-*a*:2′,3′-c]phenazine
EC_{50}	effective concentration to reduce cell viability to 50%
EtOH	ethanol
GBM	glioblastoma multiforme
GSH	glutathione
ICD	immunogenic cell death
ICP-MS	inductively coupled plasma mass spectrometry
IL	intraligand
ILCT	intraligand charge transfer
IP	imidazo[4,5-*f*][1,10]phenanthroline
IP	intellectual property
ISC	intersystem crossing
IT	intratumoral
IV	intravenous
LLCT	ligand-to-ligand charge transfer
LMCT	ligand-to-metal charge transfer
LSCM	laser scanning confocal microscopy
MeCN	acetonitrile
MeOH	methanol
MC	metal-centered
MLCT	metal-to-ligand charge transfer
MMCT	metal-to-metal charge transfer
MRI	magnetic resonance imaging
MRSA	methicillin-resistant Staphylococcus aureus
NMIBC	nonmuscle invasive bladder cancer
NSCLC	non-small cell lung cancer

PACT	photoactivated cancer therapy
PCT	photochemotherapy
PDT	photodynamic therapy
PEP	(5-pyren-1-yl)ethynyl-2,2′-bipyridine
phen	1,10-phenanthroline
pydppn	3-(pyrid-2′-yl)-4,5,9,16-tetraaza-dibenzo[*a,c*]naphthacene
PTT	photothermal therapy
PI	phototherapeutic index
PS	photosensitizer
ROS	reactive oxygen species
SA	Staphylococcus aureus
SAR	structure-activity relationship

REFERENCES

(1). Photodynamic Therapy: Basic Principles and Clinical Applications; Henderson BW, Dougherty TJ, Eds.; CRC Press, 1992.

(2). Bonnett R Chemical Aspects of Photodynamic Therapy; Gordon and Breach Science Publishers, 2000.

(3). Handbook of Photomedicine, 1st edition; Hamblin MR, Huang Y, Eds.; CRC Press: Boca Raton, FL, 2013.

(4). Hamblin MR; Mroz P Advances in Photodynamic Therapy: Basic, Translational, and Clinical; Engineering in Medicine and Biology; Artech House: Norwood, MA, 2008.

(5). Photodynamic Medicine: From Bench to Clinic, 1st edition; Kostron H, Hasan T, Eds.; Royal Society of Chemistry: Cambridge, 2016.

(6). van Straten D; Mashayekhi V; de Bruijn H; Oliveira S; Robinson D Oncologic Photodynamic Therapy: Basic Principles, Current Clinical Status and Future Directions. Cancers 2017, 9, 19.

(7). Abrahamse H; Hamblin MR New Photosensitizers for Photodynamic Therapy. Biochem. J 2016, 473, 347–364. [PubMed: 26862179]

(8). Agostinis P; Berg K; Cengel KA; Foster TH; Girotti AW; Gollnick SO; Hahn SM; Hamblin MR; Juzeniene A; Kessel D; Korbelik M; Moan J; Mroz P; Nowis D; Piette J; Wilson BC; Golab J Photodynamic Therapy of Cancer: An Update. Cancer J. Clin 2011, 61, 250–281.

(9). Dougherty TJ; Gomer CJ; Henderson BW; Jori G; Kessel D; Korbelik M; Moan J; Peng Q Photodynamic Therapy. J. Natl. Cancer Inst 1998, 90, 889–905. [PubMed: 9637138]

(10). Plaetzer K; Krammer B; Berlanda J; Berr F; Kiesslich T Photophysics and Photochemistry of Photodynamic Therapy: Fundamental Aspects. Lasers Med. Sci 2009, 24, 259–268. [PubMed: 18247081]

(11). Allison RR Photodynamic Therapy: Oncologic Horizons. Future Oncol 2014, 10, 123–124. [PubMed: 24328413]

(12). Benov L Photodynamic Therapy: Current Status and Future Directions. Med. Princ. Pract 2015, 24, 14–28. [PubMed: 24820409]

(13). Turro NJ Modern Molecular Photochemistry; University Science Books, 1991.

(14). Baptista MS; Cadet J; Di Mascio P; Ghogare AA; Greer A; Hamblin MR; Lorente C; Nunez SC; Ribeiro MS; Thomas AH; Vignoni M; Yoshimura TJ Type I and Type II Photosensitized Oxidation Reactions: Guidelines and Mechanistic Pathways. Photochem. Photobiol 2017, 93, 912–919. [PubMed: 28084040]

(15). Celli JP; Spring BQ; Rizvi I; Evans CL; Samkoe KS; Verma S; Pogue BW; Hasan T Imaging and Photodynamic Therapy: Mechanisms, Monitoring, and Optimization. Chem. Rev 2010, 110, 2795–2838. [PubMed: 20353192]

(16). Usuda J; Kato H; Okunaka T; Furukawa K; Tsutsui H; Yamada K; Suga Y; Honda H; Nagatsuka Y; Ohira T; Tsuboi M; Hirano T Photodynamic Therapy (PDT) for Lung Cancers. J. Thorac. Oncol. Off. Publ. Int. Assoc. Study Lung Cancer 2006, 1, 489–493.

(17). Matsuoka M Infrared Absorbing Dyes; Springer, 1990.

(18). Zhang J; Jiang C; Figueiró Longo JP; Azevedo RB; Zhang H; Muehlmann LA An Updated Overview on the Development of New Photosensitizers for Anticancer Photodynamic Therapy. Acta Pharm. Sin. B 2018, 8, 137–146. [PubMed: 29719775]

(19). Sternberg ED; Dolphin D Second Generation Photodynamic Agents: A Review. J. Clin. Laser Med. Surg 1993, 11, 233–241. [PubMed: 10146514]

(20). Kataoka H; Nishie H; Hayashi N; Tanaka M; Nomoto A; Yano S; Joh T New Photodynamic Therapy with next-Generation Photosensitizers. Ann. Transl. Med 2017, 5, 183. [PubMed: 28616398]

(21). Ormond AB; Freeman HS Dye Sensitizers for Photodynamic Therapy. Materials 2013, 6, 817–840. [PubMed: 28809342]

(22). Bugaj AM Targeted Photodynamic Therapy-a Promising Strategy of Tumor Treatment. Photochem. Photobiol. Sci 2011, 10, 1097–1109. [PubMed: 21547329]

(23). Zheng G; Chen J; Stefflova K; Jarvi M; Li H; Wilson BC Photodynamic Molecular Beacon as an Activatable Photosensitizer Based on Protease-Controlled Singlet Oxygen Quenching and Activation. Proc. Natl. Acad. Sci. U.S.A 2007, 104, 8989–8994. [PubMed: 17502620]

(24). Lovell JF; Liu TWB; Chen J; Zheng G Activatable Photosensitizers for Imaging and Therapy. Chem. Rev 2010, 110, 2839–2857. [PubMed: 20104890]

(25). Nakamura Y; Mochida A; Choyke PL; Kobayashi H Nanodrug Delivery: Is the Enhanced Permeability and Retention Effect Sufficient for Curing Cancer? Bioconjug. Chem 2016, 27, 2225–2238. [PubMed: 27547843]

(26). Battogtokh G; Ko YT Mitochondrial-Targeted Photosensitizer-Loaded Folate-Albumin Nanoparticle for Photodynamic Therapy of Cancer. Nanomedicine Nanotechnol. Biol. Med 2017, 13, 733–743.

(27). Jung HS; Lee J-H; Kim K; Koo S; Verwilst P; Sessler JL; Kang C; Kim JS Mitochondrial-Targeted Photosensitizer-Loaded Albumin Nanoparticles for Photodynamic Therapy of Malignant Brain Tumors. J. Pharm. Drug Deliv. Res

(28). Lv W; Zhang Z; Zhang KY; Yang H; Liu S; Xu A; Guo S; Zhao Q; Huang W A Mitochondria-Targeted Photosensitizer Showing Improved Photodynamic Therapy Effects Under Hypoxia. Angew. Chem. Int. Ed. Engl 2016, 55, 9947–9951. [PubMed: 27381490]

(29). Jung HS; Lee J-H; Kim K; Koo S; Verwilst P; Sessler JL; Kang C; Kim JS A Mi-tochondria-Targeted Cryptocyanine-Based Photothermogenic Photosensitizer. J. Am. Chem. Soc 2017, 139, 9972–9978. [PubMed: 28644025]

(30). Chakrabortty S; Agrawalla BK; Stumper A; Vegi NM; Fischer S; Reichardt C; Kögler M; Dietzek B; Feuring-Buske M; Buske C; Rau S; Weil T Mitochondria Targeted Protein-Ruthenium Photosensitizer for Efficient Photodynamic Applications. J. Am. Chem. Soc 2017, 139, 2512–2519. [PubMed: 28097863]

(31). Rui L; Xue Y; Wang Y; Gao Y; Zhang W A Mitochondria-Targeting Supramolecular Photosensitizer Based on Pillar[5]arene for Photodynamic Therapy. Chem. Commun 2017, 53 (21), 3126–3129.

(32). Muz B; de la Puente P; Azab F; Azab AK The Role of Hypoxia in Cancer Progression, Angiogenesis, Metastasis, and Resistance to Therapy. Hypoxia (Auckl.) 2015, 3, 83–92. [PubMed: 27774485]

(33). Juzeniene A; Nielsen KP; Moan J Biophysical Aspects of Photodynamic Therapy. J. Env. Pathol. Toxicol. Oncol 2006, 25, 7–28. [PubMed: 16566708]

(34). Mroz P; Hashmi JT; Huang Y-Y; Lange N; Hamblin MR Stimulation of Anti-Tumor Immunity by Photodynamic Therapy. Expert Rev. Clin. Immunol 2011, 7, 75–91. [PubMed: 21162652]

(35). Anzengruber F; Avci P; de Freitas LF; Hamblin MR T-Cell Mediated Anti-Tumor Immunity after Photodynamic Therapy: Why Does It Not Always Work and How Can We Improve It? Photochem. Photobiol. Sci 2015, 14, 1492–1509. [PubMed: 26062987]

(36). Gollnick SO; Brackett CM Enhancement of Anti-Tumor Immunity by Photodynamic Therapy. Immunol. Res 2010, 46, 216–226. [PubMed: 19763892]

(37). Gollnick SO Photodynamic Therapy and Antitumor Immunity. J. Natl. Compr. Canc. Netw 2012, 10, S40–43. [PubMed: 23055214]

(38). Shams M; Owczarczak B; Manderscheid-Kern P; Bellnier DA; Gollnick SO Development of Photodynamic Therapy Regimens That Control Primary Tumor Growth and Inhibit Secondary Disease. Cancer Immunol. Immunother 2015, 64, 287–297. [PubMed: 25384911]

(39). Seyfried TN; Huysentruyt LC On the Origin of Cancer Metastasis. Crit. Rev. Oncog 2013, 18, 43–73. [PubMed: 23237552]

(40). Haas KL; Franz KJ Application of Metal Coordination Chemistry To Explore and Manipulate Cell Biology. Chem. Rev 2009, 109, 4921–4960. [PubMed: 19715312]

(41). Mjos KD; Orvig C Metallodrugs in Medicinal Inorganic Chemistry. Chem. Rev 2014, 114, 4540–4563. [PubMed: 24456146]

(42). Storr T; Thompson KH; Orvig C Design of Targeting Ligands in Medicinal Inorganic Chemistry. Chem. Soc. Rev 2006, 35, 534–544. [PubMed: 16729147]

(43). Barry NPE; Sadler PJ Challenges for Metals in Medicine: How Nanotechnology May Help To Shape the Future. ACS Nano 2013, 7, 5654–5659. [PubMed: 23837396]

(44). Ndagi U; Mhlongo N; Soliman ME Metal Complexes in Cancer Therapy - an Update from Drug Design Perspective. Drug Des. Devel. Ther 2017, 11, 599–616.

(45). Zhang P; Sadler PJ Redox-Active Metal Complexes for Anticancer Therapy: Redox-Active Metal Complexes for Anticancer Therapy. Eur. J. Inorg. Chem 2017, 2017, 1541–1548.

(46). Romero-Canelón I; Sadler PJ Next-Generation Metal Anticancer Complexes: Multitargeting via Redox Modulation. Inorg. Chem 2013, 52, 12276–12291. [PubMed: 23879584]

(47). Wilson WR; Hay MP Targeting Hypoxia in Cancer Therapy. Nat. Rev. Cancer 2011, 11, 393–410. [PubMed: 21606941]

(48). Ardo S; Meyer GJ Photodriven Heterogeneous Charge Transfer with Transition-Metal Compounds Anchored to TiO_2 Semiconductor Surfaces. Chem. Soc. Rev 2008, 38, 115–164. [PubMed: 19088971]

(49). Hagfeldt A; Boschloo G; Sun L; Kloo L; Pettersson H Dye-Sensitized Solar Cells. Chem. Rev 2010, 110, 6595–6663. [PubMed: 20831177]

(50). Hagfeldt A; Grätzel M Molecular Photovoltaics. Acc. Chem. Res 2000, 33, 269–277. [PubMed: 10813871]

(51). Josefsen LB; Boyle RW Photodynamic Therapy and the Development of Metal-Based Photosensitisers. Metal-Based Drugs 2008, 2008, 276109. [PubMed: 18815617]

(52). Bonnet S Shifting the Light Activation of Metallodrugs to the Red and Near-Infrared Region in Anticancer Phototherapy. Comments Inorg. Chem 2015, 35, 179–213.

(53). Reeβing F; Szymanski W Beyond Photodynamic Therapy: Light-Activated Cancer Chemotherapy. Curr. Med. Chem 2017, 24, 4905–4950. [PubMed: 27601187]

(54). Heinemann F; Karges J; Gasser G Critical Overview of the Use of Ru(II) Polypyridyl Complexes as Photosensitizers in One-Photon and Two-Photon Photodynamic Therapy. Acc. Chem. Res 2017, 50, 2727–2736. [PubMed: 29058879]

(55). Liu J; Zhang C; Rees TW; Ke L; Ji L; Chao H Harnessing ruthenium(II) as Photodynamic Agents: Encouraging Advances in Cancer Therapy. Coord. Chem. Rev 2018, 363, 17–28.

(56). Poynton FE; Bright SA; Blasco S; Williams DC; Kelly JM; Gunnlaugsson T The Development of Ruthenium(II) Polypyridyl Complexes and Conjugates for in Vitro Cellular and in Vivo Applications. Chem. Soc. Rev 2017, 46, 7706–7756. [PubMed: 29177281]

(57). Knoll JD; Albani BA; Turro C Excited State Investigation of a New Ru(II) Complex for Dual Reactivity with Low Energy Light. Chem. Commun 2015, 51, 8777–8780.

(58). White JK; Schmehl RH; Turro C An Overview of Photosubstitution Reactions of Ru(II) Imine Complexes and Their Application in Photobiology and Photodynamic Therapy. Inorg. Chim. Acta 2017, 454, 7–20.

(59). Smith NA; Sadler PJ Photoactivatable Metal Complexes: From Theory to Applications in Biotechnology and Medicine. Phil. Trans. R. Soc. A 2013, 371, 20120519. [PubMed: 23776303]

(60). Zamora A; Vigueras G; Rodriguez V; Santana MD; Ruiz J Cyclometalated Iridium(III) Luminescent Complexes in Therapy and Phototherapy. Coord. Chem. Rev 2018, 360, 34–76.

(61). Jiang X; Zhu N; Zhao D; Ma Y New Cyclometalated Transition-Metal Based Photosensitizers for Singlet Oxygen Generation and Photodynamic Therapy. Sci. China Chem 2016, 59, 40–52.

(62). Lazic S; Kaspler P; Shi G; Monro S; Sainuddin T; Forward S; Kasimova K; Hennigar R; Mandel A; McFarland S; Lilge L Novel Osmium-Based Coordination Complexes as Photosensitizers for Panchromatic Photodynamic Therapy. Photochem. Photobiol 2017, 93, 1248–1258. [PubMed: 28370264]

(63). Loftus LM; White JK; Albani BA; Kohler L; Kodanko JJ; Thummel RP; Dunbar KR; Turro C New Ru(II) Complex for Dual Activity: Photoinduced Ligand Release and 1O2 Production. Chem. Eur. J 2016, 22, 3704–3708. [PubMed: 26715085]

(64). Knoll JD; Albani BA; Turro C New Ru(II) Complexes for Dual Photoreactivity: Ligand Exchange and 1O2 Generation. Acc. Chem. Res 2015, 48, 2280–2287. [PubMed: 26186416]

(65). Juris A; Campagna S; Balzani V; Gremaud G; Von Zelewsky A Absorption Spectra, Luminescence Properties, and Electrochemical Behavior of Tris-Heteroleptic Ruthenium(II) Polypyridine Complexes. Inorg. Chem 1988, 27, 3652–3655.

(66). Juris A; Balzani V; Barigelletti F; Campagna S; Belser P; von Zelewsky A Ru(II) Polypyridine Complexes: Photophysics, Photochemistry, Eletrochemistry, and Chemilumines-cence. Coord. Chem. Rev 1988, 84, 85–277.

(67). Balzani V; Juris A Photochemistry and Photophysics of Ru(II)-polypyridine Complexes in the Bologna Group. From Early Studies to Recent Developments. Coord. Chem. Rev 2001, 211, 97–115.

(68). Prier CK; Rankic DA; MacMillan DWC Visible Light Photoredox Catalysis with Transition Metal Complexes: Applications in Organic Synthesis. Chem. Rev 2013, 113, 5322–5363. [PubMed: 23509883]

(69). Bignozzi CA; Argazzi R; Boaretto R; Busatto E; Carli S; Ronconi F; Caramori S The Role of Transition Metal Complexes in Dye Sensitized Solar Devices. Coord. Chem. Rev 2013, 257, 1472–1492.

(70). Keefe M; Benkstein KD; Hupp JT Luminescent Sensor Molecules Based on Coordinated Metals: A Review of Recent Developments. Coord. Chem. Rev 2000, 205, 201–228.

(71). Friedman AE; Chambron JC; Sauvage JP; Turro NJ; Barton JK A Molecular Light Switch for DNA: Ru(bpy)2(dppz)2+. J. Am. Chem. Soc 1990, 112, 4960–4962.

(72). Mari C; Gasser G Lightening up Ruthenium Complexes to Fight Cancer? Chim. Int. J. Chem 2015, 69, 176–181.

(73). Mari C; Pierroz V; Ferrari S; Gasser G Combination of Ru(II) Complexes and Light: New Frontiers in Cancer Therapy. Chem. Sci 2015, 6, 2660–2686. [PubMed: 29308166]

(74). Knoll JD; Turro C Control and Utilization of Ruthenium and Rhodium Metal Complex Excited States for Photoactivated Cancer Therapy. Coord. Chem. Rev 2015, 282–283, 110–126.

(75). Glazer EC Light-Activated Metal Complexes That Covalently Modify DNA. Isr. J. Chem 2013, 53, 391–400.

(76). Vögtle F; Plevoets M; Nieger M; Azzellini GC; Credi A; De Cola L; De Marchis V; Venturi M; Balzani V Dendrimers with a Photoactive and Redox-Active [Ru(bpy)3]2+-Type Core: Photophysical Properties, Electrochemical Behavior, and Excited-State Electron-Transfer Reactions. J. Am. Chem. Soc 1999, 121, 6290–6298.

(77). Suzuki K; Kobayashi A; Kaneko S; Takehira K; Yoshihara T; Ishida H; Shiina Y; Oishi S; Tobita S Reevaluation of Absolute Luminescence Quantum Yields of Standard Solutions Using a

Spectrometer with an Integrating Sphere and a Back-Thinned CCD Detector. Phys. Chem. Chem. Phys 2009, 11, 9850–9860. [PubMed: 19851565]

(78). DeRosa MC; Crutchley RJ Photosensitized Singlet Oxygen and Its Applications. Coord. Chem. Rev 2002, 233/234, 351–371.

(79). Van Houten J; Watts RJ Temperature Dependence of the Photophysical and Photochemical Properties of the tris(2,2′-bipyridyl)ruthenium(II) Ion in Aqueous Solution. J. Am. Chem. Soc 1976, 98 (16), 4853–4858.

(80). Thompson DW; Ito A; Meyer TJ [Ru(bpy)3]2+* and Other Remarkable Metal-to-Ligand Charge Transfer (MLCT) Excited States. Pure Appl. Chem 2013, 85, 1257–1305.

(81). Mukuta T; Tanaka S; Inagaki A; Koshihara S; Onda K Direct Observation of the Triplet Metal-Centered State in [Ru(bpy)3]2+ Using Time-Resolved Infrared Spectroscopy. Chemis-trySelect 2016, 1, 2802–2807.

(82). Hartshorn RM; Barton JK Novel Dipyridophenazine Complexes of Ruthenium(II): Exploring Luminescent Reporters of DNA. J. Am. Chem. Soc 1992, 114, 5919–5925.

(83). Poynton FE; Hall JP; Keane PM; Schwarz C; Sazanovich IV; Towrie M; Gunnlaugsson T; Cardin CJ; Cardin DJ; Quinn SJ; Long C; Kelly JM Direct Observation by Time-Resolved Infrared Spectroscopy of the Bright and the Dark Excited States of the [Ru(phen)2(dppz)]2+ Light-Switch Compound in Solution and When Bound to DNA. Chem. Sci 2015 7, 3075–3084. [PubMed: 26029356]

(84). Olofsson J; Önfelt B; Lincoln P Three-State Light Switch of [Ru(phen)2dppz]2+: Distinct Excited-State Species with Two, One, or No Hydrogen Bonds from Solvent. J. Phys. Chem. A 2004, 108, 4391–4398.

(85). Önfelt B; Olofsson J; Lincoln P; Nordén B Picosecond and Steady-State Emission of [Ru(phen)2dppz]2+ in Glycerol: Anomalous Temperature Dependence. J. Phys. Chem. A 2003, 107, 1000–1009.

(86). Brennaman MK; Alstrum-Acevedo JH; Fleming CN; Jang P; Meyer TJ; Papanikolas JM Turning the [Ru(bpy)2dppz]2+ Light-Switch On and Off with Temperature. J. Am. Chem. Soc 2002, 124, 15094–15098. [PubMed: 12475355]

(87). Brennaman MK; Meyer TJ; Papanikolas JM [Ru(bpy)2dppz]2+ Light-Switch Mechanism in Protic Solvents as Studied through Temperature-Dependent Lifetime Measurements. J. Phys. Chem. A 2004, 108, 9938–9944.

(88). Mari C; Pierroz V; Rubbiani R; Patra M; Hess J; Spingler B; Oehninger L; Schur J; Ott I; Salassa L; Ferrari S; Gasser G DNA Intercalating Ru(II) Polypyridyl Complexes as Effective Photosensitizers in Photodynamic Therapy. Chem. - Eur. J 2014, 20, 14421–14436. [PubMed: 25213439]

(89). Mari C; Pierroz V; Leonidova A; Ferrari S; Gasser G Towards Selective Light-Activated Ru(II)-Based Prodrug Candidates: Towards Selective Light-Activated Ru(II)-Based Prodrug Candidates. Eur. J. Inorg. Chem 2015, 2015, 3879–3891.

(90). Hess J; Huang H; Kaiser A; Pierroz V; Blacque O; Chao H; Gasser G Evaluation of the Medicinal Potential of Two Ruthenium(II) Polypyridine Complexes as One-and Two-Photon Photodynamic Therapy Photosensitizers. Chemistry 2017, 23, 9888–9896. [PubMed: 28509422]

(91). Yam VW-W; Lo KK-W; Cheung K-K; Kong RY-C Deoxyribonucleic Acid Binding and Photocleavage Studies of Rhenium(I) Dipyridophenazine Complexes. J. Chem. Soc. Dalton Trans 1997, 2067–2072.

(92). Foxon SP; Alamiry MAH; Walker MG; Meijer AJHM; Sazanovich IV; Weinstein JA; Thomas JA Photophysical Properties and Singlet Oxygen Production by Rutheni-um(II) Complexes of benzo[i]dipyrido[3,2-a:2′,3′-c]phenazine: Spectroscopic and TD-DFT Study. J. Phys. Chem. A 2009, 113, 12754–12762. [PubMed: 19791785]

(93). Jenkins Y; Friedman AE; Turro NJ; Barton JK Characterization of Dipyridophenazine Complexes of Ruthenium(II): The Light Switch Effect as a Function of Nucleic Acid Sequence and Conformation. Biochemistry 1992, 31, 10809–10816. [PubMed: 1420195]

(94). Sun Y; Joyce LE; Dickson NM; Turro C Efficient DNA Photocleavage by [Ru(bpy)2(dppn)]2+ with Visible Light. Chem. Commun 2010, 46, 2426–2428.

(95). Liu Y; Hammitt R; Lutterman DA; Joyce LE; Thummel RP; Turro C Ru(II) Complexes of New Tridentate Ligands: Unexpected High Yield of Sensitized 1O2. Inorg. Chem 2009, 48, 375–385. [PubMed: 19035764]

(96). Zhao R; Hammitt R; Thummel RP; Liu Y; Turro C; Snapka RM Nuclear Targets of Photodynamic Tridentate Ruthenium Complexes. Dalton Trans 2009, 10926–10931. [PubMed: 20023923]

(97). Steenken S; Jovanovic SV How Easily Oxidizable Is DNA? One-Electron Reduction Potentials of Adenosine and Guanosine Radicals in Aqueous Solution. J. Am. Chem. Soc 1997, 119, 617–618.

(98). Elias B; Creely C; Doorley GW; Feeney MM; Moucheron C; Kirsch-DeMesmaeker A; Dyer J; Grills DC; George MW; Matousek P; Parker A; Towrie M; Kelly JM Photooxidation of Guanine by a Ruthenium Dipyridophenazine Complex Intercalated in a Double-Stranded Polynucleotide Monitored Directly by Picosecond Visible and Infrared Transient Absorption Spectroscopy. Chem. Eur. J 2008, 14, 369–375. [PubMed: 17886324]

(99). Lecomte J-P; Kirsch-De Mesmaeker A; Feeney MM; Kelly JM Ruthenium(II) Complexes with 1,4,5,8,9,12-Hexaazatriphenylene and 1,4,5,8-Tetraazaphenanthrene Ligands: Key Role Played by the Photoelectron Transfer in DNA Cleavage and Adduct Formation. Inorg. Chem 1995, 34, 6481–6491.

(100). Mesmaeker A; Lecomte J-P; Kelly J Photoreactions of Metal Complexes with DNA, Especially Those Involving a Primary Photo-Electron Transfer In Electron Transfer II; Mattay J, Ed.; Topics in Current Chemistry; Springer Berlin / Heidelberg, 1996; 177, 25–76.

(101). Ortmans I; Elias B; Kelly JM; Moucheron C; Kirsch-DeMesmaeker A [Ru(TAP)2(dppz)]2+: A DNA Intercalating Complex, Which Luminesces Strongly in Water and Undergoes Photo-Induced Proton-Coupled Electron Transfer with Guanosine-5′-Monophosphate. Dalton Trans 2004, 668–676. [PubMed: 15252532]

(102). Elias B; Kirsch-De Mesmaeker A Photo-Reduction of Polyazaaromatic Ru(II) Complexes by Biomolecules and Possible Applications. Coord. Chem. Rev 2006, 250, 1627–1641.

(103). Ortmans I; Moucheron C; Kirsch-De Mesmaeker A Ru(II) Polypyridine Complexes with a High Oxidation Power. Comparison between Their Photoelectrochemistry with Transparent SnO2 and Their Photochemistry with Desoxyribonucleic Acids. Coord. Chem. Rev 1998, 168, 233–271.

(104). Yin H; Stephenson M; Gibson J; Sampson E; Shi G; Sainuddin T; Monro S; McFarland SA In Vitro Multiwavelength PDT with ^{3}IL States: Teaching Old Molecules New Tricks. Inorg. Chem 2014, 53, 4548–4559. [PubMed: 24725142]

(105). Mackay FS; Woods JA; Heringova P; Kasparkova J; Pizarro AM; Moggach SA; Parsons S; Brabec V; Sadler PJ A Potent Cytotoxic Photoactivated Platinum Complex. Proc. Natl. Acad. Sci 2007, 104, 20743–20748. [PubMed: 18093923]

(106). Ford WE; Rodgers MAJ Reversible Triplet-Triplet Energy Transfer within a Covalently Linked Bichromophoric Molecule. J. Phys. Chem 1992, 96, 2917–2920.

(107). Harriman A; Hissler M; Khatyr A; Ziessel R A Ruthenium(II) tris(2,2′-Bipyridine) Derivative Possessing a Triplet Lifetime of 42 μs. Chem. Commun 1999, 735–736.

(108). Hissler M; Harriman A; Khatyr A; Ziessel R Intramolecular Triplet Energy Transfer in Py-rene-Metal Polypyridine Dyads: A Strategy for Extending the Triplet Lifetime of the Metal Complex. Chem. Eur. J 1999, 5, 3366–3381.

(109). McClenaghan ND; Leydet Y; Maubert B; Indelli MT; Campagna S Excited-State Equilibration: A Process Leading to Long-Lived Metal-to-Ligand Charge Transfer Luminescence in Supramolecular Systems. Coord. Chem. Rev 2005, 249, 1336–1350.

(110). Kozlov DV; Tyson DS; Goze C; Ziessel R; Castellano FN Room Temperature Phosphorescence from Ruthenium(II) Complexes Bearing Conjugated Pyrenylethynylene Subunits. Inorg. Chem 2004, 43, 6083–6092. [PubMed: 15360260]

(111). Goze C; Kozlov DV; Tyson DS; Ziessel R; Castellano FN Synthesis and Photophysics of Ruthenium(II) Complexes with Multiple Pyrenylethynylene Subunits. New J. Chem 2003, 27, 1679–1683.

(112). Lincoln R; Kohler L; Monro S; Yin H; Stephenson M; Zong R; Chouai A; Dorsey C; Hennigar R; Thummel RP; McFarland S Exploitation of Long-Lived ^{3}IL Excited States for Metal-Organic

Photodynamic Therapy: Verification in a Metastatic Melanoma Model. J. Am. Chem. Soc 2013, 135, 17161–17175. [PubMed: 24127659]

(113). Monro S; Scott J; Chouai A; Lincoln R; Zong R; Thummel RP; McFarland SA Photobiological Activity of Ru(II) Dyads Based on (Pyren-1-yl)ethynyl Derivatives of 1,10-Phenanthroline. Inorg. Chem 2010, 49, 2889–2900. [PubMed: 20146527]

(114). Cruickshank B; Giacomantonio M; Marcato P; McFarland S; Pol J; Gujar S Dying to Be Noticed: Epigenetic Regulation of Immunogenic Cell Death for Cancer Immunotherapy. Front. Immunol 2018, 9, Article 654.

(115). Swavey S; Brewer KJ Visible Light Induced Photocleavage of DNA by a Mixed-Metal Supramolecular Complex: [{(bpy)2Ru(dpp)}2RhCl2]5+. Inorg. Chem 2002, 41, 6196–6198. [PubMed: 12444759]

(116). Holder AA; Swavey S; Brewer KJ Design Aspects for the Development of Mixed-Metal Supramolecular Complexes Capable of Visible Light Induced Photocleavage of DNA. Inorg. Chem 2004, 43, 303–308. [PubMed: 14704081]

(117). Holder AA; Zigler DF; Tarrago-Trani MT; Storrie B; Brewer KJ Photobiological Impact of [{(bpy)2Ru(dpp)}2RhCl2]Cl5 and [{(bpy)2Os(dpp)}2RhCl2]Cl5 [bpy=2,2′-bipyridine; dpp=2,3-bis(2-pyridyl)pyrazine] on Vero Cells. Inorg. Chem 2007, 46, 4760–4762. [PubMed: 17488069]

(118). Stemp EDA; Arkin MR; Barton JK Oxidation of Guanine in DNA by Ru(phen)2(dppz)3+ Using the Flash-Quench Technique. J. Am. Chem. Soc 1997, 119, 29212925.

(119). Purugganan MD; Kumar CV; Turro NJ; Barton JK Accelerated Electron Transfer between Metal Complexes Mediated by DNA. Science 1988, 241, 1645–1649. [PubMed: 3420416]

(120). Majewski MB; de Tacconi NR; MacDonnell FM; Wolf MO Ligand-Triplet-Fueled Long-Lived Charge Separation in Ruthenium(II) Complexes with Bithienyl-Functionalized Ligands. Inorg. Chem 2011, 50, 9939–9941. [PubMed: 21936493]

(121). Howerton BS; Heidary DK; Glazer EC Strained Ruthenium Complexes Are Potent Light-Activated Anticancer Agents. J. Am. Chem. Soc 2012, 134, 8324–8327. [PubMed: 22553960]

(122). Wachter E; Heidary DK; Howerton BS; Parkin S; Glazer EC Light-Activated Ruthenium Complexes Photobind DNA and Are Cytotoxic in the Photodynamic Therapy Window. Chem. Commun 2012, 48, 9649–9651.

(123). Albani BA; Peña B; Leed NA; de Paula NABG; Pavani C; Baptista MS; Dunbar KR; Turro C Marked Improvement in Photoinduced Cell Death by a New Tris-Heteroleptic Complex with Dual Action: Singlet Oxygen Sensitization and Ligand Dissociation. J. Am. Chem. Soc 2014, 136, 17095–17101. [PubMed: 25393595]

(124). Hanson BJ Composition and Assays for Determining Cell Viability U.S. Patent 2013/0210063 A1, 8 15, 2013.

(125). Berlanda J; Kiesslich T; Engelhardt V; Krammer B; Plaetzer K Comparative in Vitro Study on the Characteristics of Different Photosensitizers Employed in PDT. J. Photochem. Photobiol. B 2010, 100, 173–180. [PubMed: 20599390]

(126). Kiesslich T; Gollmer A; Maisch T; Berneburg M; Plaetzer K A Comprehensive Tutorial on In Vitro Characterization of New Photosensitizers for Photodynamic Antitumor Therapy and Photodynamic Inactivation of Microorganisms. BioMed Res. Int 2013, 2013, 1–17.

(127). Ji S; Wu W; Wu W; Song P; Han K; Wang Z; Liu S; Guo H; Zhao J Tuning the Luminescence Lifetimes of Ruthenium(II) Polypyridine Complexes and Its Application in Luminescent Oxygen Sensing. J. Mater. Chem 2010, 20, 1953–1963.

(128). Kalinina S; Breymayer J; Reeβ K; Lilge L; Mandel A; Rück A Correlation of Intracellular Oxygen and Cell Metabolism by Simultaneous PLIM of Phosphorescent TLD1433 and FLIM of NAD(P)H. J. Biophotonics 2018, e201800085. [PubMed: 29877627]

(129). Biner M; Buergi HB; Ludi A; Roehr C Crystal and Molecular Structures of [Ru(bpy)3](PF6)3 and [Ru(bpy)3](PF6)2 at 105 K. J. Am. Chem. Soc 1992, 114, 5197–5203.

(130). Pérez-Cordero EE; Campana C; Echegoyen L X-Ray Structure of[Ru(bpy)3]0: An Expanded Atom or a New Electride? Angew. Chem. Int. Ed. Engl 1997, 36, 137–140.

(131). Wang Z Radziszewski Reaction In Comprehensive Organic Name Reactions and Reagents; John Wiley & Sons, Inc., 2010.

(132). Han M-J; Gao L-H; Wang K-Z Ruthenium(II) Complex of 2-(9-anthryl)-1H-imidazo[4,5-f] [1,10]phenanthroline: Synthesis, Spectrophotometric pH Titrations and DNA Interaction. New J. Chem 2006, 30, 208–214.

(133). Li Z-S; Yang H-X; Zhang A-G; Luo H; Wang K-Z pH Effects on Optical and DNA Binding Properties of a Thiophene-Containing Ruthenium(II) Complex. Inorg. Chim. Acta 2011, 370, 132–140.

(134). Kato Y; Ozawa S; Miyamoto C; Maehata Y; Suzuki A; Maeda T; Baba Y Acidic Extracellular Microenvironment and Cancer. Cancer Cell Int 2013, 13, 89. [PubMed: 24004445]

(135). Reichardt C; Sainuddin T; Wächtler M; Monro S; Kupfer S; Guthmuller J; Gräfe S; McFarland S; Dietzek B Influence of Protonation State on the Excited State Dynamics of a Photobiologically Active Ru(II) Dyad. J. Phys. Chem. A 2016, 120, 6379–6388. [PubMed: 27459188]

(136). Becker RS; Seixas de Melo J; Maçanita AL; Elisei F Comprehensive Evaluation of the Absorption, Photophysical, Energy Transfer, Structural, and Theoretical Properties of α-Oligothiophenes with One to Seven Rings. J. Phys. Chem 1996, 100, 18683–18695.

(137). Gierschner J; Cornil J; Egelhaaf H-J Optical Bandgaps of “-Conjugated Organic Materials at the Polymer Limit: Experiment and Theory. Adv. Mater 2007, 19, 173–191.

(138). Mauer R; Howard I; Laquai F Energy and Charge Transfer In Semiconducting Polymer Composites: Principles, Morphologies, Properties and Applications; Wiley-VCH Verlag.

(139). Johansson T; Mammo W; Svensson M; Andersson MR; Inganäs O Electrochemical Bandgaps of Substituted Polythiophenes. J. Mater. Chem 2003, 13, 1316–1323.

(140). Köhler A; Beljonne D The Singlet-Triplet Exchange Energy in Conjugated Polymers. Adv. Funct. Mater 2004, 14, 11–18.

(141). Scaiano JC; Redmond RW; Mehta B; Arnason JT Efficiency of the Photoprocesses Leading to Singlet Oxygen (1δg) Generation by Alpha-Terthienyl: Optical Absorption, Optoa-coustic Calorimetry and Infrared Luminescence Studies. Photochem. Photobiol 1990, 52, 655659.

(142). Wasserberg D; Marsal P; Meskers SCJ; Janssen RAJ; Beljonne D Phosphorescence and Triplet State Energies of Oligothiophenes. J. Phys. Chem. B 2005, 109, 4410–4415. [PubMed: 16851510]

(143). Scaiano JC; MacEachern A; Arnason JT; Morand P; Weir D Singlet Oxygen Generating Efficiency of α-Terthienyl and Some of Its Synthetic Analogues. Photochem. Photobiol 1987, 46, 193–199.

(144). Shi G; Monro S; Hennigar R; Colpitts J; Fong J; Kasimova K; Yin H; DeCoste R; Spencer C; Chamberlain L; Mandel A; Lilge L; McFarland SA Ru(II) Dyads Derived from α-Oligothiophenes: A New Class of Potent and Versatile Photosensitizers for PDT. Coord. Chem. Rev 2015, 282–283, 127–138.

(145). Reyftmann JP; Kagan J; Santus R; Morliere P Excited State Properties of α-Terthienyl and Related Molecules. Photochem. Photobiol 1985, 41, 1–7. [PubMed: 3983243]

(146). Ciofalo M; Petruso S; Schillaci D Quantitative Assay of Photoinduced Antibiotic Activities of Naturally-Occurring 2,2′:5′,2′′-Terthiophenes. Planta Med 1996, 62, 374–375. [PubMed: 8792675]

(147). Alberto ME; Pirillo J; Russo N; Adamo C Theoretical Exploration of Type I/Type II Dual Photoreactivity of Promising Ru(II) Dyads for PDT Approach. Inorg. Chem 2016, 55, 1118511192.

(148). Millis KK; Weaver KH; Rabenstein DL Oxidation/Reduction Potential of Glutathione. J. Org. Chem 1993, 58, 4144–4146.

(149). Sainuddin T; Pinto M; Yin H; Hetu M; Colpitts J; McFarland SA Strained Ruthenium Metal-organic Dyads as Photocisplatin Agents with Dual Action. J. Inorg. Biochem 2016, 158, 45–54. [PubMed: 26794708]

(150). Fong J; Kasimova K; Arenas Y; Kaspler P; Lazic S; Mandel A; Lilge L A Novel Class of Ruthenium-Based Photosensitizers Effectively Kills in Vitro Cancer Cells and in Vivo Tumors. Photochem. Photobiol. Sci 2015, 14, 2014–2023. [PubMed: 25666432]

(151). Svensson FR; Matson M; Li M; Lincoln P Lipophilic Ruthenium Complexes with Tuned Cell Membrane Affinity and Photoactivated Uptake. Biophys. Chem 2010, 149, 102–106. [PubMed: 20471741]

(152). Du H; Xiang J; Zhang Y; Tang Y; Xu G Binding of VIV to Human Transferrin: Potential Relevance to Anticancer Activity of Vanadocene Dichloride. J. Inorg. Biochem 2008, 102, 146–149. [PubMed: 17825420]

(153). Guo W; Zheng W; Luo Q; Li X; Zhao Y; Xiong S; Wang F Transferrin Serves as a Mediator to Deliver Organometallic Ruthenium(II) Anticancer Complexes into Cells. Inorg. Chem 2013, 52, 5328–5338. [PubMed: 23586415]

(154). Kaspler P; Lazic S; Forward S; Arenas Y; Mandel A; Lilge L A Ruthenium(II) Based Photosensitizer and Transferrin Complexes Enhance Photo-Physical Properties, Cell Uptake, and Photodynamic Therapy Safety and Efficacy. Photochem. Photobiol. Sci 2016, 15, 481–495. [PubMed: 26947517]

(155). Kratz F; Hartmann M; Keppler B; Messori L The Binding Properties of Two Antitumor Ruthenium(III) Complexes to Apotransferrin. J. Biol. Chem 1994, 269, 2581–2588. [PubMed: 8300587]

(156). Mazuryk O; Kurpiewska K; Lewiński K; Stochel G; Brindell M Interaction of Apo-Transferrin with Anticancer Ruthenium Complexes NAMI-A and Its Reduced Form. J. Inorg. Biochem 2012, 116, 11–18. [PubMed: 23010324]

(157). Pongratz M; Schluga P; Jakupec MA; Arion VB; Hartinger CG; Allmaier G; Kep-pler BK Transferrin Binding and Transferrin-Mediated Cellular Uptake of the Ruthenium Coordination Compound KP1019, Studied by Means of AAS, ESI-MS and CD Spectroscopy. J. Anal. At. Spectrom 2004, 19, 46–51.

(158). Sun H; Li H; Sadler PJ Transferrin as a Metal Ion Mediator. Chem. Rev 1999, 99, 2817–2842. [PubMed: 11749502]

(159). Gollnick SO; Vaughan L; Henderson BW Generation of Effective Antitumor Vaccines Using Photodynamic Therapy. Cancer Res 2002, 62, 1604–1608. [PubMed: 11912128]

(160). Castano AP; Mroz P; Hamblin MR Photodynamic Therapy and Anti-Tumour Immunity. Nat. Rev. Cancer 2006, 6, 535–545. [PubMed: 16794636]

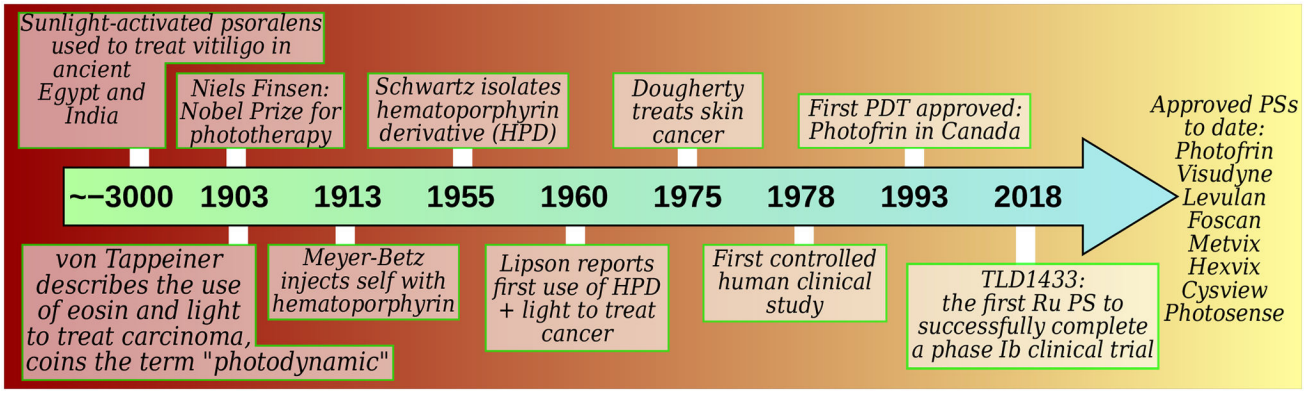

Figure 1.

Historical development of PDT according to selected milestones.[15] PS=photosensitizer.

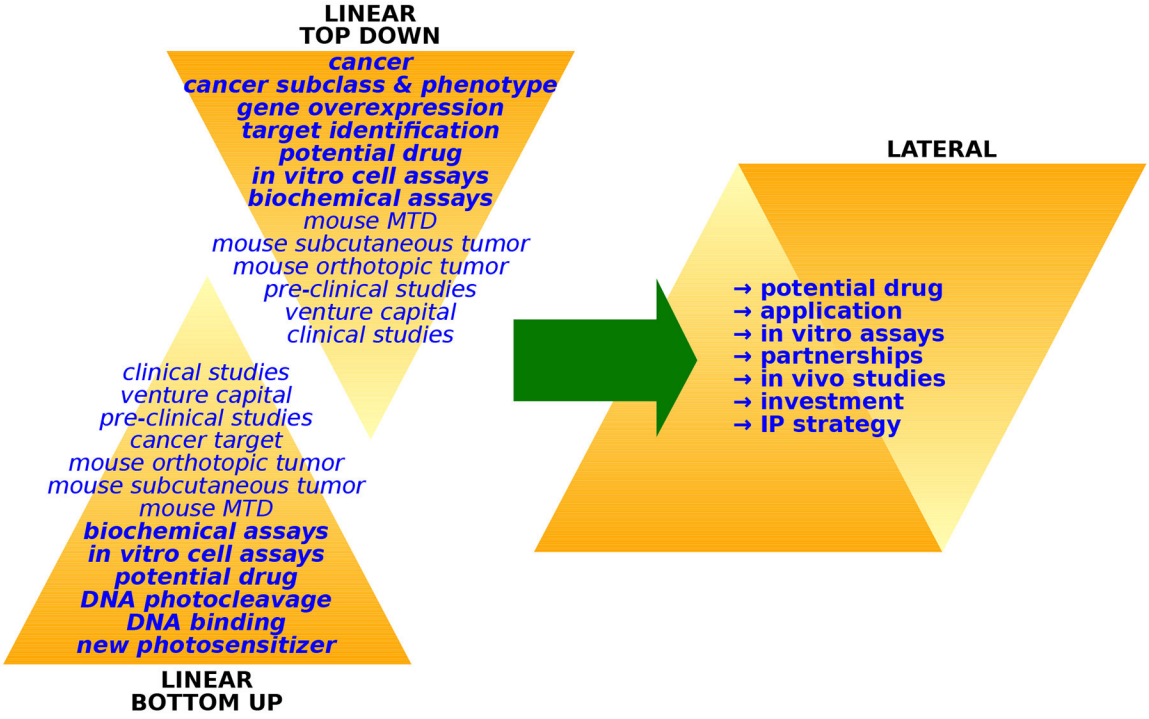

Figure 2.
Academic (left) and multi-dimensional (right) approaches to PDT research.

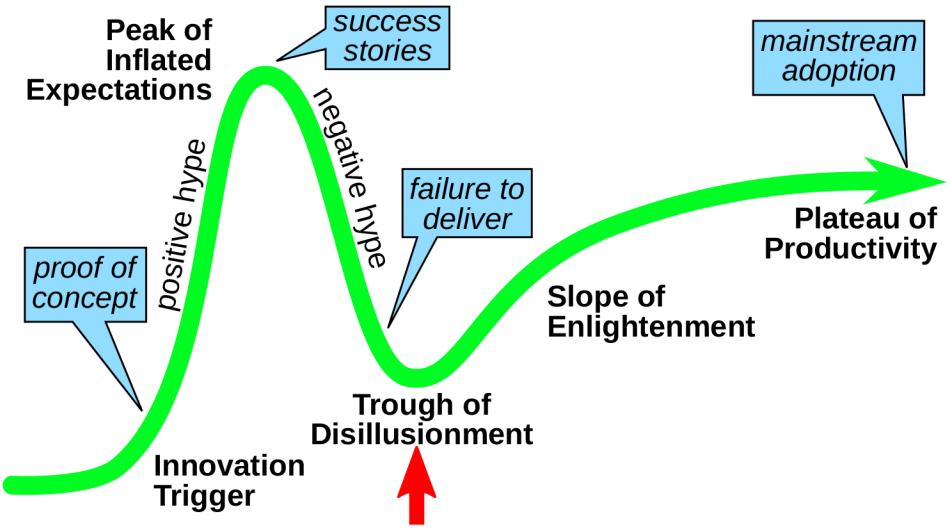

Figure 3.
Gartner hype cycle for innovative technologies.

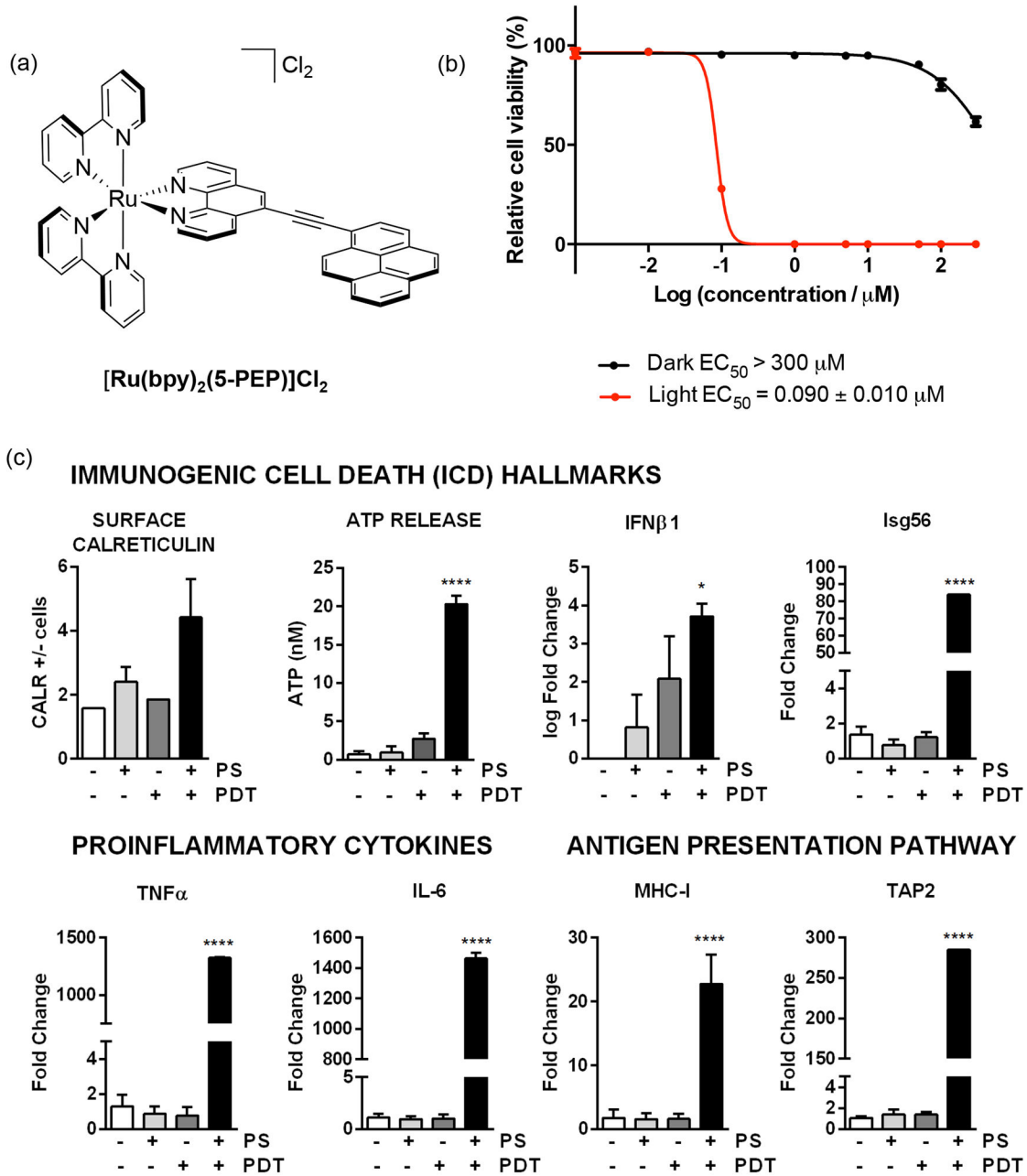

Figure 4.

(a) Chemical structure of metal-organic dyad $[Ru(bpy)_2(5\text{-PEP})]Cl_2$ (only Λ isomer shown), (b) (Photo)cytotoxicity against SKMEL28 melanoma cells for $[Ru(bpy)_2(5\text{-PEP})]^{2+}$ with and without transferrin (Tf). PS=photosensitizer. (c) Immunomodulatory potential of $[Ru(bpy)_2(5\text{-PEP})]Cl_2$ (100 nM) toward B16F10 melanoma cells. The light treatment was 100 J cm^{-2} of broadband visible (400–700 nm) light delivered at a rate of ~28 mW cm^{-2}. The PS-to-light interval was 16 h.

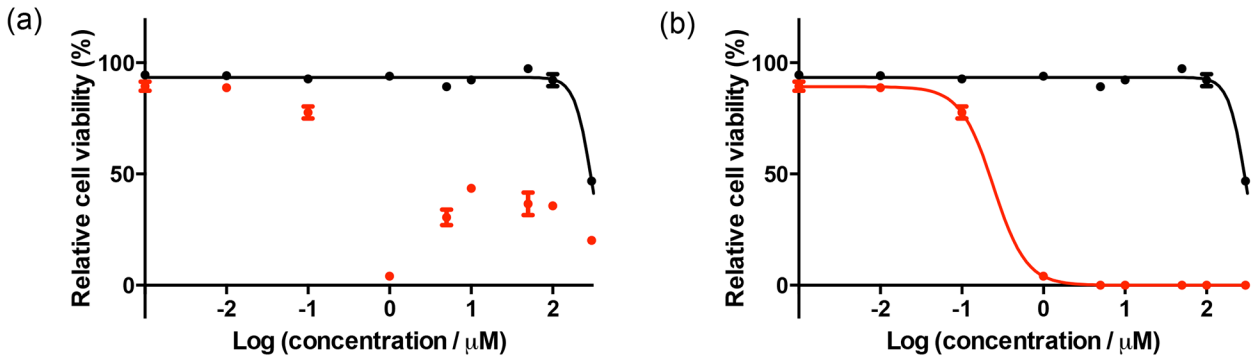

Figure 5.

Dose-response curves for HL-60 human leukemia cells treated with TLD1433 with (red) or without (black) a light treatment, (a) Uncorrected data, (b) corrected data. The light treatment was 100 J cm^{-2} of broadband visible (400–700 nm) light delivered at a rate of ~28 mW cm^{-2}. The photosensitizer-to-light interval was 16 h.

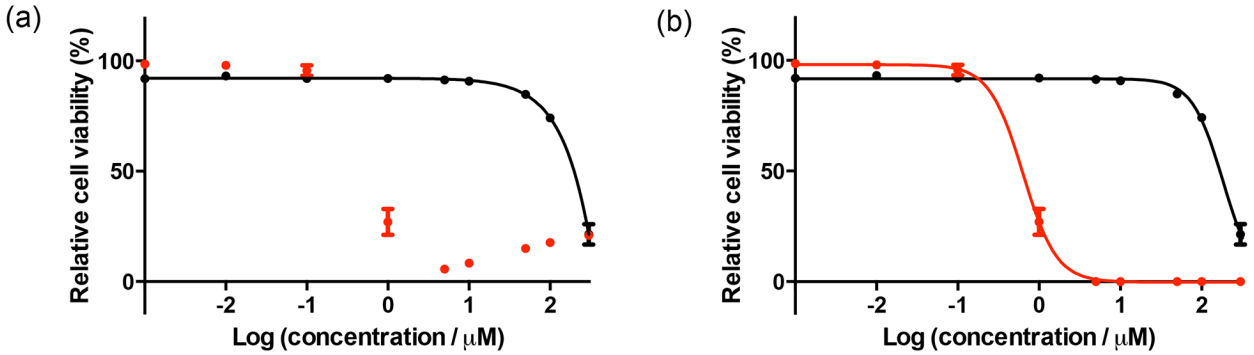

Figure 6.

Dose-response curves for SKMEL28 human melanoma cells treated with $[Ru(bpy)_2(dppn)]CL$ with (red) or without (black) a light treatment, (a) Uncorrected data, (b) corrected data. The light treatment was 100 J cm^{-2} of broadband visible (400–700 nm) light delivered at a rate of ~28 mW cm^{-2}. The photosensitizer-to-light interval was 16 h.

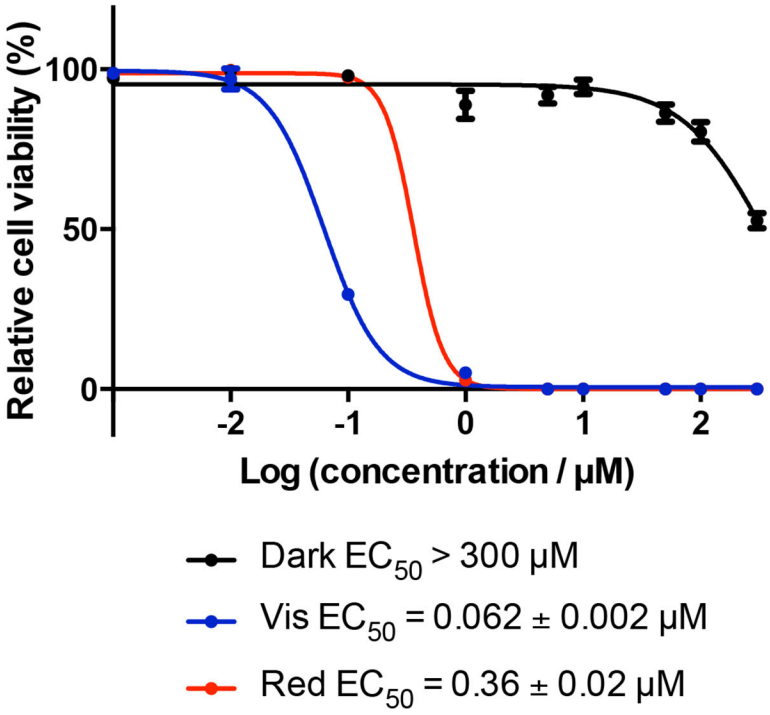

Figure 7.
In vitro dose-response curves for SKMEL28 cells treated with $[Ru(bpy)_2(dppn)]Cl_2$ using the standard assay conditions.

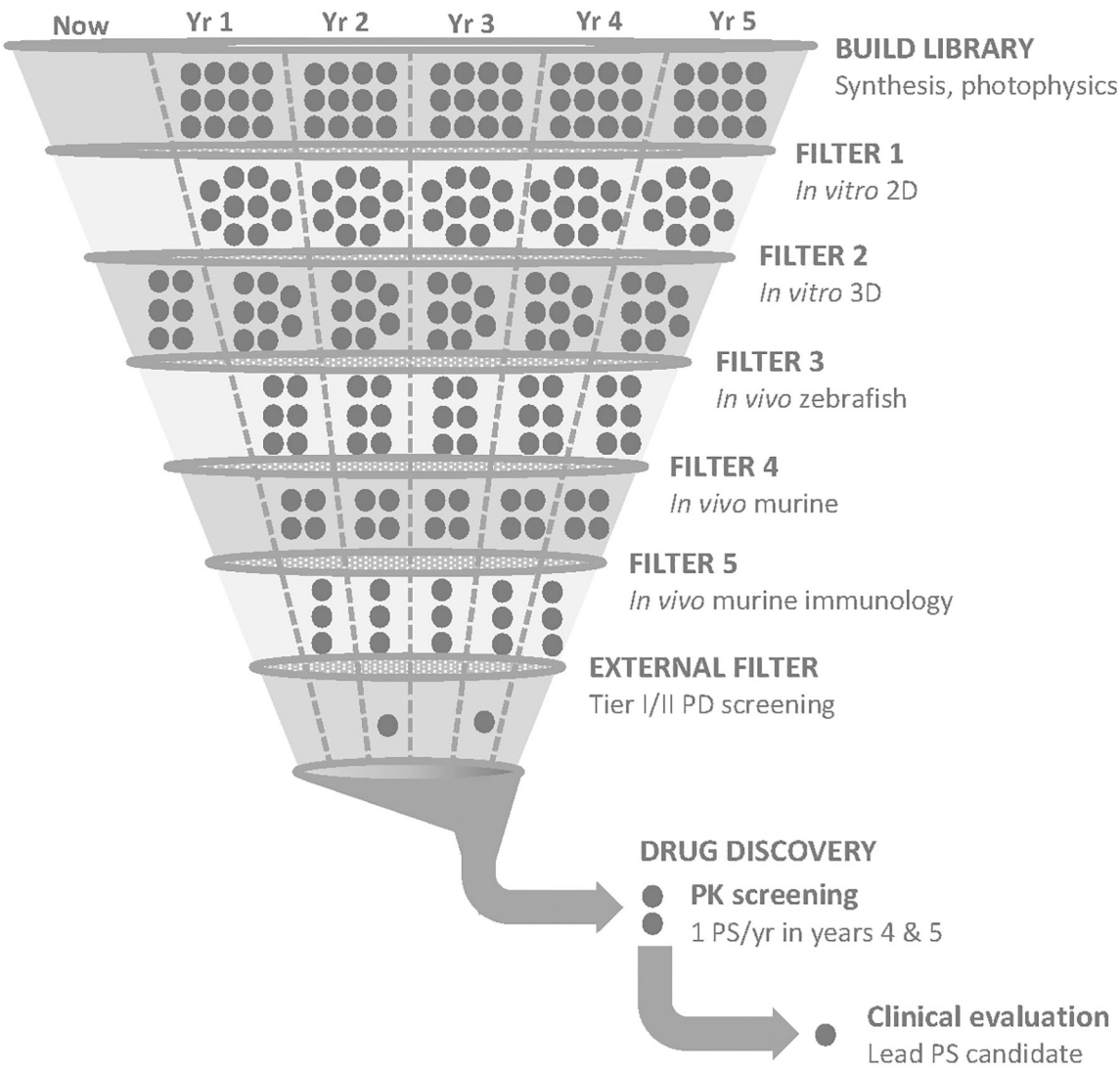

Figure 8.

Filter process for hit (lead) identification. Image used with permission from Mr. Martin Greenwood, CEO, Photodynamic Inc.®

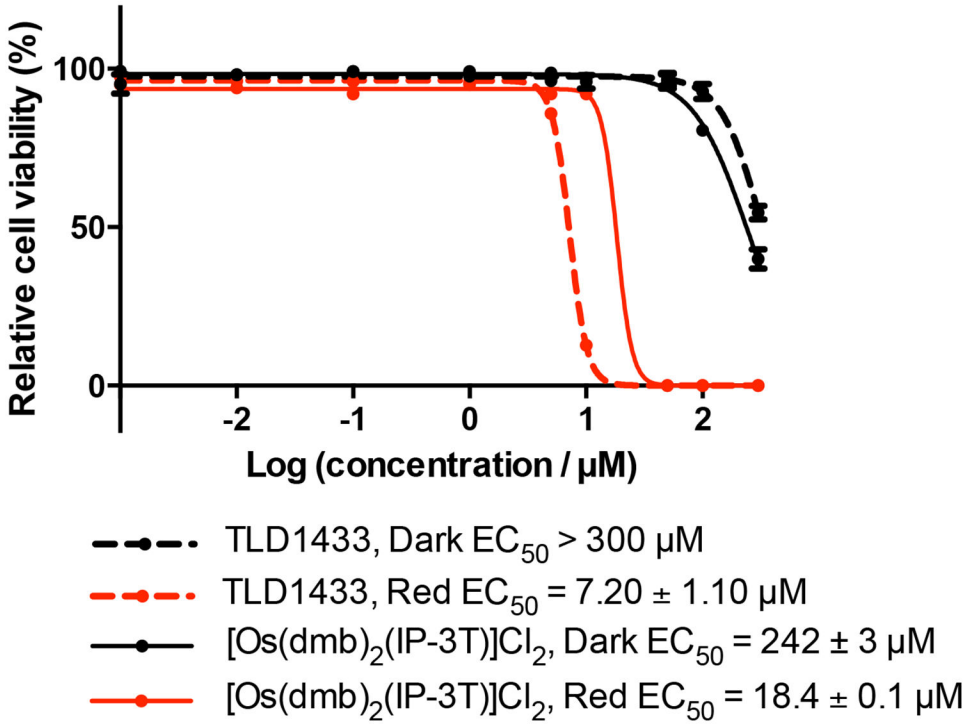

Figure 9.

(Photo)cytotoxicity dose-response profiles toward HL-60 human leukemia cells for Ru(II) versus Os(II) dyads derived from the IP-3T ligand. Light treatments were 100 J cm^{-2} of red (625 nm) light delivered at a rate of ~28 mW cm^{-2}. The photosensitizer-to-light interval was 16 h.

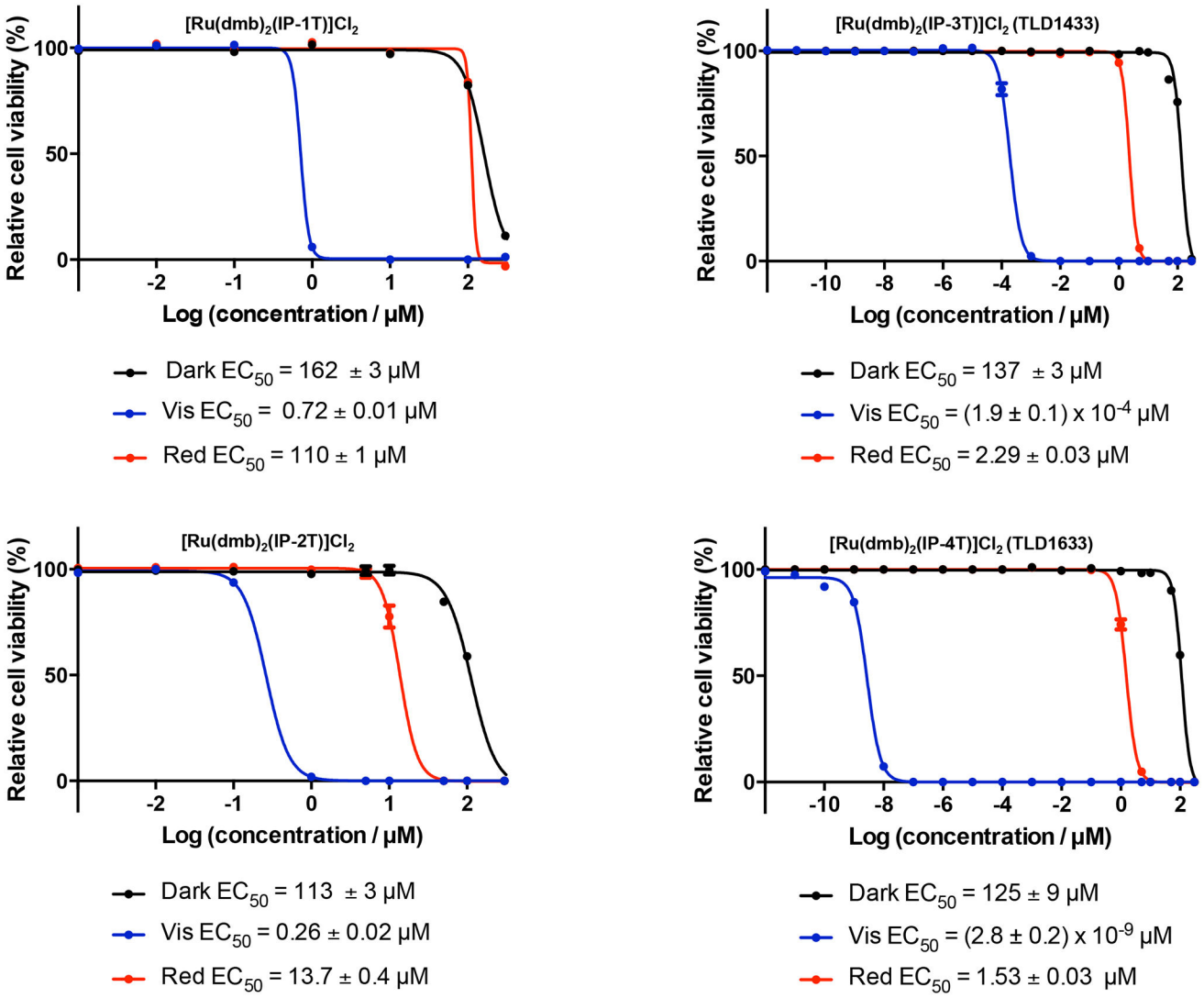

Figure 10.

(Photo)cytotoxicity dose-response profiles toward SK-MEL-28 melanoma cells for Ru(II) dyads derived from the functional IP-*n*T ligand, where *n*=1–4. Light treatments were 100 J cm^{-2} of broadband visible (400–700 nm) or monochromatic red (625 nm) light delivered at a rate of ~28 mW cm^{-2}. The photosensitizer-to-light interval was 16 h.

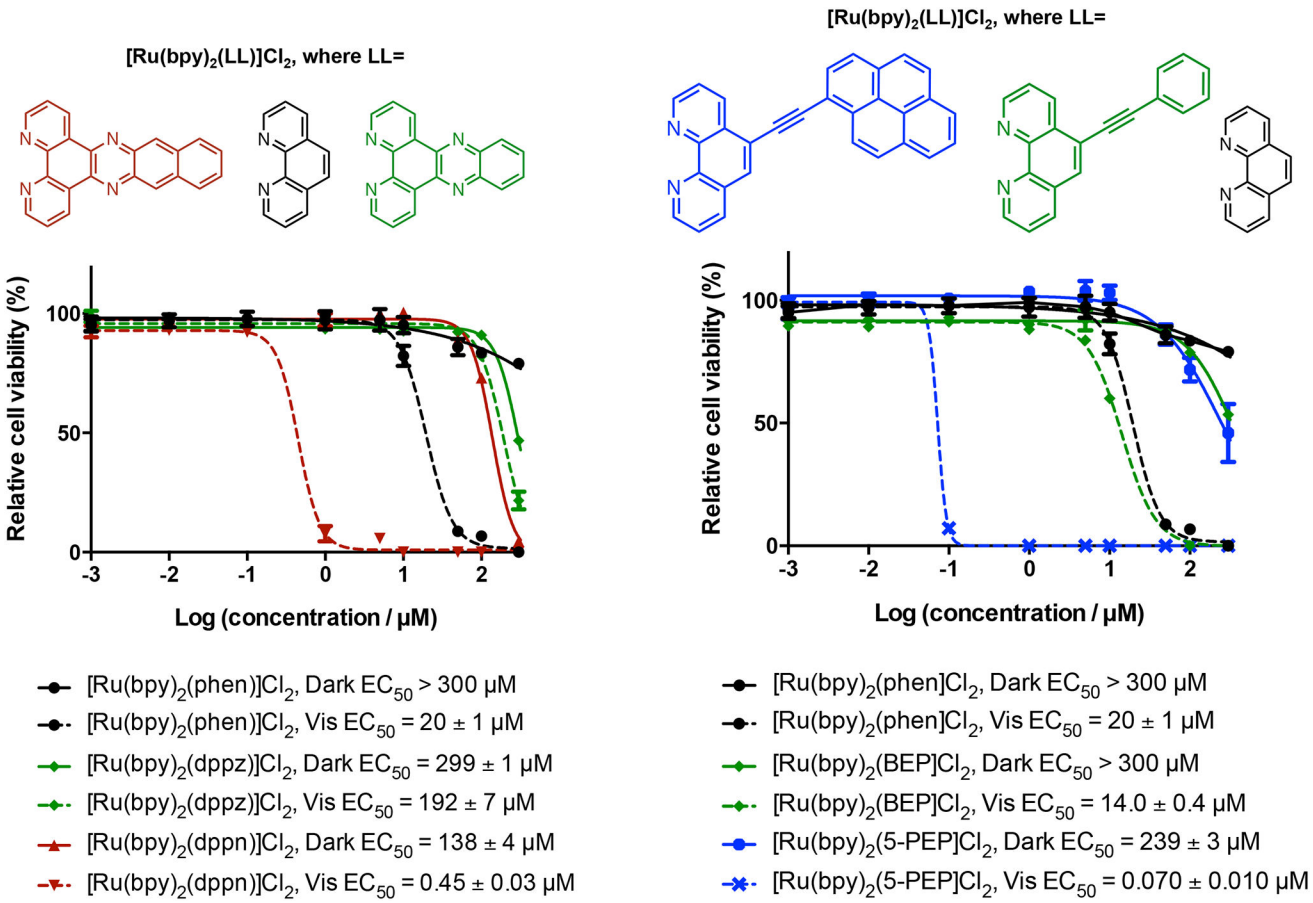

Figure 11.

(Photo)cytotoxicity dose-response profiles toward HL-60 human leukemia cells for Ru(II) dyads of two different families. Light treatments were 100 J cm^{-2} of broadband visible (400–700 nm) light delivered at a rate of ~28 mW cm^{-2}. The photosensitizer-to-light interval was 16 h.

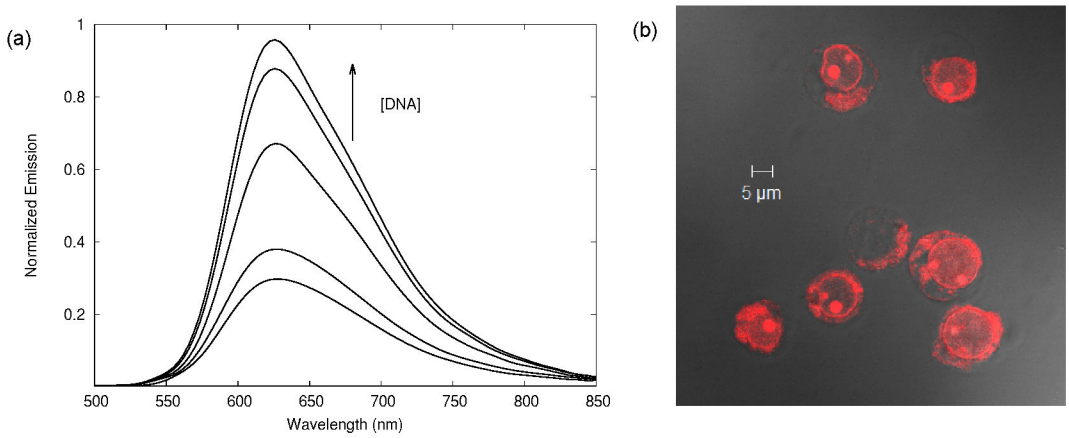

Figure 12.

(a) Emission of TLD1433 titrated with calf-thymus DNA. (b) Human leukemia cells dosed with TLD1433 and viewed using laser scanning confocal microscopy (LSCM).

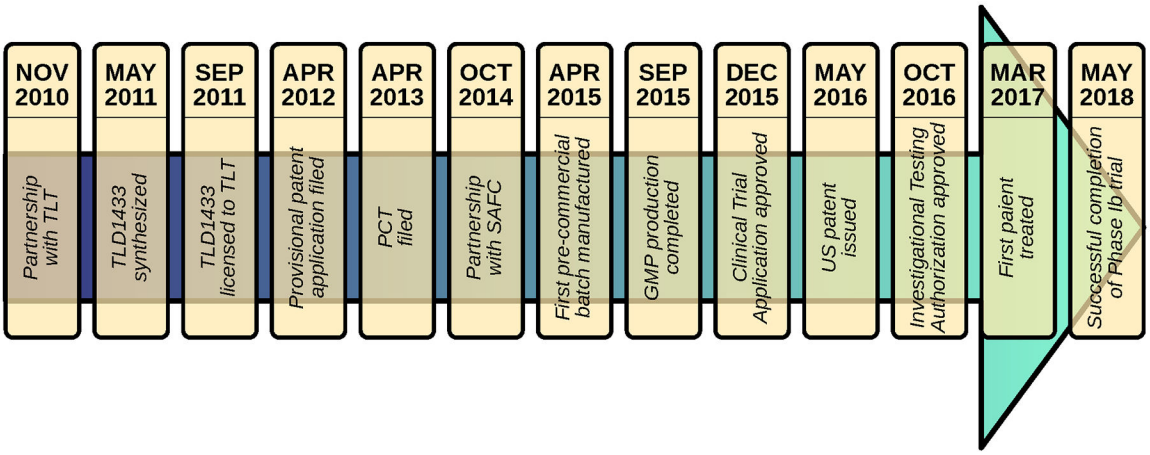

Figure 13.
Timeline for developing TLD1433.

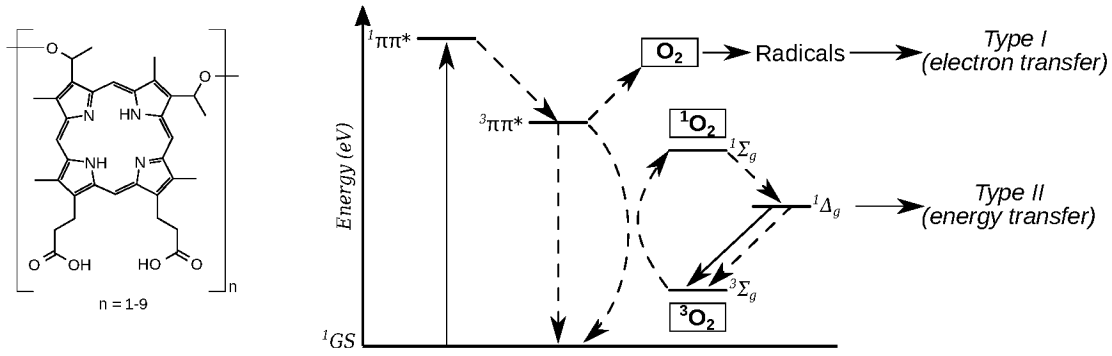

Scheme 1.

Chemical structure of Photofrin®, where n indicates the possible oligomeric components of a poorly defined mixture (left), and a Jablonski diagram showing Type I and Type II photoreactions (right).

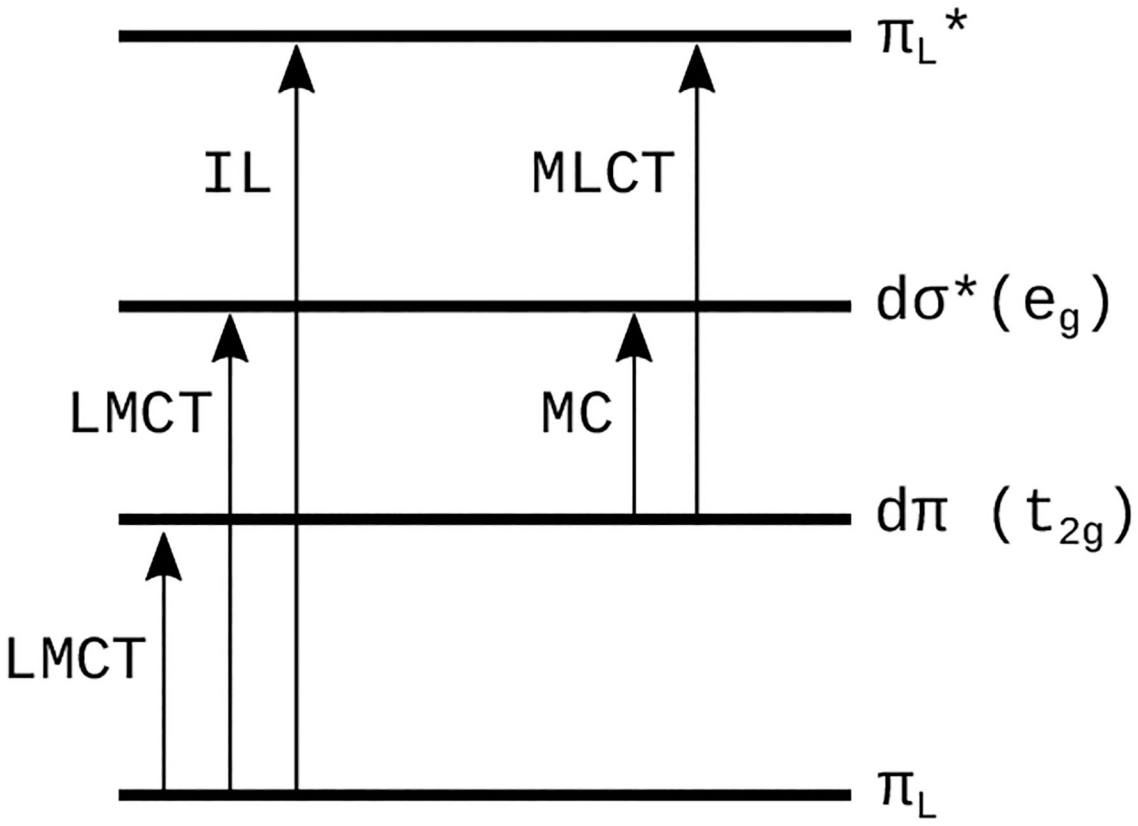

Scheme 2.
Some of the electronic transitions available to transition metal complexes.

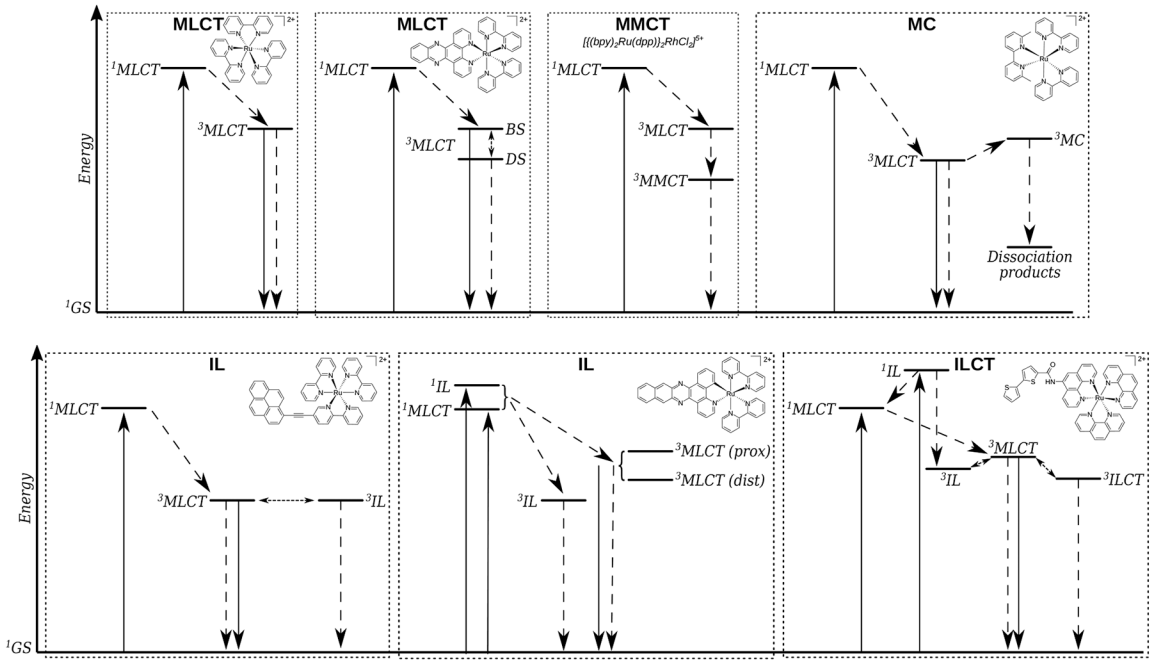

Scheme 3.

Jablonski diagrams for different excited-state electronic configurations in Ru(II)-based transition metal complexes.

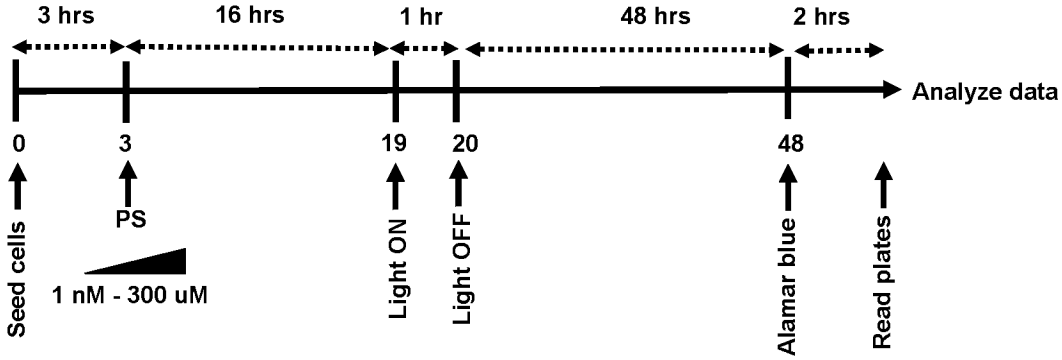

Scheme 4.
Timeline for standard PDT/PCT assay.

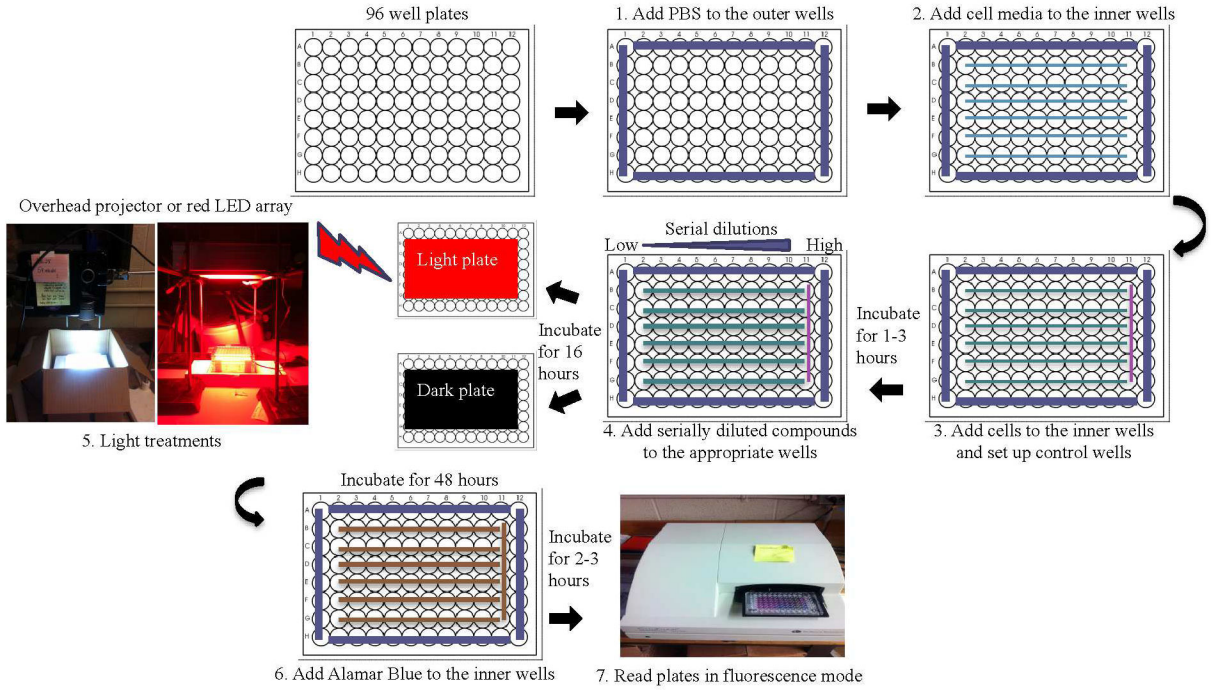

Scheme 5.
Microplate layout and organization of the standard PDT/PACT assay.

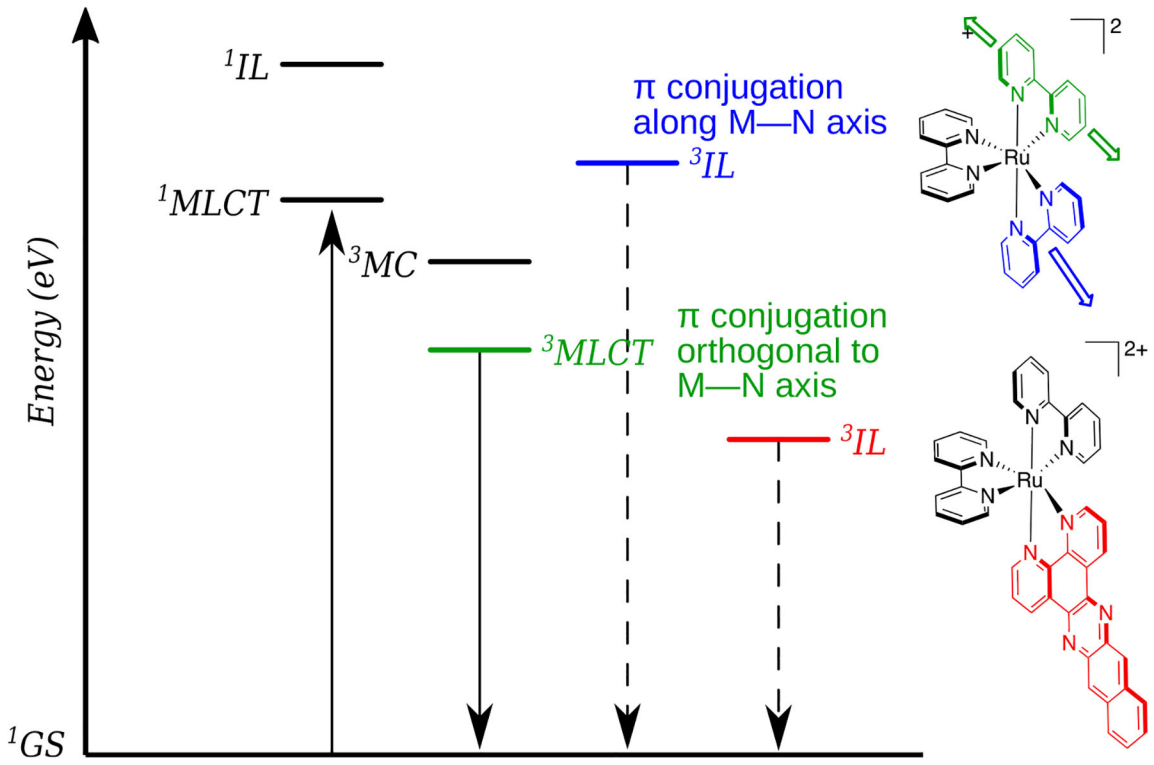

Scheme 6.

Some excited state energies in Ru(II) polypyridyl complexes that can be altered with **π**-conjugation.

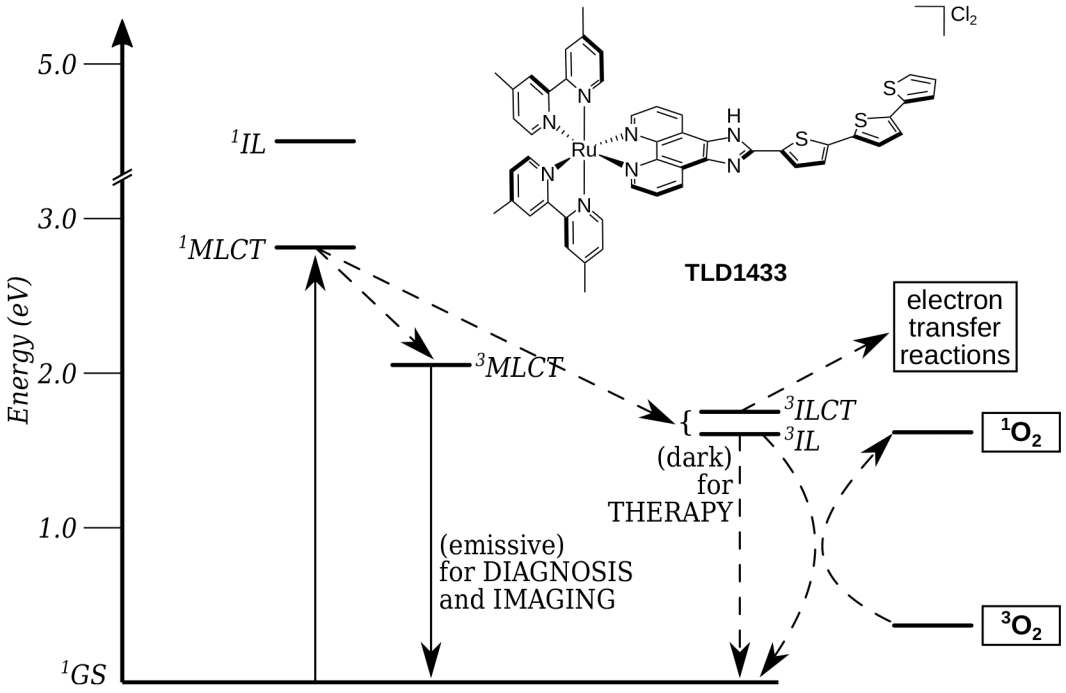

Scheme 7.
Excited-state deactivation pathways accessible to TLD1433 with visible light activation.

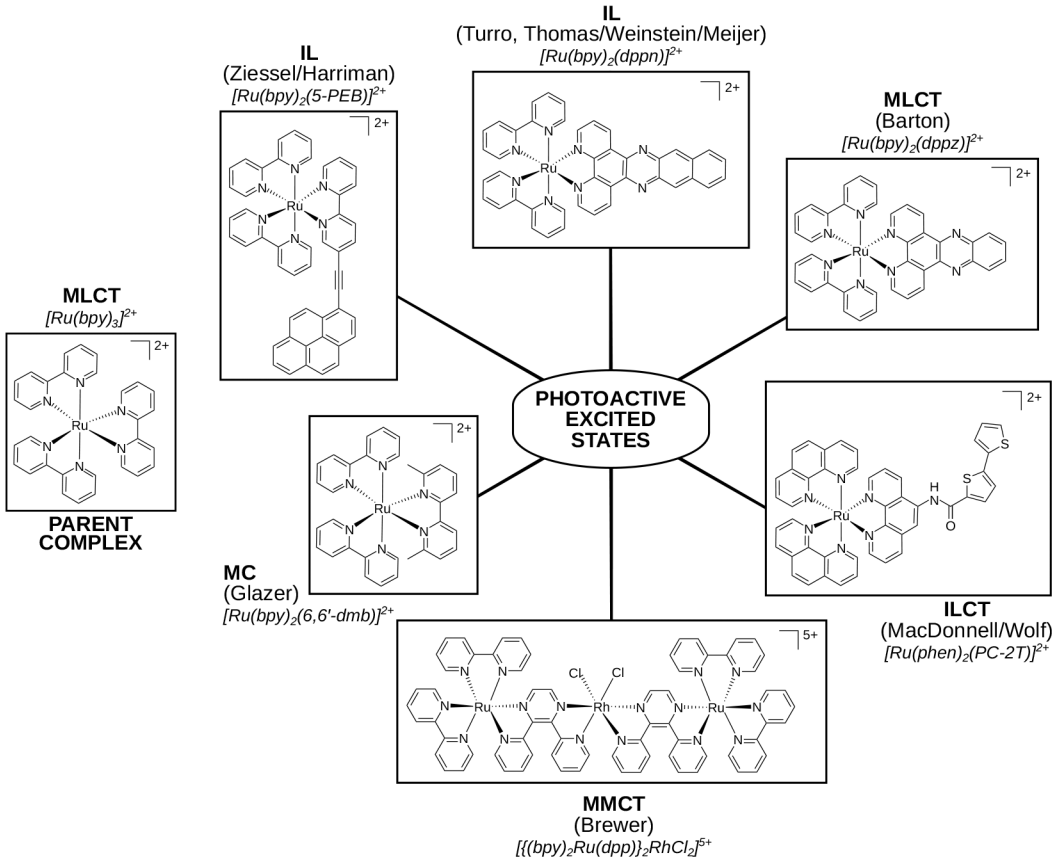

Chart 1.

Compounds that serve as examples of the different types of accessible excited states in Ru(II) transition metal complexes (only one stereoisomer shown for simplicity).

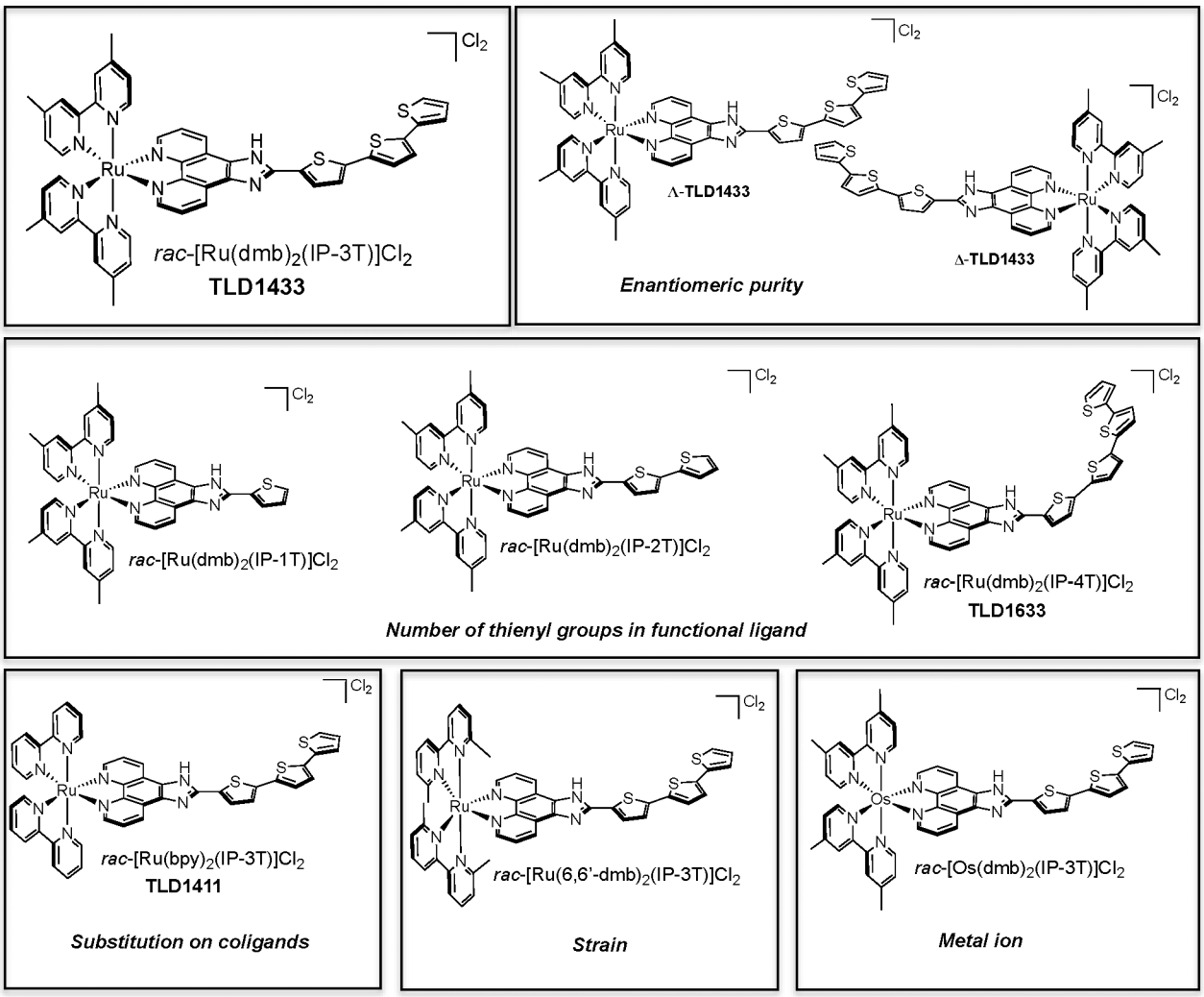

Chart 2.

Molecular Structures Used to Establish SARs for Ru(II) Dyads that Incorporate α-Oligothiophenes (dmb=4,4′-dmb).

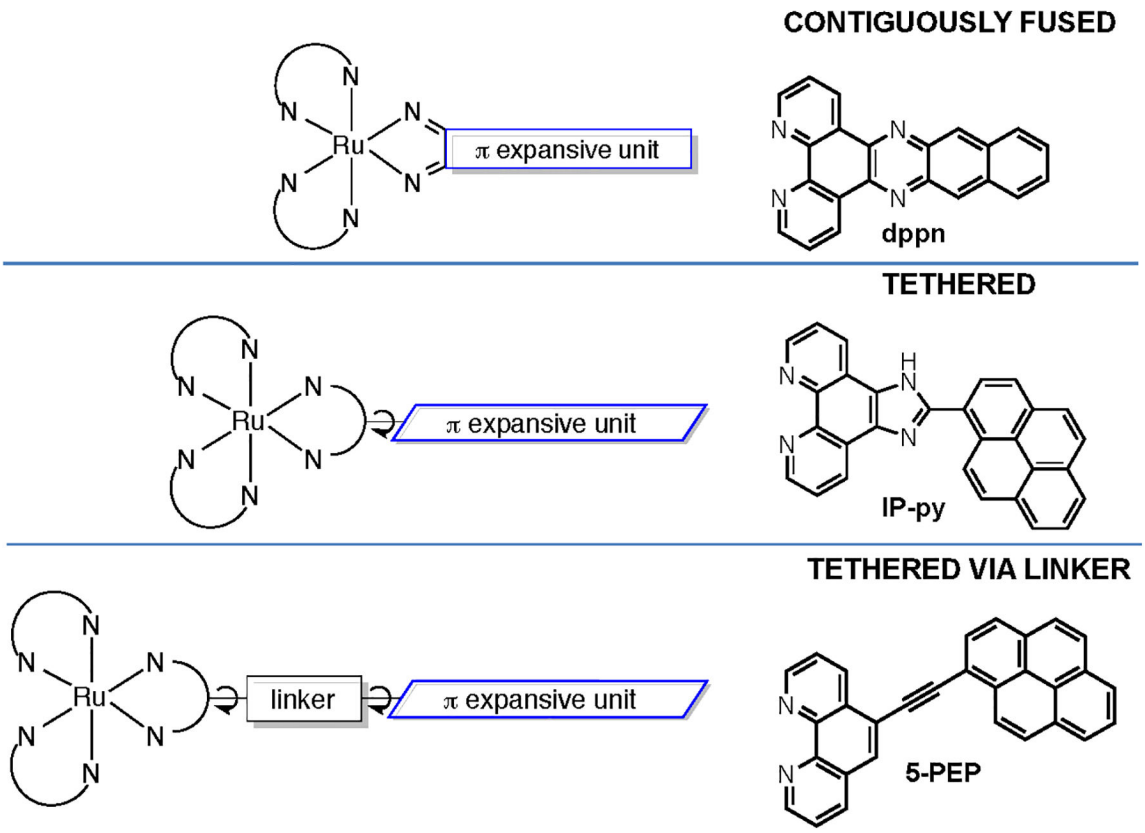

Chart 3.
Various ways of introducing π-expansion into polypyridyl ligands to make Ru(II)-dyads.

Table 5.

Search Hits Related to Metal Complexes and Ruthenium as Photoactive Anticancer Agents.

Search terms (2008–2018)	PubMed	Scopus	SciFinder®	Google Scholar
metal complex and photodynamic therapy	170	295	429	18,600
metal complex and photoactivated cancer therapy	7	61	4	10,100
metal complex and photochemotherapy	114	25	70	2,200
metal complex and photoactivated chemotherapy	26	15	24	5,780
ruthenium and photodynamic therapy	128	56	427	5,040
ruthenium and photoactivated cancer therapy	8	56	8	2,270
ruthenium and photochemotherapy	71	25	94	535
ruthenium and photoactivated chemotherapy	22	15	43	1.600
Total	456[a]	548[a]	1,099[a]	46,125[a]

[a]Numbers not corrected for duplicate hits.